DISS. ETH NO. 24794

FATE AND POTENTIAL OF MSCS IN MICRO-VASCULARIZED TISSUE MODELS

A thesis submitted to attain the degree of

DOCTOR OF SCIENCES of ETH ZURICH

(Dr. sc. ETH Zurich)

presented by

ULRICH BLACHE

M. Sc., Universität Leipzig

born on 01.02.1986

citizen of Germany

accepted on the recommendation of

Prof. Dr. Jess Snedeker,

Prof. Dr. Katrien De Bock, PD Dr. Martin Ehrbar

2017

Fate and potential of MSCs in micro-vascularized tissue models

Acknowledgements

I would like to thank the following persons for their support during my time as PhD student:

PD Dr. Martin Ehrbar for accepting me as a member of his research group at the University Hospital of Zurich, for always being responsive, for triggering good ideas but also for supporting my silly ideas, for providing me with the Marie Curie Fellowship and for reading and commenting on my paper works. I am very glad to have worked in his lab. **Prof. Jess Snedeker** for accepting me as doctoral student at the ETH Zurich, for guiding me through the PhD studies, for the trust in my work and for making me be part of the team that in 2017 almost won the SOLA-Stafette. **Prof. Katrien De Bock** for accepting to read, criticize and evaluate this thesis and my work. **Prof. Roland Zimmermann** for the support of the research unit at the Obstetrics Department of the University Hospital of Zurich.

I thank **all lab members** of the famous and unique Ehrbar Lab. It has been really a big pleasure to be part of this amazing group… In particular, I thank **Esther Kleiner, Aida Kurmanaviciene, Yvonne Eisenegger** and **Corina von Arx** for the continuous and always reliable technical and administrative support, and for the jokes in the mornings. **Dr. Vincent Milleret** for 24/7 answering the tons of questions I asked. **Dr. Stéphanie Metzger** for being my great bench neighbor for many years and for the friendship. **Dr. Panagiota Papageorgiou** for traveling with me around Europe and for fighting my fear of flying. **Yannick Devaud** for being a perfect French and English teacher. **Queralt Vallmajó-Martin** for the truly infectious enthusiasm and for fighting my conservative scientific behavior. **Eva Avilla Royo** for the lessons on the color code, **Dr. Philipp Lienemann** for paving the way in PEG hydrogels, **Dr. Anna-Sofia Kiveliö** for running with me around all that Swiss lakes and **Lisa Krattiger** for the proofreading.

Furthermore, I would like to thank **Dr. Unai Silvan**, **Stefania Wunderli** and **Angelina Schönenberger** for perfectly integrating me into the Snedeker Lab. **Prof. Ivan Martin**, **PD Dr. Arnaud Scherberich**, **Dr. Julien Guerrero, Dr. Michael Prummer, Dr. Edward Horton** and **Prof. Valentin Djonov** for the good and fruitful collaborations. **Werner Graber** for acquiring the most beautiful images of this thesis. **Philipp Fisch** for helping me with rheology experiments, **Anette Schütz** for helping me with FACS experiments and **Eric Parigoris** for the English proofreading.

Finally, I thank **Dr. Martin Kräter** for exchanging with me many silly E-mails and for being my partner in crime in the academic jungle and **Sebastian Greiser** for being the one among my friends who is able to understand what it means to do a PhD. Most of all I thank **Elisabeth Bormann** and **Florin Blache** for the love and patience.

Summary

Diseases related to vascular malfunction, hyper-vascularization, or lack of vascularization are among the leading causes of morbidity and mortality. Although the first generation of pro- and anti-vascular treatment strategies has delivered promising results in basic research, clinical trials have not met expectations. One reason for this discrepancy lies in the differences between basic research involving animal models and human biology. Additionally, the evaluation of vascular treatment strategies on the cellular level is challenging in animal models and even more so in human patients. Three-dimensional (3D) tissue models show great potential for overcoming these limitations by establishing controlled and near-physiological in vitro conditions for the detailed study of vessel formation and regulation. The engineering of vascularized tissue models requires appropriate scaffold materials that support cell-specific functions and at best are compatible with (micro)-manufacturing techniques. Furthermore, scaffold materials for tissue models should be highly defined in their composition and properties to achieve reproducible and controlled cell environments. Additionally, tissue models that address cell biology questions would benefit from scaffold materials that can be tailored towards specific cellular needs. Hydrogels made of fully synthetic materials that mimic the extracellular matrix (ECM) fulfill these requirements and have been established in the last decade. For the development of vascularized tissue models, it is now important to integrate such versatile hydrogel systems with recent advances in vascular biology and manufacturing techniques.

In the presented thesis, we engineer micro-capillary networks in poly (ethylene glycol) PEG-based hydrogels by the 3D co-culture of endothelial cells and mesenchymal stem/progenitor cells (MSCs). In this setup, endothelial cells self-assemble into lumenized micro-capillaries surrounded by cell-derived ECM and stabilized by MSCs that serve as support cells. While myriads of studies have investigated the endothelial component of micro-capillaries, we bring the anonymous support cells into the limelight and ask what fate decision MSCs undergo in the perivascular microenvironment. This question is of general biological interest because in vivo MSCs likely reside in the perivascular microenvironment of blood vessel capillaries. Transcriptome analysis of human bone marrow MSCs, when isolated from engineered micro-capillaries, revealed a prominent switch in ECM production of vascular basement membrane components and perivascular differentiation including Notch signaling. By making use of the modular and flexible design of PEG-hydrogels we functionalized them with the Notch-activating ligand Jagged1 and could recapitulate the ECM phenotypic switch of MSCs in the absence of endothelial cells. In doing so we show that the ECM switch is a novel attribute of perivascular MSCs and that vascular ECM components in MSCs are likely controlled by cell-cell communication via the Notch pathway.

MSCs are not just vascular supporters but also progenitor cells of mesenchymal tissues. Therefore, in an effort to establish vascularized bone mimicking tissue we took advantage of the full potential of MSCs by simultaneously using them as pro-vascular and tissue progenitor cells. While bone marrow MSCs together with endothelial cells assembled into micro-capillary structures in 3D co-cultures, we used growth factors to direct the fate of MSCs towards osteogenic cells. In this study, bone morphogenetic protein-2 (BMP-2) or fibroblast growth factor-2 (FGF-2) promotes

the formation of vascular networks. However, while osteogenic differentiation is achieved with BMP-2, treatment with FGF-2 suppressed osteogenic differentiation. Thus, our study shows that co-cultures of MSCs and endothelial cells in PEG-hydrogels can be directed towards bone-like and bone marrow-like 3D tissue constructs.

Taken together, this thesis provides micro-capillary networks as building block for the generation of vascularized tissue models in synthetic hydrogels. Two proof of concept studies show that engineered micro-capillary networks can be used 1) as valuable models in 3D vascular cell biology and 2) in a tissue engineering approach towards the generation of vascularized tissue mimics.

Zusammenfassung

Krankheiten, welche das vaskuläre System betreffen, gehören zu den häufigsten Todesursachen. Vaskuläre Erkrankungen umfassen z.B. eine zu starke Blutgefässbildung bei Tumoren, Durchblutungsschwierigkeiten bei Diabetes oder das Fehlen von Blutgefässen bei nekrotischen Geweben. Die Grundlagenforschung hat in der Vergangenheit Erfolg versprechende Blutgefäss-fördernde und -inhibierende Strategien entwickelt. Jedoch konnten Resultate der Grundlagenforschung nur selten in klinischen Studien bestätigt werden. Eine Ursache für diese Diskrepanz liegt im Unterschied zwischen den in der Grundlagenforschung angewandten Tiermodellen und der menschlichen Biologie begründet. Des Weiteren gestaltet es sich als schwierig, vaskuläre Therapiestrategien in Tiermodellen sowie in Patienten auf zellulärer Ebene zu untersuchen. 3-dimensionale (3D) Gewebsmodelle haben das Potential, diesen Schwierigkeiten entgegenzuwirken, indem sie unter kontrollierten und der menschlichen Physiologie ähnlichen Bedingungen die Studie der Blutgefässbiologie ermöglichen. Das Züchten von vaskularisierten Gewebsmodellen benötigt angemessene Gerüstmaterialien, welche 3D Konditionen erlauben, zell-spezifische Funktionen unterstützen und kompatibel mit modernen 3D Produktionsverfahren sind. Darüber hinaus sollten solche Materialien bezüglich ihrer Bestandteile und Eigenschaften exakt definiert sein, um reproduzierbare und kontrollierte Zellumgebungen zu ermöglichen. Zusätzlich ist es für die Adressierung von zellbiologischen Fragestellungen von Vorteil, wenn diese Materialien flexibel sind und zell-spezifischen Anforderungen angepasst werden können. In den letzten Jahren wurden Hydrogele aus synthetischen Materialien entwickelt, welche die extrazelluläre Matrix (EZM) nachahmen und die genannten Bedingungen erfüllen. Um vaskularisierte Gewebsmodelle zu etablieren ist es nun wichtig, synthetische Hydrogelsysteme mit Fortschritten in der Blutgefässbiologie und modernen Produktionsverfahren zu verknüpfen.

In der vorliegenden Arbeit wird die Entwicklung von künstlichen, kleinen Blutgefässen (Mikrokapillaren) durch die Ko-Kultur von Endothelzellen und Mesenchymalen Stammzellen (MSC) in Polyethylenglykol (PEG)-Hydrogelen gezeigt. In diesem 3D in vitro System fusionieren Endothelzellen zu Mikrokapillaren, welche Lumen aufweisen, von zell-eigener EZM umgeben sind und von MSC stabilisiert und unterstützt werden. Während vorherige Studien die Endothelzellen der Mikrokapillaren untersucht haben, werden in dieser Arbeit die Helferzellen in den Mittelpunkt gerückt. Dazu wird die Frage, welchen Phänotyp MSC in der künstlichen, perivaskulären Umgebung annehmen, adressiert. Diese Frage ist von breiterem zellbiologischen Interesse, weil MSC in vivo wahrscheinlich in der perivaskulären Umgebung von kleinen Blutgefässen angesiedelt sind. Genexpressions-Analysen von humanen Knochenmark-MSC, welche von den künstlichen Mikrokapillaren zurückgewonnen wurden, weisen eine deutliche Veränderung von Komponenten der vaskulären EZM und von Indikatoren für eine perivaskuläre Differenzierung inklusive des Notch-Signalweges auf. Durch die Design-Flexibilität des verwendeten PEG-Hydrogels konnte der Notch-Signalweg-Aktivator Jagged1 in das Hydrogel eingebaut werden und dadurch die Veränderung der vaskulären EZM Komponenten in MSC in Abwesenheit von Endothelzellen induziert werden. Dadurch konnte gezeigt werden, dass die Veränderung der EZM ein neues Attribut von perivaskulären MSC ist und, dass die vaskuläre EZM in MSC wahrscheinlich mittels

Zell-Zell-Kommunikation durch den Notch-Signalweg kontrolliert wird.

Abgesehen von ihrer Helferfunktion für Endothelzellen besitzen MSC mesenchymale Stammzelleigenschaften. In der vorliegenden Arbeit wurden diese beiden Eigenschaften von MSC in einem vaskularisierten Gewebsmodell mit osteogenen Knocheneigenschaften kombiniert. Dazu wurden MSC/Endothelzell-Kulturen und die beiden Wachstumsfaktoren Knochen-induzierendes Protein 2 (bone morphogenetic protein-2: BMP-2) und Fibroblasten Wachstumsfaktor 2 (fibroblast growth factor-2: FGF-2) benutzt. Beide Wachstumsfaktoren unterstützen die Formierung von Endothelzellen zu Mikrokapillaren. Während BMP-2 jedoch die osteogene Differenzierung von MSC hervorruft, unterdrückt FGF-2 diesen Effekt. Dieses Resultat zeigt, dass MSC/Endothelzell-Kulturen in PEG-Hydrogelen benutzt werden können, um einfache, vaskularisierte 3D Gewebsmodelle von Knochen und Knochenmark zu generieren.

Zusammengefasst zeigt die vorliegende Arbeit, dass künstliche Blutgefässnetzwerke in synthetischen Hydrogelen etabliert werden können. Diese mikrokapillaren Netzwerke können als Bausteine für vaskularisierte Gewebsmodelle benutzt werden, wie in zwei Beispielstudien demonstriert wird. Es wird gezeigt, dass die mikrokapillaren Netzwerke A) als 3D Modell für grundlegende Blutgefässbiologie und B) als Teil von vaskularisierten Knochenmodellen fungieren können.

Abbreviations and acronyms

2D / 3D / 4D = two / three / four dimensional

ACTA2 = alpha-actin 2; gene

ALP = alkaline phosphatase

ALPL = alkaline phosphatase liver / bone / kidney; gene

ANG-1 / ANG-2 = angiopoietin 1 / 2

ANOVA = analysis of variance

ASC = adipose-derived stromal cells

BGLAP = bone gamma-carboxyglutamic acid-containing protein; gene

BMP-2 / BMP-4 = bone morphogenetic protein 2 / 4

BSA = bovine serum albumin

CD = cluster of differentiation

CDH2 = cadherin-2; gene

Col = collagen; protein

COL = collagen; gene

Ct-value = cycle threshold value

DEG = differentially expressed gene

DLL-4 = delta-like ligand 4

EC = endothelial cell

ECFC = endothelial colony-forming cells

ECM = extracellular matrix

EDTA = ethylenediaminetetraacetic acid

EEF1A1 = eukaryotic translation elongation factor 1 alpha 1; gene

EGF = epidermal growth factor

FACS = fluorescence-activated cell sorting

FBS = fetal bovine serum

FDR = false discovery rate

FGF-2 = fibroblast growth factor 2

FN = fibronectin

FXIII = blood coagulation factor XIII

GAG = glycosaminoglycan

GAPDH = glyceraldehyde-3-phosphate dehydrogenase; gene

GelMA = gelatin methacrylate

GF = growth factor

Gln = glutamine

GO = gene ontology

GUCY = guanylate cyclase; gene

HA = hyaluronic acid

HEPES = hydroxyethyl piperazineethanesulfonic acid

HEY 1 / HEY 2 = hairy/enhancer-of-split related with YRPW motif 1 / 2; genes

HEYL = hairy/enhancer-of-split related with YRPW motif; gene

HRP = horseradish peroxidase

HSPG-2 = heparin-sulfate-proteoglycan-2

HUVEC = human umbilical vein endothelial cells

ICC = immunocytochemistry

IgG = immunoglobulin G

ITGB3 = integrin beta 3; gene

JAG1 = jagged1; gene

KCN8J = potassium voltage-gated channel subfamily J member 8; gene

LAMA / LAMB / LAMC = laminin alpha / beta / gamma; genes

Lys = lysine

MMP = matrix metalloproteinase

MSC = mesenchymal stem cell

MYOCD = myocardin; gene

NID = nidogen; gene

NRARP = NOTCH regulated ankyrin repeat protein; gene

NTN = netrin 4; gene

OEC = outgrowth endothelial cell

PBS = phosphate-buffered saline

PDGF-BB = platelet derived growth factor BB

PDGFRB = platelet derived growth factor receptor beta; gene

PE = phycoerythrin

PEG = poly(ethylene glycol)

PFA = paraformaldehyde

qRT-PCR = quantitative real-time polymerase chain reaction

RGD = cell adhesion peptide: arginine–glycine–aspartic acid

RGS5 = regulator of G-protein signaling 5; gene

RT = room temperature

RUNX-2 = runt-related transcription factor 2; gene

SD = standard deviation

SDC2 = syndecan 2; gene

SDF-1α = stromal cell-derived factor 1α

siRNA = small interfering RNA

SPARC = secreted protein acidic and rich in cysteine; gene

SSP1 = secreted phosphoprotein1; gene

TCP = tissue culture plastic

TEM = transmission electron microscopy

TG = transglutaminase

TGF-β = transforming growth factor β

TIMP = tissue inhibitors of metalloproteinase

VEGF-A = vascular endothelial growth factor A

VEGFR = vascular endothelial growth factor receptor

VMT = vascularized microtumors

VSMC = vascular smooth muscle cell

WB = western blot

YWHAZ = tyrosine 3-monooxygenase/tryptophan 5-monooxygenase activation protein zeta; gene

Contents

Main concept

Motivation

Diseases related to vascular malfunction, hyper-vascularization, or lack of vascularization are among the leading causes of morbidity and mortality. On the one hand, patients suffer from insufficient vascular perfusion of the heart, the brain or even peripheral tissues. On the other hand, excessive vascular growth contributes to the pathogenesis of cancer, psoriasis or diabetic retinopathy. Despite the fact that treatments towards insufficient perfusion by growth factor-mediated induction of neovascularization have delivered promising results in basic research, clinical trials have not met expectations. Additionally, therapeutic approaches towards the reduction and normalization of vascularization for most cancers have only resulted in minimal extension of progression free survival. Obviously, there is a great need for relevant in vitro models to investigate treatment approaches and novel therapeutics towards the re-establishment, normalization, or reduction of vessels under near-physiological conditions. Furthermore, also basic research in blood vessel biology will benefit from vascularized tissue models. The engineering of vascularized tissue constructs for both in vivo transplantation as well as in vitro modeling requires appropriate scaffold materials. Such materials must support cell-specific functions and be compatible with innovative (micro)-manufacturing techniques. Extracellular matrix (ECM)-inspired hydrogels fulfill these requirements and are extremely versatile materials**.** Today, engineers and biologists can draw on several natural or synthetic ECM-mimicking hydrogel systems to vascularize tissues and establish models of vascular diseases in vitro. In the future, engineered vascularized tissues will build an important basis to study basic questions of vascular biology, to develop perusable tissues for transplantation, and to test novel therapeutics under controlled near-physiological conditions. In this regard, it is of fundamental importance for the success of vascular engineering to continuously integrate advances in vascular biology with hydrogel innovations. Synthetic hydrogel materials are flexible in design, biologically inert and chemically defined, which facilitates matrix engineering and biological modifications. Furthermore, since they are produced from scratch, synthetic hydrogels are free of animal products and biological confounding signals, which are important features for the reproducibility and medical relevance of tissue models. Therefore, the presented thesis aims to establish 3D micro-capillary networks within synthetic ECM-mimicking poly(ethylene glycol) (PEG) hydrogels as basic modules for vascularized tissue models.

Objectives

To establish micro-capillary networks in synthetic PEG hydrogels, we co-culture endothelial cells with mesenchymal stem/progenitor cells (MSCs). Endothelial cells represent the building block of every vascular engineering approach since they form the inner cell layer of all blood vessels. MSCs

were used in the first place as mesenchymal support cells since they have previously displayed pro-vascular properties, in vitro. However, the most prominent characteristic of MSCs is certainly not their pro-vascular, but rather their stem cell properties. Due to this tissue progenitor capacity, MSCs have become a major tool in regenerative medicine and tissue engineering approaches that aim to replace, treat or model mesenchymal tissues. It is interesting to note that in vivo mesenchymal tissue progenitor cells reside in close proximity to blood vessels (in the perivascular space). This perivascular localization in vivo together with the pro-vascular properties of MSCs in vitro have led to the constantly debated hypothesis that MSCs and perivascular (mural) cells are closely related or even equivalent cell types. Regardless of the actual degree of relationship, the given similarity of MSCs and perivascular cells is a lucky find for the engineering of vascularized tissues. In the presented thesis, the following objectives towards the establishment of vascularized in vitro tissue models are addressed:

Objective 1: Micro-capillary network engineering. The gold standard materials to engineer 3D micro-capillary networks are natural ECM hydrogels composed of fibrin or collagen type I. The first goal of this thesis is to engineer micro-capillary networks in fully synthetic, ECM-free PEG hydrogels.

Objective 2: Vascular biology. MSCs have pro-vascular properties and support the capillary morphogenesis by endothelial cells. The second goal of this thesis is to investigate how MSCs are regulated by endothelial cells, and what the fate of MSCs in the perivascular microenvironment is.

Objective 3: Tissue model. MSCs have pro-vascular and tissue progenitor properties. Therefore, we hypothesize that both MSC properties can be combined in 3D PEG hydrogels to build vascularized bone-mimicking tissues.

Thesis outline

The presented thesis consists of four chapters. In **Chapter 1,** we discuss the history, development and application of hydrogels in vascular engineering. We start by looking at the molecular and cellular aspects of neovascularization since these aspects are key to understanding the requirements concerning vascular engineering. Based on this, we will examine how different hydrogel materials and designs have fulfilled the requirements and have been successfully engineered for blood vessel growth. Starting with the hydrated protein meshwork fibrin, which is the naturally occurring scaffold for neovascularization during wound healing, we review hydrogel materials from natural ECM via semi-synthetic to synthetic components. We finish **Chapter 1** by considering the current limitations of hydrogel usage for vascular engineering and by giving a brief summary of novel trends in the context of vascularized tissue models. The content of **Chapter 1** is adapted from an accepted review article. As briefly discussed, engineering micro-capillary networks in hydrogels requires not only endothelial cells, but also mesenchymal support cells. In **Chapter 2,** we establish micro-capillaries in synthetic PEG hydrogels. In these assays, MSCs act as perivascular-like cells and support endothelial capillary morphogenesis. Here, we bring MSCs, which in vascular engineering are usually applied as supporters, into the limelight and ask what

adaptations they undergo in the perivascular environment of engineered endothelial capillaries. **Chapter 2** also partially addresses the question of the modification of ECM-free synthetic PEG hydrogels by cell-deposited ECM, which is an understudied topic in the field of synthetic materials research. The content of **Chapter 2** is taken from a manuscript that is prepared for submission as a full article. **Chapter 3** is motivated by the idea of combining the pro-vascular and the tissue progenitor properties of MSCs towards a micro-vascularized bone-mimicking model. Similar to Chapter 2, micro-capillaries were generated in PEG hydrogels by co-culturing endothelial cells with MSCs. At the same time, MSCs in 3D co-cultures were also differentiated into osteoblasts by the bone morphogenetic protein-2 (BMP-2) or prevented from differentiation by the fibroblast growth factor 2 (FGF-2). The content of **Chapter 3** is taken from a manuscript that is published as a full article. **Chapter 4** will conclude this thesis and try to develop a vision as to how this project or the findings thereof could be used in future work. To do so, we will summarize what we have learned in this project and evaluate the potential of the findings. In this context, the general limitations of the setup in addition to limitations of the thesis design will be discussed.

Chapter I:

Inspired by nature: hydrogels as versatile tools for vascular engineering

The content of this chapter is accepted for publication as comprehensive review article: U. Blache and M. Ehrbar (2018): Inspired by nature: hydrogels as versatile tools for vascular engineering; *Advances in Wound Care*

Abstract

Diseases related to vascular malfunctions are among the leading causes of morbidity and mortality in the industrialized world. While patients suffer from insufficient vascular perfusion of the heart, the brain, or even peripheral tissues, excessive vascular growth contributes to the pathogenesis of cancer, psoriasis, or diabetic retinopathy. Even though treatments towards insufficient perfusion by growth factor-mediated induction of angiogenesis have delivered promising results in basic research, clinical trials have not met expectations. Additionally, anti-angiogenic approaches towards the reduction of vascularization in most cancers have only resulted in the minimal extension of progression free survival. Obviously, relevant in vitro models to study blood vessel biology and treatment approaches under near-physiological conditions are needed. The engineering of vascularized tissue constructs for in vivo transplantation as well as for modeling diseases in vitro requires appropriate scaffold materials that support cell-specific functions and are compatible with innovative (micro)-manufacturing techniques. Extracellular matrix (ECM)-inspired hydrogels fulfill these requirements and are extremely versatile scaffold materials for vascular engineering**.** Importantly, essential to the success of vascular engineering is the continuous integration of hydrogel innovations with advances in vascular biology and manufacturing techniques. In this review, we discuss hydrogels in vascular engineering, including their in vivo application. We specifically focus on the advancements related to materials research and on the development of vascularized three-dimensional (3D) tissue models.

Neovascularization

Mechanisms of blood vessel development, maturation, and remodeling

The cardiovascular system supplies almost all tissues with gas, nutrients, signaling molecules, and cells. Neovascularization, the formation of new blood vessels, is a fundamental part of tissue formation and repair involving two distinct morphogenetic processes: vasculogenesis and angiogenesis (**Fig. 1A**). Vasculogenesis denotes the de novo formation of blood vessels from mesodermal-derived precursor cells called angioblasts. The differentiation of angioblasts into endothelial cells and their subsequent assembly into a new primitive blood vessel network mainly occurs during embryonic development. Initially described to take place in the yolk sac of the developing mouse embryo, it became clear that blood vessel initiation by vasculogenesis independently occurs at both intra-embryonic and extra-embryonic sites of the embryo[1]. Interestingly, circulatory endothelial progenitor cells have been shown to enable vasculogenesis in the adult organism where they could play a significant role in tissue repair and regeneration[2-4]. Although relatively limited information on the molecular mechanism of vasculogenesis is available, genetic ablation studies showed that fibroblast growth factor (FGF)-2, bone morphogenetic protein (BMP)-4, and vascular endothelial growth factor (VEGF) are centrally involved in the process of vasculogenesis[5]. In contrast, angiogenesis is the formation of new blood vessels from preexisting ones and occurs throughout the whole lifespan. Sprouting angiogenesis describes the branching of endothelial cells from existing blood vessels due to the local environment's provision of angiogenic signals[6-8]. Intussusceptive angiogenesis occurs from the formation of pillars in the inside of preexisting capillaries resulting in their longitudinal division "within itself"[9]. However, molecular mechanisms leading to intussusceptive angiogenesis remain largely obscure.

Under homeostatic conditions small-caliber blood vessels are composed of an endothelial cell tube and perivascular cells. In this constellation, endothelial cells are quiescent and form stable interactions with each other and with a specialized ECM layer, the basement membrane[10]. Upon metabolic demand or hypoxic conditions pro-angiogenic molecules, such as VEGF, FGF, platelet derived growth factor (PDGF)-BB, stromal cell-derived factor (SDF)-1α and Angiopoietin (ANG)-2 become available in the local environment and cause the proteolytic remodeling of the vessel basement membrane, the destabilization of endothelial cell-cell contacts, and the extravasation of blood plasma proteins that contribute to the formation of a provisional ECM[11-13]. Interestingly, inflammatory cells upon injury establish quite similar angiogenic growth factor milieus. Subsequently, some endothelial cells via VEGF receptor (VEGFR)-2 and VEGFR-3 mediated signaling acquire a tip cells phenotype, become motile, and form filopodia[14, 15]. Tip cells upregulate the delta-like ligand (DLL)-4 that binds to the Notch receptor of neighboring endothelial cells where it suppresses the expression of VEGFR-2 and VEGFR-3 and promotes the expression of VEGFR-1[15]. As a consequence of the changed VEGFR expression, these cells become less responsive to VEGF-signals and exhibit a stalk cell phenotype showing stronger proliferation and the initiation of lumen formation. To form new vascular networks two tip cells undergo anastomosis, which is initiated by filopodia contacts and results in the fusion of different endothelial sprouts.

Primitive endothelial tube maturation into mature vessels is initiated by the recruitment of perivascular cells that ultimately enwrap the endothelial tubes. Perivascular cells are of mesenchymal origin and classified as pericytes or vascular smooth muscle cells depending on their localization to small or large vessels, respectively[16, 17]. Among the factors known to play an important role in the recruitment, proliferation, and differentiation of perivascular cells are PDGF-BB, ANG-1, and transforming growth factor (TGF)-β. Due to their stabilizing and regulating role, perivascular cells are generally considered as vascular support cells. Additionally, debate continues over whether perivascular cells are mesenchymal tissue progenitor cells since these cells also reside in the perivascular microenvironment of blood vessels[18-24].

Angiogenesis is a partially overshooting process and endothelial cells become calmed by perivascular cells once in contact. However, overproduced or redundant vessels need to be pruned. The main cause of vessel regression is interrupted blood flow[25-27]. Mechanistically, upon lumen collapse vessel regression is achieved by increased apoptosis or migration of endothelial cells[27-30]. However, and conversely, the lumen collapse during vessels regression has also been shown to be the consequence of endothelial cell apoptosis[31]. Furthermore, the finding that perivascular cells are actively involved in vessel pruning supports the idea that vessel regression is not a passive process[32]. Remarkably, vessel formation and vessel pruning can occur simultaneously within the same vascular network[33].

Extracellular matrix as template for neovascularization during tissue repair

Neovascularization is crucial to tissue development and homeostasis. Hence, neovascularization is also key to wound healing and tissue repair. The pivotal step of blood vessel establishment during wound healing is the recruitment of participating cells into the defective tissue. This cell recruitment requires a supportive matrix, which is established during the initial steps of wound healing by the release of fibrinogen, plasma fibronectin, and platelets from leaky blood vessels. The resulting fibronectin and platelet enriched fibrin clot acts as a temporary matrix for early healing promoting factors and supports the infiltration of cells[34]. Subsequently, mobilized neutrophils and macrophages release growth factors into the matrix. Importantly, several angiogenic growth factors, such as VEGF-A, FGF-2, and PDGF-BB can bind to fibrin and fibronectin and thereby render the wound matrix a growth factor presentation platform[35-39]. This angio-competent milieu attracts endothelial, perivascular, and stromal cells that, by secretion of cellular fibronectin and fibrillar collagen, remodel the initial fibrin clot into a provisional matrix. During tube formation, endothelial and perivascular cell types start to lay ECM components around the blood vessels and thereby establish the basement membrane of mature blood vessels. The main components of the basement membrane are collagen type IV, laminins, nidogens, fibronectin, and perlecan. However, many more ECM components, such as collagen type XV and XVIII and glycosaminoglycans contribute to the basement membrane[40, 41].

Besides providing structural and physical support to cells, the vascular ECM acts as a pro-angiogenic signal transducer. The ECM composition itself exerts an instructive role for vascular development covering, e.g., early endothelial lumen formation, endothelial quiescence, and

mature vessel stabilization[10, 40, 42, 43]. On the other hand, the anti-angiogenic effects of collagen IV, XV, and XVIII cleavage products actively regulate blood vessel formation and stability[40, 44]. Since neovascularization is strongly associated with the dynamic remodeling of the ECM, enzymes that disintegrate ECM components are key regulators of neovascularization. Plasmin and the members of the large matrix metalloproteinase (MMP) family are proteases able to cleave ECM proteins. This proteolytic ECM breakdown enables three fundamental processes: 1) disintegration of the basement membrane and cell-cell junctions resulting in breakout of endothelial and perivascular cells, 2) liberation of angiogenic growth factors from their ECM storage, and 3) turnover and maturation of the ECM during vessel formation and maturation. But, to achieve a strictly controlled degradability-stability equilibrium, the proteolytic activity of both plasmin and MMPs is controlled by direct counterparts, such as alpha 2-antiplasmin and tissue inhibitors of metalloproteinases (TIMP).

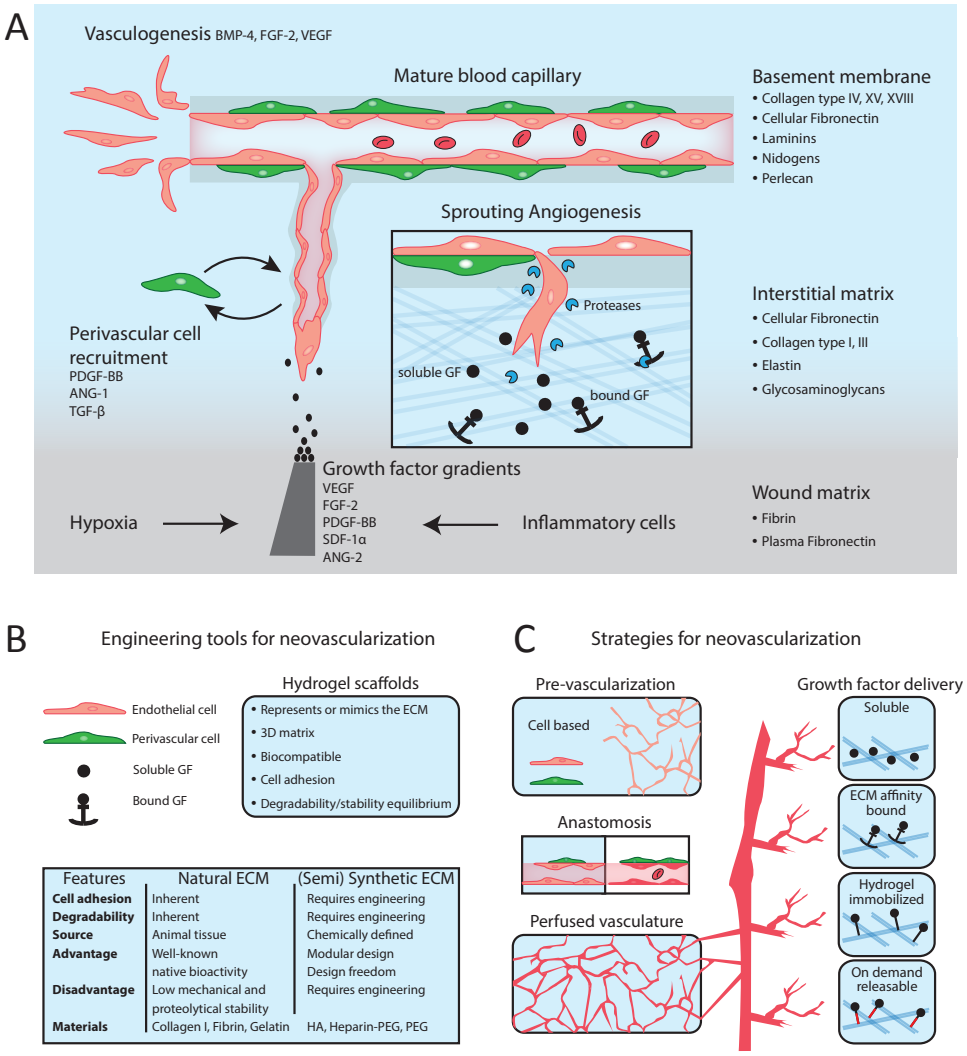

Figure 1: Engineering neovascularization in hydrogels inspired by the template function of the extracellular matrix (ECM) during blood vessel development and maturation. A) The establishment of new blood capillaries occurs through vasculogenesis and angiogenesis in an angio-competent milieu generated by growth factors and the ECM. B) Tools for vascular engineering derived from the natural processes of blood vessel development include vascular cells, growth factors, and ECM-inspired hydrogel scaffolds. Hydrogels can be engineered from natural ECM components or synthetic ECM analogues. C) Hydrogel-based strategies to generate new functional vascular networks in vivo. Pre-vascularization follows the concept of engineering vascular networks within hydrogels in vitro by the application of endothelial cells that self-assemble into micro-capillary networks. Upon transplantation, pre-vascularized hydrogel constructs can anastomose to the host vasculature and become perfused. In an alternative strategy, the delivery of soluble, matrix bound, or on demand releasable angiogenic growth factors can promote the formation of new vessels in situ.

Hydrogels for vascular engineering

Vascular-deficient tissues can be treated by either the delivery of angiogenic growth factors or the transplantation of pre-vascularized tissues. While the delivery of growth factors builds on the individual´s endogenous vascularization potential, the transplantation of pre-vascularized tissues is applicable even if the wound-healing cascade is strongly impaired. Looking at the natural processes of blood vessel development and regeneration, vascular engineering minimally requires angiogenic growth factors or vascular cells in combination with adequate 3D scaffolds (**Fig. 1B**). Although completely scaffold-free strategies exist (e.g., spheroid or cell sheet technology[45-47]), most vascular engineering strategies require appropriate scaffolds that enable the transport of growth factors or cells and provide a 3D matrix for blood vessel (in)growth and formation (**Fig. 1C**).

Hydrogel materials have become valuable 3D scaffolds for vascular engineering since they share many features with the natural ECM, including high water content and viscoelastic properties. Naturally occurring or synthetic polymers that are hydrophilic and form interconnected networks by physical interactions or chemical bonds can form hydrogels. By controlling the chemical properties of the polymer, its initial concentration and the distance between molecular interactions in the network, hydrogel parameters, such as stiffness, swelling, and pore size can be readily adapted[48, 49]. To date, a variety of biocompatible, natural, or synthetic ECM-mimicking hydrogels are commercially available for a broad spectrum of users (see Caliari and Burdick[50]). Many of these hydrogel systems can be used to engineer pre-vascularized tissue constructs in vitro prior to in vivo implantation by drawing the evolutionary memory of endothelial cells to assemble into micro-capillary networks when co-cultured with perivascular or other mesenchymal cells.

Natural ECM hydrogels and modified ECM protein-based (semi-synthetic) hydrogels

The main class of hydrogel materials directly derived from natural ECM is protein polymers. Protein polymers' great advantage is their intrinsic bioactivity, which includes the provision of cell adhesion and proteolytic degradable sites. Moreover, the application of ECM protein polymers has a long tradition in vascular biology and existing knowledge of this materials class is profound. Pioneering work in the 1980s from Nicosia et al. and Montesano et al. showed that fibrin and collagen type I hydrogels can host micro-capillary-like structures ex vivo[51-55]. Based on this early work, ECM protein-based hydrogels have become the most widely used scaffold materials for vascular engineering.

The first matrix vascular cells encounter during vascularization in vivo is fibrin. Fibrin hydrogels result from the enzymatic activation of fibrinogen by thrombin, followed by terminal factor XIIIa-mediated, enzymatic cross-linking. In vitro, fibrin hydrogels are suitable templates for endothelial and mesenchymal cells, which under appropriate co-culture conditions readily form micro-capillaries. Studies from different labs have proven that such in vitro established pre-vascularized fibrin constructs connect (inosculate) to the host vasculature when transplanted into mice[56-60]. Importantly, one study provided experimental evidence for the general assumption that an in

vitro pre-vascularization step is indeed beneficial over only cell delivery (**Fig. 2**)[56]. Collagen type I is part of the interstitial ECM and has the intrinsic capacity to self-assemble into hydrogels under physiological conditions. In a seminal series of in vitro studies, Davis and co-workers have shown that collagen hydrogels allow for the formation of 3D micro-capillary networks by endothelial and perivascular cells[61-65]. Other studies showed that capillaries engineered within collagen hydrogels successfully inosculate after in vivo implantation[66-70]. However, native collagen hydrogels might miss the optimal degradability-stability equilibrium since the low collagen concentrations suitable for 3D culture of micro-capillary networks result in mechanically weak scaffolds. To overcome this dilemma, collagen hydrogels have been modified by plastic compression[71-73] or by chemical modifications as discussed below.

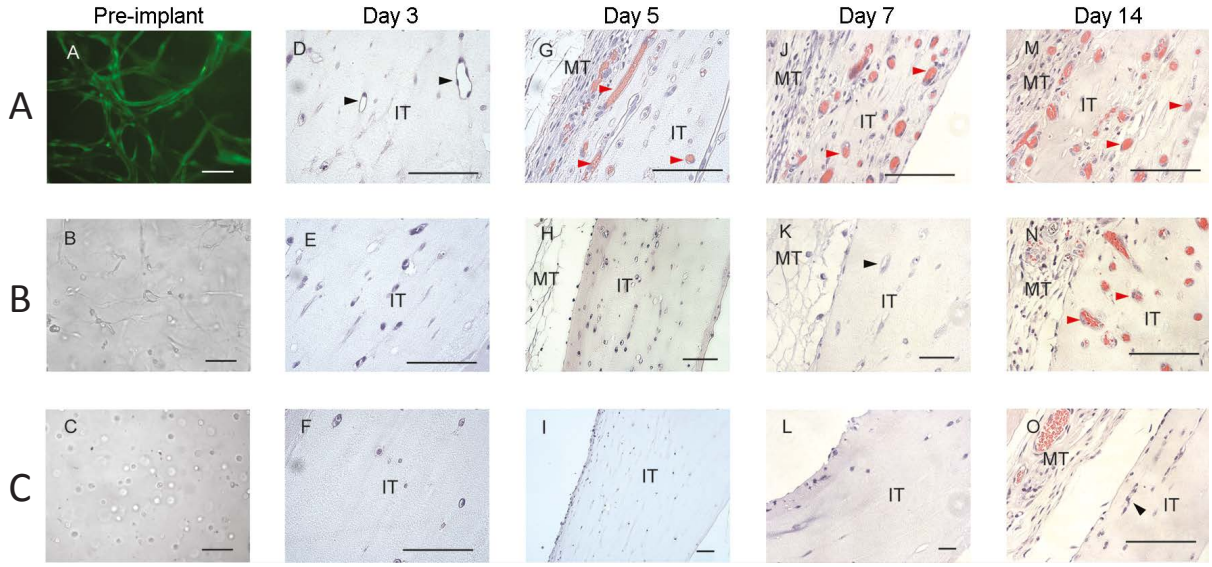

Figure 2: Pre-vascularization of fibrin hydrogels leads to the rapid anastomosis of engineered micro-capillaries with the host vasculature. A, B) Micro-capillaries were engineered in vitro by the co-culture of human fibroblasts with human umbilical vein endothelial cells (HUVEC) in fibrin hydrogels. Pre-vascularized tissue (A, 7 days in vitro pre-culture) was perfused by host blood cells more rapidly than non-pre-vascularized tissue (B, 1 day in vitro pre-culture) upon implantation. C) HUVEC-cultures in the absence of supporting fibroblasts do not form perfusable structures. Histological tissue sections from 3–14 days post-implantation, with red blood cells being evident in the pre-vascularized tissue starting at day 5 post-implantation. MT, mouse tissue; IT, implant tissue. Scale bars: 100 µm. Adapted figure reproduced from Chen et al.[56] with permission from *Mary Ann Liebert, Inc*.

To combine their cell-instructive and biocompatible features with desired mechanical properties, natural ECM components can be tuned by chemical modifications. The resulting semi-synthetic biomaterials are beneficial, especially when using highly proteolytic cells as is the case in vascular engineering. In this regard, a photo-cross-linkable collagen-poly(ethylene glycol) (PEG) hybrid material, in which the mechanical properties could be increased independently of the material density, has been developed[74]. Within this collagen-PEG hydrogel micro-capillary networks can be generated. Another promising and widely used ECM-based material is gelatin, which is derived from collagens by hydrolytic breakage. Like its mother material, gelatin can form physical hydrogels of quite weak mechanical properties. Unfortunately, gelatin hydrogels are just stable below 37 °C, which makes them inappropriate as independent scaffolds. However, methacrylic anhydride modification renders gelatin into photo-cross-linkable gelatin methacrylate (GelMA) hydrogels of excellent tissue engineering properties[75-77]. Using GelMA as vascularization scaffold, micro-capillary networks that anastomose with a murine host can be achieved either through

in vitro pre-vascularization or subcutaneous injection of polymerizing hydrogel precursors and vascular cells[78, 79]. These studies clearly demonstrate the benefits of chemically modified ECM polymers because the bioactivity of gelatin allowed for micro-capillary network formation and the photo-cross-link mechanism for stable material properties.

Modified GAG-based (semi-synthetic) hydrogels and PEG-based (synthetic) hydrogels

While natural and chemically modified ECM protein-based hydrogels are excellent substrates for the culture of vascularized tissues, they exhibit inherent materials properties. To gain further control over materials properties, carbohydrate-based materials, such as glycosaminoglycans (GAG) serve as the basis for hydrogel engineering. Upon modification with cross-linkable chemical groups, GAG hydrogels can be produced with defined physical properties. Although GAGs as components of the natural ECM are known to be degraded by enzymes, to bind growth factors and to interact with cell-surface receptors, their modification with additional biologically functional modules, such as small peptides or protein domains is key for vascular engineering. As we can learn from hyaluronic acid (HA), two biological features from the natural ECM are required to turn these semi-synthetic scaffolds into cell-friendly hydrogels for neovascularization: sites for integrin-dependent cell adhesion and sites for proteolytic remodeling. Indeed, acrylated HA when modified with the cell-adhesion peptide arginine–glycine–aspartic acid (RGD) and polymerized by a thiol-cross-linker containing MMP-sensitive peptides results in a bioactive hydrogel, which allows cell adhesion and proteolytic remodeling[80]. These HA hydrogel modifications are sufficient to enable in vitro formation of micro-capillary networks that upon in vivo transplantation anastomose with the host vasculature[81-84]. Not surprisingly, hybrid hydrogels built by the cross-linking of the GAG heparin and poly(ethylene glycol) (PEG) can host micro-capillary networks when biologically modified by RGD and MMP-sensitivity[85, 86]. However, in contrast to HA hydrogels, heparin-based hydrogels through the high abundance of sulfate groups and the resulting negative charge enables the affinity binding of various growth factors.

We have seen that hydrogels derived from naturally occurring ECM components are suitable scaffolds for vascular engineering, and that they can be engineered within a certain range towards desired functions. Reverse engineered synthetic hydrogels aim to mimic the natural ECM but rely on fully controlled design and synthesis[87-90]. Since manufactured from scratch, synthetic hydrogel materials can be seen as blank slates free of animal products and confounding biological factors, per se. Conceivably, in these initially cell-inert synthetic materials biological modifications are essential to render them cell-friendly and biologically functional. Interestingly, it seems that the minimalistic approach of facilitating cell adhesion by RGD and matrix remodeling by MMP-sensitive peptides is generally sufficient for micro-capillary network formation in synthetic hydrogels. Although these materials are still less used than natural ECM hydrogels, some work proving the potential of synthetic hydrogels for vascular engineering has been reported within the last decade. Hydrogels exclusively composed of PEG allow neovascularization in vitro and in vivo when RGD sites and MMP-sensitivity optimized the material. In this regard, several studies showed that co-culturing of endothelial and mesenchymal cells in PEG hydrogels is a promising approach for the formation of 3D pre-vascularized scaffolds with fully defined properties[91-94].

Controlled delivery of vascular endothelial growth factor by hydrogel immobilization

In vitro engineered vascular networks hold great promise to become transplantable functional tissue units. However, their production relies on the expansion of autologous cells under complex production environments and is labor- and cost-intensive. By contrast, the concept of therapeutic angiogenesis builds on the idea that upon proper stimulation with key pro-angiogenic factors, the body´s innate angiogenic program initiates the formation of new vessels. Early therapeutic angiogenesis attempts, conducted by the infusion of plasmid DNA encoding the expression VEGF or recombinant VEGF proteins into various tissue sites as well as into blood vessels, showed promising results in preclinical studies that could not be reproduced in clinical trials[95]. To improve therapeutic angiogenesis by at least partially localized delivery, hydrogels with no or weak affinities for growth factors were employed for release by passive or slowed-down diffusion[96]. In recent years, multiple sophisticated strategies that enable the tailoring of growth factor release towards specific requirements have been developed (for a comprehensive review see Briquez et al.[97]). Here, we look at examples of VEGF delivery to demonstrate how hydrogel and growth factor engineering can boost the response of angiogenic growth factors.

An elegant strategy to functionalize fibrin hydrogels with growth factors has been developed by emulating the factor XIII (FXIII)-mediated cross-linking taking place in native fibrin. In detail, a short peptide sequence (NQEQVSPL) responsible for linking α2-plasmin inhibitor to fibrin allows the covalent XIIIa-mediated binding of growth factors to fibrin when fused to the N-terminus of growth factors or peptides[98, 99]. Resulting growth factor-modified fibrin hydrogels enable the release of their growth factor payload upon cell-mediated matrix degradation. Applying this engineering approach in vivo resulted in an improved angiogenic performance of fibrin-immobilized as compared to freely diffusible $VEGF_{121}$ (**Fig. 3A**)[100-102]. However, a considerable downside of fibrin hydrogels is their relatively fast degradation kinetics in vivo, resulting in the robust induction of new vessels that are not stabilized and regress due to the short duration of

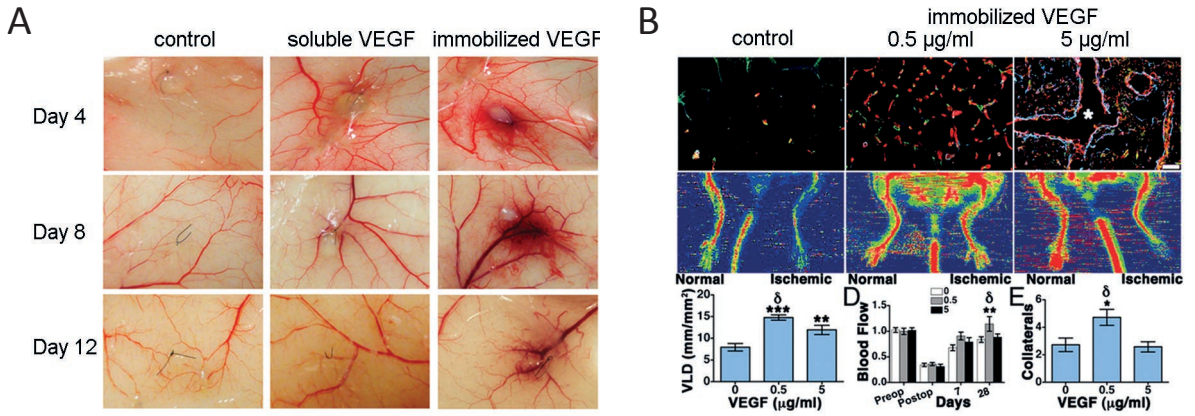

Figure 3: In situ neovascularization by engineered, hydrogel-immobilized VEGF delivery. A) Skin vascularization response to fibrin hydrogels containing no VEGF (control), soluble VEGF, or engineered, fibrin-immobilized VEGF. Although the immobilized VEGF outperforms soluble VEGF, the vascularization response decreases as the fibrin hydrogel becomes degraded over time. Reproduced from Largo et al.[102] with permission from the Royal Society of Chemistry. B) Improvement of fibrin-immobilized VEGF treatment by aprotinin engineered, long-lasting fibrin hydrogels. No VEGF (control) or engineered, fibrin-immobilized VEGF (0.5 µg/mL and 5 µg/mL) were compared in a hindlimb ischemia mouse model. Fibrin hydrogels used for the delivery were stabilized by fibrin-immobilization of the fibrinolysis inhibitor aprotinin. Tissues analyzed 4 weeks after hydrogel delivery for endothelial cells (CD31, in red), pericytes (NG2, in green), and smooth-muscle cells (α-SMA, in cyan, scale bar: 20 µm) or for microcirculation by Laser-Doppler-Imaging of non-ischemic and ischemic limbs (left and right legs, respectively). Figure reproduced from Sacchi et al.[105].

VEGF-treatment[102]. Although this material´s degradability-stability equilibrium related problem could be partially addressed by changing the fibrin amount, conceivably a higher material density is negatively correlated with vascular morphogenesis[103, 104]. Therefore, degradation-resistant and VEGF-releasing fibrin hydrogels were engineered by modifying fibrin with the covalently bound fibrinolysis inhibitor aprotinin and $VEGF_{164}$ at the same time (**Fig. 3B**). These long-lasting fibrin hydrogels enable a cell-demanded, continuous, and slow release of $VEGF_{164}$ and were shown to induce the formation of lasting blood vessels in skeletal muscles and to improve the perfusion of ischemic hind-limbs and skin flaps in mice[105].

Another way of controlling the stability of growth factor releasing hydrogels is to engineer them from the bottom-up using defined components. The degradability of synthetic PEG hydrogels, for instance, can be tailored by introducing peptide sequences with variable sensitivities for the proteolytic degradation by MMPs and Plasmin[106, 107]. For in situ vascularization, different VEGF-variants were immobilized to cell-free, MMP-sensitive PEG hydrogels and liberated by host cells[108, 109]. These studies showed that for synthetic hydrogels, bound VEGF outperformed soluble VEGF in inducing neovascularization in vivo in a qualitative as well as quantitative way.

Current efforts to immobilize growth factors to hydrogels are directed towards more flexible engineering strategies. On the one hand, the binding of various native growth factors could be achieved by modifying hydrogels, for example with fibronectin domains, fibrinogen derived peptides, or heparin[110-112]. On the other hand, growth factors were engineered with affinities such that they bind to hydrogels comprising ECM-components, streptavidin, or barnase[113-115].

Limitations of current hydrogel-based vascularization strategies

Despite tremendous progress in hydrogel-based vascularization strategies, major problems have emerged from the application of hydrogels as scaffolds for vascularized tissues. So far, except for skin, which is a relatively thin tissue, only small-size constructs have been successfully pre-vascularized and implanted in vivo, due mostly to limitations in fabrication techniques and the soft material properties of cell-friendly hydrogels. Nevertheless, soft hydrogels can be applied as a gelatinous cell carrier solution within porous and solid scaffolds. For instance, endothelial and perivascular cells can be suspended in fibrinogen or matrigel solutions and poured into macroporous sponges prior to gel polymerization. Applying this technique in poly(lactic-co-glycolic acid)/poly(L-lactic acid) co-polymers-based sponges facilitated the establishment of pre-vascularized capillary networks, which were shown to anastomose in vivo[116, 117]. Although overcoming the stability problems of soft hydrogels, such a scaffold-in-scaffold strategy still relies on the “spontaneous” self-assembly of mono-dispersed cell mixtures, which per default result in micro-capillaries with diameters of about 10 μm. However, clinical relevant tissue constructs of large size require large-caliber vessels as well.

For therapeutic angiogenesis, a substantial repertoire of angiogenic growth factors is known today. However, knowledge on the spatiotemporal availability and dynamics of growth factors (often described as 4^{th} dimension) in tissues is still quite limited and remains a major challenge. Although it is widely accepted that growth factors appear in gradients resulting from diffusion and

binding to the ECM, the characteristics of these growth factor gradients are highly complex, tissue-specific, and therefore difficult to determine. Furthermore, for the engineering of specific tissue factors controlling vascularization as well as factors directing differentiation need to be present at the same time. Hence, potential cross-talks between angiogenic and tissue specific signals and cells need to be considered.

Novel (hydrogel-based) technologies for vascularized tissue models

In vascular biology, much knowledge has been generated using various well established in vivo evaluations and transgenic animal models[118, 119]. Additionally, cellular and molecular mechanism controlling capillary architecture, morphogenesis, and EC-perivascular cell communication have been dissected in 3D in vitro systems using natural ECM hydrogels. Furthermore, engineered micro-capillary networks or molecules with blood vessel-modulating functions have been delivered in vivo using hydrogels. Yet, large-caliber vessels are still missing in current pre-vascularization systems. Furthermore, while angiogenesis inhibitors proved successful for the treatment of ocular vascular diseases, their use for cancer treatments in many instances did not lead to the targeted effects[120, 121].

The study of basic vascular biology, the development of novel therapeutic strategies, and the establishment of in vitro platforms for personalized therapies will benefit from physiologically relevant and reproducible 3D tissue models. Since novel materials and manufacturing technologies are key to achieve such models, we will discuss their impact on the generation of vascularized tissue models in the next sections.

Synthetic hydrogel materials to study basic vascular biology

The American Heart Association states that collagen type I and fibrin hydrogels are the gold standard materials for 3D in vitro vascular biology assays[122]. Indeed, these systems have provided invaluable insight into the morphogenesis of blood vessel capillaries. However, biological outcomes might be influenced by ECM hydrogel properties. In contrast, semi-synthetic and synthetic hydrogels enable study of the function of ECM components on vascular morphogenesis and signaling in the absence of confounding ECM signals. Such defined conditions will further allow control over growth factor presentation and the evaluation of growth factor gradients, for example during sprouting angiogenesis and pericyte recruitment[123]. The in vitro recapitulation of angiogenic processes under controlled matrix and growth factor presentation conditions will be important to the study of spontaneous morphogenic processes and associated molecular and biochemical functions. A recent publication shows the adequacy of fully synthetic hydrogels to provide insights into the heterocellular communication between perivascular and endothelial cells[124]. Moreover, in synthetic hydrogels established vascular models could provide a platform to manipulate morphogenic processes by using sophisticated and ideally remotely controllable cells and materials components as they are becoming available[125, 126]. For example, cells that upon

chemical-, temperature-, or light-mediated activation induce the expression of angiogenic stimuli, receptors, or even cell-cell adhesion molecules could be used to study cellular communication during vessel formation and remodeling. Furthermore, hydrogels whose stiffness, cell adhesion, or growth factor binding properties can be modulated by light could serve to control the local activation of sprouting angiogenesis.

Vascularized models of specific types of tissues

Vessel properties vary among different tissues and reciprocally vessels can influence the development and function of tissues. Therefore, vessel functions should be studied in tissue specific models consisting of multiple properly arranged and differentiated cell types. Since they are relatively simple in structure, dermo-epidermal tissue models were among the first engineered differentiated tissues with an established functional vascularization[58, 59]. However, in tissues with high structural complexity, the localization of growth factor stimulation relies on a spatial patterning to prevent a potential interference of different signaling cues. The need for the spatial separation of growth factors has been shown in engineered bone and bone marrow mimicking environments, as they require at least two different growth factors[94]. While the osteogenic signal BMP-2 directed mesenchymal progenitor cells towards osteogenic commitment, FGF-2 supported the maintenance of an undifferentiated phenotype. Since in this system both factors promote the formation of a 3D micro-capillary network, the localized presentation of the factors could be used to study vascular functions responsible for the maintenance of hematopoietic stem cells in their bone marrow compartment.

Vascularized cancer models

Cancer is known to continuously promote angiogenesis and to benefit from excessive vascularization. Therefore, the inhibition of angiogenesis was considered as a strategy to reduce cancer progression. Surprisingly, the treatment of cancer patients with VEGF inhibitors in many instances did result only in the minimal extension of progression free survival[127]. The cause of limited treatment efficiency can be manifold and includes the compensation of treatment effects through non-angiogenic mechanisms. Nevertheless, mechanisms also related to angiogenesis, such as the co-option of preexisting vessel structures or the compensation for the lack of one angiogenic cue by the upregulation of another cue, are currently seen as important aspects to be carefully studied. Moreover, within the last decade, the dogma of vascularization-based cancer treatment has shifted from the inhibition of blood vessel formation to a normalization of the structurally and functionally aberrant cancer induced blood vessels[128]. Due to the enormous need for meaningful in vitro screening assays, 3D models of cancer have become one of the fastest growing research topics in both cancer biology and tissue engineering. Since angiogenesis is one of the hallmarks of cancer, vascularization has been integrated into engineered 3D cancer models. While first vascularized cancer models were established in naturally occurring ECM hydrogels, models engineered in semi-synthetic and synthetic hydrogels are now becoming available and have the potential to give rise to highly structured, vascularized tumor environments[129-133].

Manufacturing channels in hydrogels to engineer large-caliber vessels

Vascular engineering can benefit from novel biofabrication techniques, such as bioprinting, micro-molding and lithography, in moving towards the development of larger diameter vessels. By applying these techniques, hydrogel materials that contain imbedded channels of several hundred micrometers can be obtained. Subsequently, the created channels can be lined by endothelial cells and can serve as potential access sites for perfusion. For example, Bertassoni et al. have molded channels into stiff GelMA and PEG hydrogels using agarose rods and seeded the channels with endothelial cell suspensions after removing the rods[134]. In two other studies, gold rods coated with oligopeptides and ECs have been used to couple channel creation and endothelialization. After hydrogel formation, the endothelial cells were electrochemically transferred from the gold rod to the hydrogel and thereby formed an endothelialized channel[135, 136]. Another strategy to establish endothelialized channels is to combine micro-molding and additive manufacturing as excellently shown in collagen hydrogels[137, 138]. The general concept of leaving behind a channel in hydrogels can also be implemented by printing temperature dissolvable materials into temperature stable hydrogels and release them on demand by an adequate temperature shift[139-141]. To save labor, channels can be created in hydrogels by laser-based photo-ablation of the bulk hydrogel material, a technique that renounces molding and allows for high spatiotemporal control over the channel design[142]. Independent of the fabrication method and the employed material, the channel-based vascularization concept holds great potential for tissue engineering applications. But, the transfer of big channels to in vivo applications remains to be realized.

Microfluidic technology for the perfusion of vascularized tissue models

Today, most vascularization models are still based on non-perfused micro-capillary networks. Factors that control flow-mediated vessel maturation and remodeling are not accessible in non-perfused systems and consequently cannot be studied. Additionally, drugs distributed using the vasculature cannot be the tested in non-perfused systems. Therefore, novel vascularization models build on the formation of 3D vascular structures in microfluidic devices, which can be perfused with cell culture medium and permit the testing of pro- and anti-angiogenic compounds. Large channels can be formed, as we discussed above, and connected to microfluidic devices. When such microfluidic channels are fused with micro-capillary networks the whole engineered vascularized model can be perfused[143-146]. Conceivably, the dominant field in microfluidics perfused tissue models is cancer[147]. In this regard, vascularized microtumors (VMT) have been generated in hydrogels[148, 149]. When such VMT models were connected to perfusion, they allowed for the efficient screening of anti-cancer drugs that are affecting the microtumors as well as the tumor vasculature (**Fig. 4**). Furthermore, the combination of large vascular structures with self-arranged micro-capillaries would allow for the formation of hierarchically organized vascular trees.

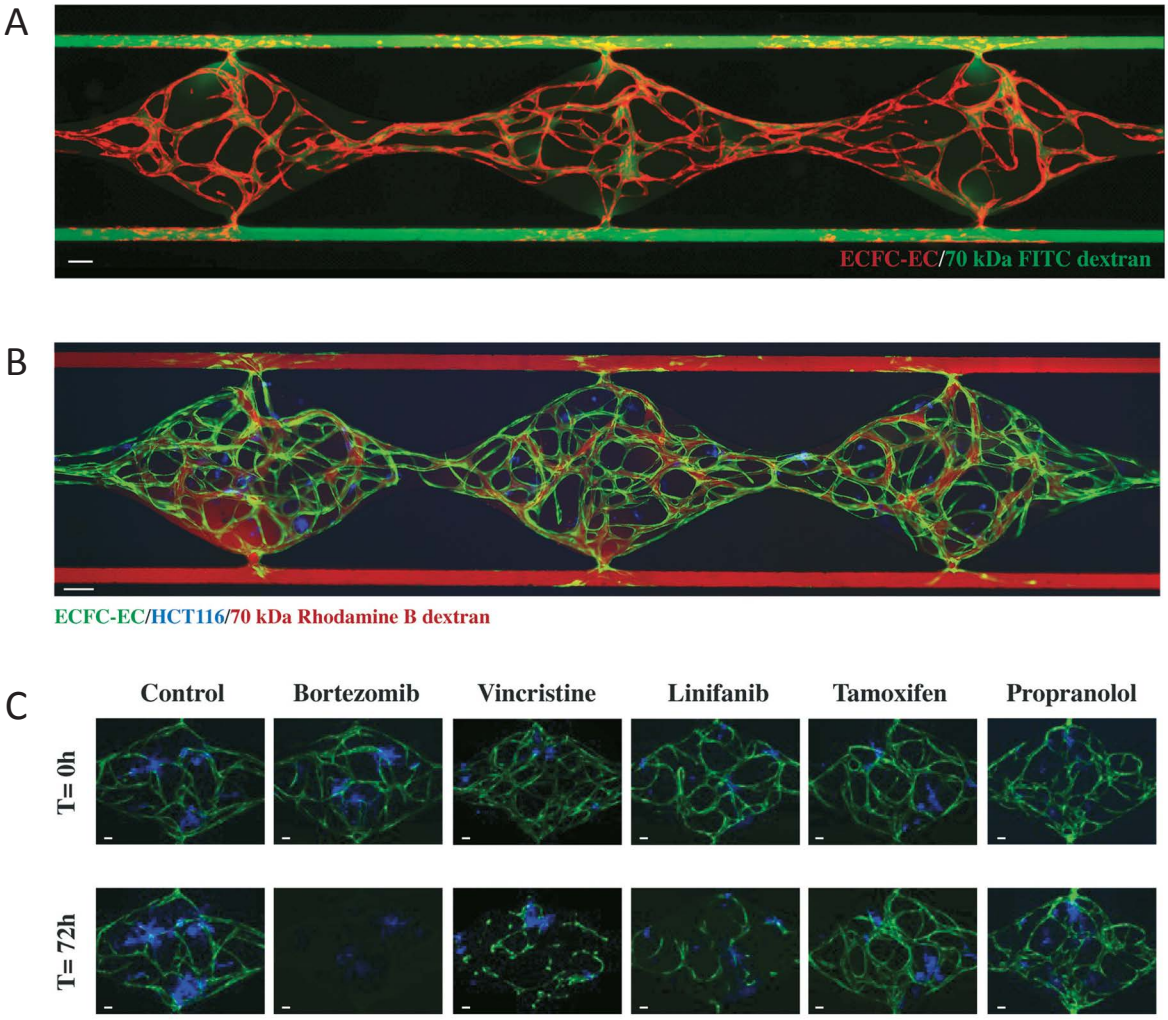

Figure 4: Perfused vasculature on-a-chip model as potential cancer and drug screening platform. A) Vascular networks formed by co-culture of human endothelial colony forming cells (ECFC-EC) and human fibroblasts in fibrin hydrogels. Vascular networks inside the three tissue chambers connect to microfluidic channels and can be perfused (70 kDa FITC-dextran). B) Vascularized microtumors (VMTs). HCT116 cancer cells were embedded together with endothelial/fibroblast co-cultures into fibrin hydrogels and grow into microtumors surrounded by perfused vascular networks. Scale bars A, B: 100 μm. C) VMTs used for anti-cancer drug screening. The collapse of the tumor (vasculature) can be monitored upon treatment with FDA-approved anti-cancer drugs. Scale bars: 50 μm. Adapted figure reproduced from Phan et al.[148] with permission from the *Royal Society of Chemistry*.

Outlook: Standardized platforms for drug screening and personalized medicine

The above-described approaches to engineer vessel models are mainly designed to gain insight into physiological and pathological tissue functions. By using human cells, engineered vessel models avoid species-related false positive and negative results and therefore are interesting alternatives to preclinical animal models. However, to speed up the development of novel vascular drugs, the integration of vessel models with reproducible high throughput platforms is required. The potential benefit of such platforms was recently shown by using induced pluripotent stem cells and PEG hydrogels[150]. Since similar assays could be run with adult stem or induced pluripotent stem cells derived from healthy or diseased human individuals, these assays can also help to bring forward personalized medicine in the field of vascular diseases.

Summary

Engineered pre-vascularized tissues and the delivery of angiogenesis promoting or inhibiting therapeutics are promising approaches to treat diseases related to malfunction of the vasculature. Additionally, emerging vascularized tissue models (summarized in **Fig. 5**) enable the study of basic vessel biology under near-physiological and pathology mimicking conditions in vitro. If scalable, vascularized tissue models would allow screening for therapeutic compounds under controlled and highly standardized conditions. The development of next-generation vascularized tissues critically depends on hydrogel systems tailorable towards cell-specific functions and compatible with innovative (micro)-manufacturing technologies. Therefore, the development of novel clinically translatable vascular treatments as well as personalized tissue models require the continuous integration of knowhow from basic vascular biology, hydrogel engineering, biofabrication, and medical needs.

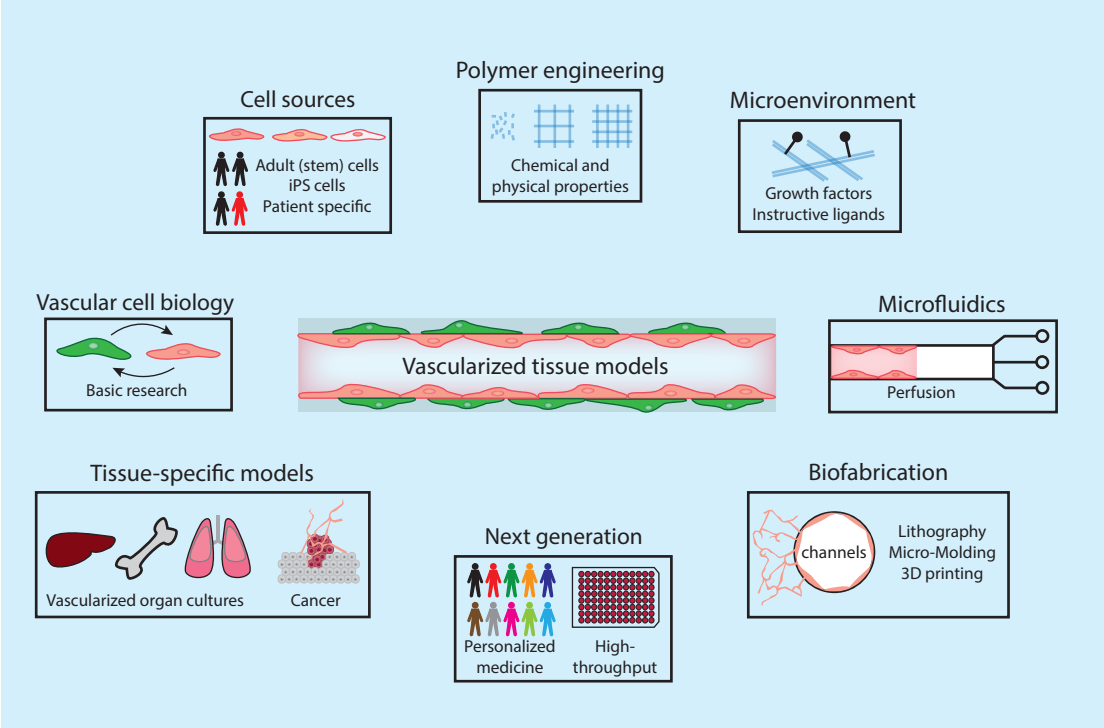

Figure 5: Engineering of vascularized tissue models using hydrogels. Vascularized tissue models largely depend on engineered hydrogel-based, cell-instructive microenvironments. The culture of adult (stem) cells in these cell-instructive microenvironments enables the study of basic vascular biology under defined in vitro conditions. Engineering physiologically relevant human tissue and cancer models requires the integration of knowhow from vascular biology and biofabrication techniques. In the future, the use of defined 3D culture systems together with patient derived cells will allow for the screening of therapeutics and the testing for treatment towards personalized medicine.

Acknowledgments

This work has been supported by the European Union's Seventh Framework Programme (iTERM grant agreement No. 607868) and by the Swiss National Science Foundation (310030-169808/1).

Chapter II:

Notch-inducing PEG-hydrogels mimic the extracellular matrix switch of MSCs in the perivascular microenvironment

The content of this chapter is prepared for submission as full article with the following co-authors: U. Blache, Q. Vallmajo-Martin, E.R. Horton, J. Guerrero, V. Djonov, A. Scherberich, J.T. Erler, I. Martin, J.G. Snedeker, V. Milleret and M. Ehrbar

Abstract

Mesenchymal stem cells (MSCs) are debated to reside in the perivascular microenvironment of blood vessel capillaries. However, the fate of MSCs in the perivascular microenvironment as well as factors controlling their fate is not understood. Here, we engineered synthetic poly (ethylene glycol) PEG-based hydrogels for the growth of capillaries by endothelial cells and MSCs in extracellular matrix (ECM)-free biomaterials in vitro. Transcriptome analysis of human bone marrow-derived MSCs, when isolated from engineered micro-capillaries, showed a prominent switch in ECM production of vascular basement membrane components and perivascular differentiation, including Notch signaling. Interestingly, functionalization of PEG-hydrogels with Notch-activating Jagged1 could recapitulate the ECM phenotypic switch of MSCs in the absence of endothelial cells, further demonstrating direct cell-cell dependent, Notch-induced ECM remodeling by MSCs.

This work demonstrates an interesting loop approach, in that biomaterials-based tissue mimetics serve to obtain novel biological knowledge, which immediately reinstructs the design of biomaterials.

Introduction

Blood vessels consist of an inner endothelial cell layer and a surrounding wall of perivascular cells (mural cells). Perivascular cells are sub-classified into vascular smooth muscle cells or pericytes by their distribution to either large-caliber vessels or micro-capillaries, respectively[16, 17]. During the formation of new blood vessels, perivascular cells are recruited by endothelial cells and contribute to the stabilization and regulation of newly formed endothelial capillaries (**Fig. 1A**). Due to this stabilizing function, perivascular cells are considered as endothelial cell supporters. Interestingly, the perivascular microenvironment of endothelial capillaries within different tissues has been proposed to potentially function as a reservoir for mesenchymal stem/progenitor cells (MSCs)[18-21, 23, 151, 152]. This has led to the hypothesis that MSCs and perivascular cells are closely related, or may even be considered as equivalent cell types. In support of this hypothesis, a sub-fraction of human MSCs, characterized by their expression of CD146, has been shown to home to the perivascular niche of the bone marrow and self-renew[20]. However, how MSCs adapt to the perivascular environment has not been addressed comprehensively, mainly due to the lack of MSC-specific markers allowing for cell tracing experiments and difficulties in specifically manipulating cells within their perivascular niche in vivo[153]. Therefore, in vitro models are required to systematically address the regulation of MSCs in a defined perivascular microenvironment.

In vitro, MSCs comparable to perivascular cells can act as vascular support cells and have been successfully used for blood vessel engineering within natural ECM hydrogels[69, 154-158]. However, the elucidation of specific microenvironmental signals in ECM hydrogels remains difficult due to inherent bioactivities. The influence of individual niche determinants on MSC function and behavior has been investigated by engineering 2D cell substrate materials towards stiffness, the presentation of cell-cell or cell-ECM adhesion ligands and by controlling cell shape and spreading[159-164]. However, to mimic native cell niches, 3D microenvironments with application-specific and systematically tailored properties are required[165]. Fully synthetic materials, such as poly (ethylene glycol) (PEG)-based or hyaluronic acid (HA)-based hydrogels[50, 89, 166], can be generated with defined physical and chemical properties and provide reproducible and tunable platforms for the creation of defined cell microenvironments. These synthetic materials provide 3D scaffolds suited to mimic developmental processes as recently demonstrated for the promotion of angiogenesis, neural tube formation, epithelial cyst formation and culture of small intestine organoids[91, 167-171]. To specifically control the fate of MSCs in engineered 3D microenvironments, stiffness and degradability as well as the presentation of matrix-immobilized small molecules and growth factors have been engineered in synthetic hydrogels[115, 172, 173]. However, there is still a lack of basic knowledge on MSC function and commitment within the perivascular niche, and how this niche might be successfully mimicked by a minimal synthetic microenvironment. Thus, identifying key factors of the communication with a disparate cell population, such as occurs in the perivascular niche between MSCs and endothelial cells, could help the rational engineering of highly defined synthetic microenvironments that control the fate of MSCs.

Here, we engineer 3D perivascular microenvironments within PEG-hydrogels to control and determine the fate of MSCs in a fully defined environment that closely mimics their native niche

(**Fig. 1B**). We show this synthetic system can promote ECM deposition from human bone marrow MSCs, which defines the cellular microenvironment and MSC-matrix interactions required immediately after cell embedment. In co-culture with human endothelial cells, we describe that MSCs behave as perivascular-like cells and efficiently support the formation of endothelial micro-capillaries as a function of PEG-hydrogel stiffness. Furthermore, we show that MSCs together with endothelial cells become embedded within a dense perivascular ECM that consists of multiple matrix components. Unbiased transcriptome analysis of perivascular MSCs demonstrated a prominent switch in the production of basement membrane ECM and Notch signaling compared to control MSCs. In the absence of endothelial cells, we recapitulated the induction of the perivascular MSC phenotype by engineering PEG-hydrogels with the Notch-activating ligand Jagged1. These remarkable findings demonstrate the potential of synthetic hydrogels to be specifically engineered to create perivascular microenvironments that mimic endothelial cell-derived signals, enabling the identification of mechanisms of perivascular lineage commitment of MSCs under defined conditions.

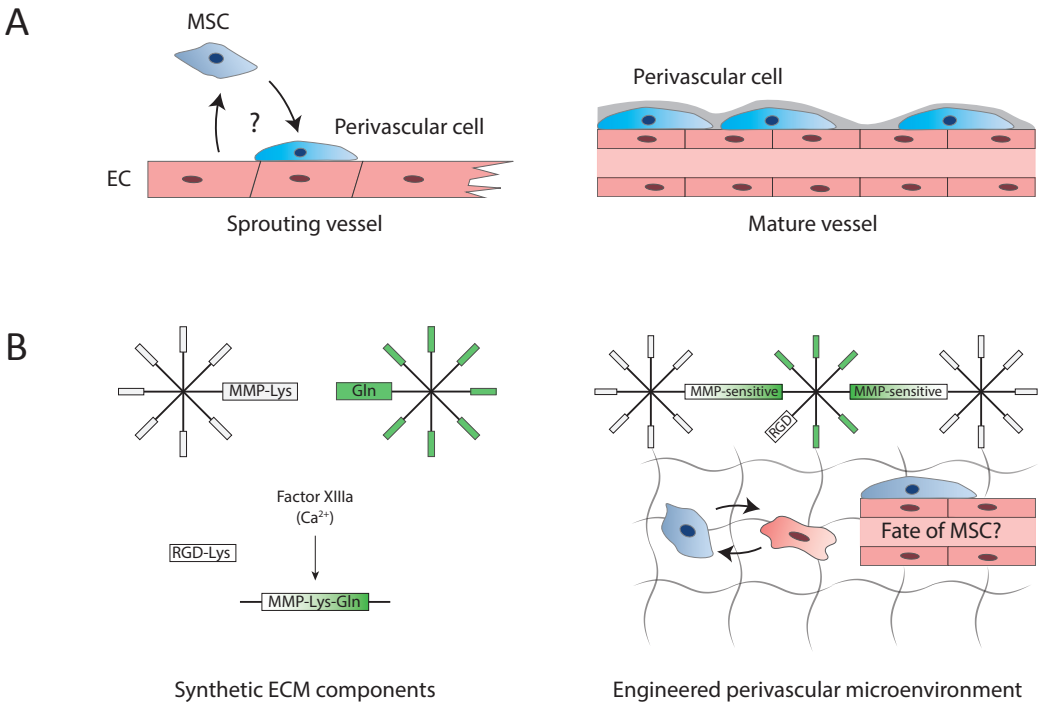

Figure 1: Engineering perivascular microenvironments to study their role in MSC commitment. A) Schematic representation of the recruitment of perivascular cells during blood vessel formation by endothelial cells (EC). B) Schematic of synthetic, FXIIIa cross-linked PEG-hydrogels containing the integrin adhesion ligand RGD and MMP-sensitive sites, and their usage for the engineering of perivascular microenvironments. These ECM-free modular designed PEG-hydrogels enable the defined co-culture of MSCs and endothelial cells, resulting in the cell-autonomous establishment of micro-capillaries containing perivascular localized MSCs.

Results

MSCs rapidly modify engineered microenvironments with their own ECM

3D microenvironments were engineered by enzymatically cross-linking *star-shaped* 8-arm PEG precursor molecules that are end-functionalized by substrate-sequences for FXIIIa (**Fig. 1B**) [174,

[175]. A matrix metalloproteinase (MMP)-sensitive degradation domain in one of the precursor molecules and the simultaneously cross-linked integrin-adhesion peptide RGD render this synthetic environment bioactive. To address the contribution of human bone marrow MSCs (BM-MSCs) to the engineered microenvironment, we embedded BM-MSCs in PEG-hydrogels and selectively visualized deposited cell-derived ECM components by immunostaining without cell membrane permeabilization. We found BM-MSCs weave a fibrillar meshwork of structural ECM proteins into the surrounding environment within 7 days (**Fig. 2A**). This cell-derived ECM meshwork comprised cellular fibronectin (FN) and heparin-sulfate-proteoglycan-2 (HSPG-2/perlecan), as well as collagen type 1 (Col1) and type 3 (Col3). To gain deeper insight into the initial changes of the engineered microenvironment, we analyzed ECM deposition at earlier time points (**Fig. 2B**). Intriguingly, we found that 4 hours post-embedment BM-MSCs were not yet spread but already lined their encapsulation cavities by a shell of cellular FN. Notably, after 24 hours cells started to spread and to move out from their ECM-cavities, which are made up also by other ECM components than FN including HSPG-2 and Col3. Based on the very early appearance of cell-derived ECM proteins, we asked whether the cell-derived ECM influence the interaction of cells with the engineered microenvironment. To address this question, we knocked down FN in BM-MSCs by siRNA (**Fig. S1A;** supporting figures are found at the end of this chapter at pages 38-40) and embedded FN-depleted cells in PEG-hydrogels containing 50 μM RGD (**Fig. 2C**). When cultured on 2D controls (**Fig. S1B**) or in engineered 3D microenvironments (**Fig. 2C**), these FN-depleted BM-MSCs could not form FN-networks. Additionally, in 3D cultures FN-depleted cells were less elongated and less spread than their control cells after 3 days of culture (**Fig. 2C**). To quantitatively analyze this effect we determined the spreading index of cells by automated measurement of cell elongation. In doing so, we confirmed a significantly reduced spreading behavior of FN-depleted cells using several FN1-siRNAs as well as several BM-MSC donors (**Fig. 2D**). Nevertheless, cell-matrix interactions do occur in FN-depleted cells despite significantly reduced spreading. To further decouple the role of the cellular FN from the hydrogel-presented RGD, we embedded FN-depleted and control siRNA cells in matrices without RGD and analyzed their spreading. Intriguingly, control cells still spread in matrices without RGD, but less than in RGD-containing matrices. However, when FN-depleted cells were analyzed in RGD-free matrices their spreading index decreased dramatically and cells remained almost completely round. Together these data show that hydrogel-embedded BM-MSCs, in addition to RGD-mediated cell spreading, change their microenvironment by depositing ECM components, including FN. In summary, PEG-hydrogels provide a 3D system to study MSCs within MSC-derived ECM.

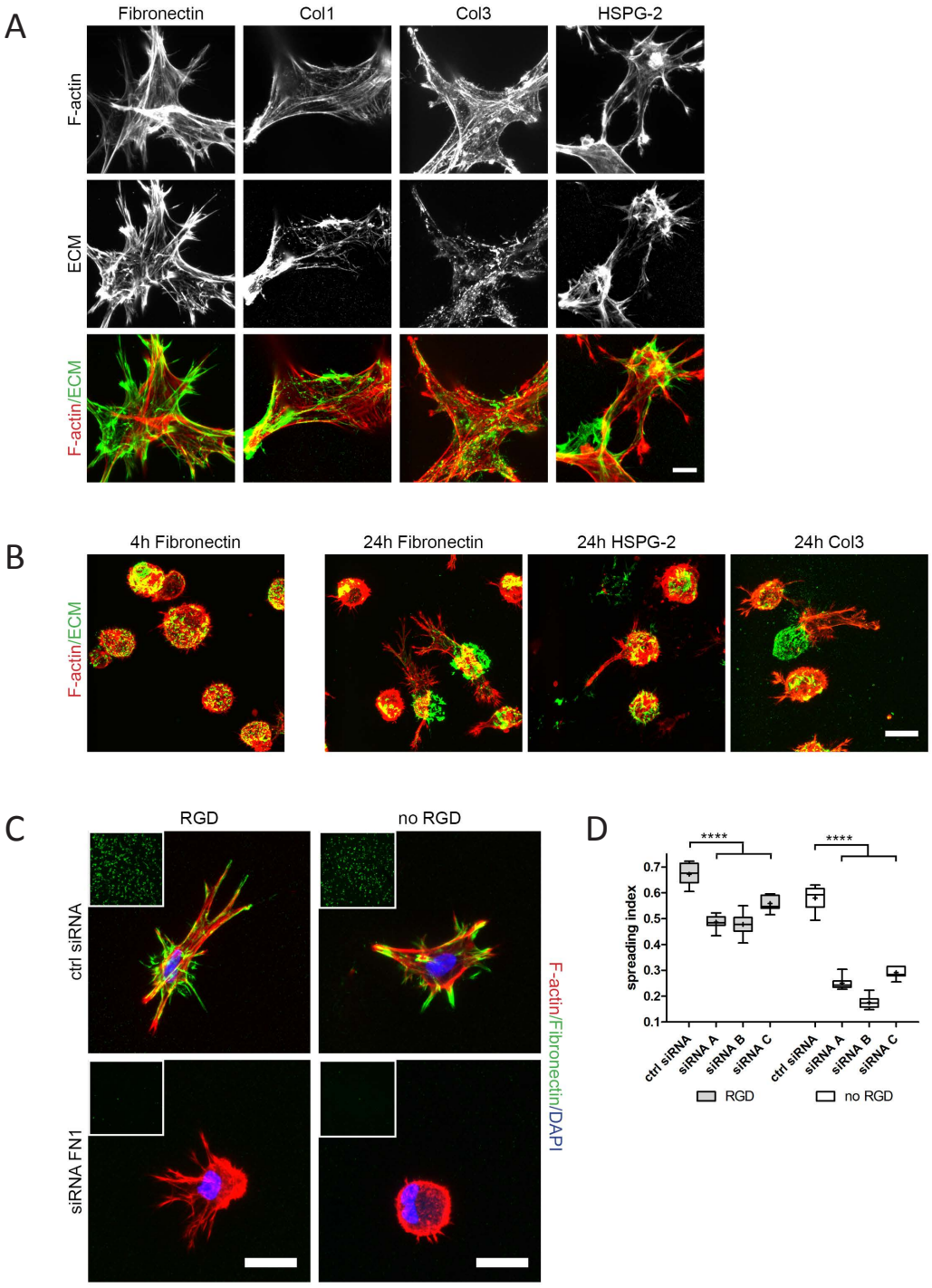

Figure 2: ECM secreted by BM-MSCs modifies PEG-hydrogels and alters cell-substrate interactions in engineered microenvironments. A) Representative immunofluorescence images of BM-MSCs (F-actin, red) and deposited ECM components (green) after 7 days of culture within RGD-modified PEG-hydrogels. Scale bar, 10 μm. B) BM-MSC (F-actin, red) secreted and deposited cell-derived ECM (green) to sites of initial embedment in RGD-modified PEG-hydrogels after 4 and 24h of culture. Scale bar, 20 μm. C) Cellular fibronectin modulated spreading of BM-MSCs with intact or knocked-down fibronectin expression after 3 days of culture within RGD-modified and RGD-free PEG-hydrogels. Scale bar, 20 μm. Insets: 1.55x1.55 mm overview images of fibronectin staining. D) Quantification of cell spreading of BM-MSCs with intact or knocked-down fibronectin expression within RGD-modified and RGD-free PEG-hydrogels. The spreading of BM-MSCs treated with control siRNA and 3 different siRNAs to FN1 is shown as spreading index between 0 for circular cells and 1 for elongated cells. Box plot (25th and 75th percentiles) with whiskers (5th and 95th percentiles), median (line) and mean (+). (n = 9 samples from 3 donors. ANOVA with Bonferroni's post hoc test **** $p < 0.0001$). All depicted images are Z-projections and exclusively present the extracellular deposited protein.

FGF-2 stimulation, PEG-hydrogel stiffness and degradability control micro-capillary network assembly

Next, to convert the MSC-derived microenvironment presented above into a perivascular microenvironment, we aimed at tailoring PEG-hydrogel properties and culture conditions for optimal in vitro vessel morphogenesis and micro-capillary network formation. Towards this aim, we 3D embedded BM-MSCs together with human umbilical vein endothelial cells (HUVEC) in a 1:1 ratio in PEG-hydrogels containing RGD. After 7 days of culture, we evaluated the formation of 3D micro-capillary networks by CD31 immunostaining of endothelial cells (**Fig. 3A-C**). BM-MSCs and endothelial cells failed to assemble into micro-capillary networks in the absence of FGF-2. However, when co-cultures were conducted in the presence of FGF-2, micro-capillary network formation occurred in a dose-dependent manner up to 50 ng/ml FGF-2 (**Fig. 3A** and **Fig. S2A**). We next examined the impact of matrix stiffness and material density on network formation by comparing hydrogels of varying PEG amounts (dry mass content 1% - 3% with corresponding storage moduli 74 Pa - 2157 Pa, respectively) in the presence of 50 ng/ml FGF-2 (**Fig. 3B**, **Fig. S2B** and **Fig S2C**). The overall length of CD31-positive micro-capillaries was equally high in very soft matrices (1% - 1.3% PEG with 74-276 Pa, respectively), while there was a slight reduction in 1.7% PEG matrices (470 Pa). However, in matrices above 2% PEG (>762 Pa) the length of micro-capillaries decreased significantly and CD31-networks were almost completely absent in the stiffest matrices tested of 3% PEG (2157 Pa). Taken together, a combination of FGF-2 and soft PEG matrices supports the robust formation of 3D micro-capillary networks by endothelial cells (CD31-positive) and BM-MSCs (CD31-negative) (**Fig. 3C**).

To gain insights into the structural details of these micro-capillaries we investigated PEG-hydrogels by light and electron microscopy (**Fig. 3D).** We show that BM-MSCs (and derivatives) reside around and between the endothelial capillaries. By transmission electron microscopy (TEM) we demonstrate that micro-capillaries have lumens of several micrometers in diameter and are surrounded by a layer of cell-derived ECM. Moreover, endothelial cells were in very tight contact with perivascular localized BM-MSCs that are enshrouded in the cell-derived ECM layer. Ultrastructural analysis indicates that the deposited ECM layer is of heterogeneous composition, includes collagen microfibrils, and facilitates physical interactions with cellular extensions (**Fig. 3E**). We next investigated the composition of the perivascular ECM network by means of immunofluorescence analysis without cell membrane permeabilization (**Fig. 3F**). We found FN, Col1 and Col3 to be present in the extra-cellular space around the micro-capillaries. Notably, the perivascular ECM layer also consists of the basement membrane components collagen type 4 (Col4), laminin and HSPG-2. However, matrix remodeling in synthetic hydrogels is not just featured by newly deposited cellular ECM but is also dependent on the proteolytic breakdown of the synthetic matrix. To confirm this assumption we blocked matrix metalloproteinase (MMPs) activity using chemical inhibitors (**Fig. S2D**). Indeed, the broadband MMP-Inhibitor GM6001, as well as inhibitors of MMP-2 and MMP-9, completely prevented the formation of micro-capillary network formation at high concentrations. Taken together, favorable conditions for the culture of 3D micro-capillaries were featured by balanced hydrogel degradation and cell-derived ECM deposition, enabling hetero-cellular adhesions and morphogenesis to occur.

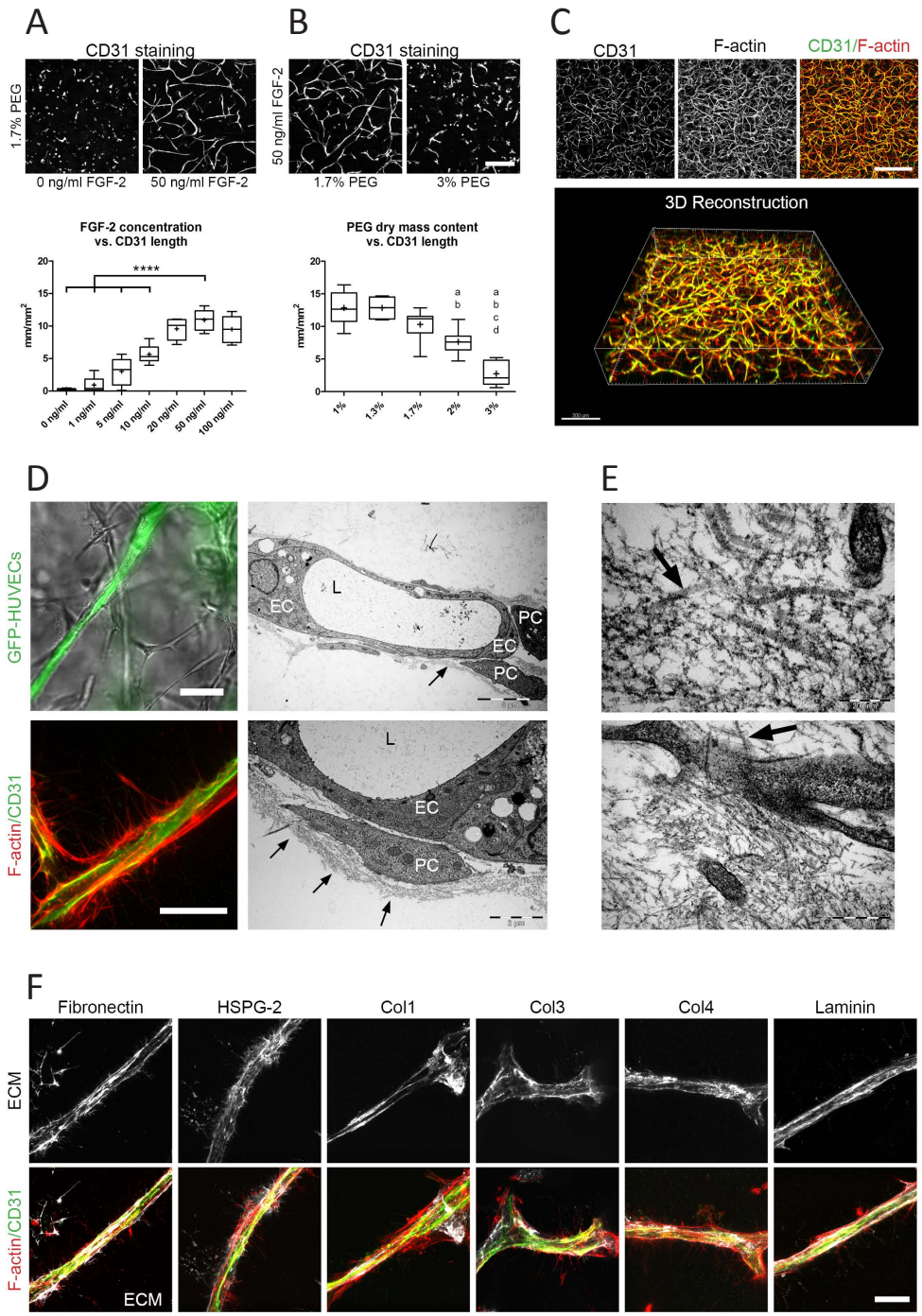

Figure 3: Engineering of 3D perivascular microenvironments by defining parameters for micro-capillary formation. A-C) Representative immunofluorescence images of micro-capillary networks formed by BM-MSC and endothelial cells (CD31) after 7 days of 3D co-culture in PEG-hydrogels. Scale bars, 200 µm. (A) Quantitative analysis of the absolute length of CD31-positve networks depending on FGF-2 concentration (n = 6 samples from 3 donors. ANOVA with Bonferroni's post hoc test **** $p < 0.0001$) and (B) physical matrix properties by PEG dry mass content (n = 8 samples from 5 donors. ANOVA with Bonferroni's post hoc test shows significant differences from 1% PEG (a), 1.3% PEG (b), 1.7% PEG (c) and 2% PEG (d)). Box plots in A and B show 25th and 75th percentiles with whiskers at 5th and 95th percentiles, median (line) and mean (+). C) 3D micro-capillary network formed by co-cultures of BM-MSC and endothelial cells in 1.7% PEG matrices and in the presence of 50 ng/ml FGF-2. Scale bars Z-projection 500 µm and for 3D reconstruction 300 µm. D) Qualitative assessment of micro-capillaries by light (scale bar, 50 µm), fluorescence (scale bar, 20 µm) and TEM microscopy (scale bars of upper and lower panel, 5 µm and 2 µm). Images show endothelial cells (EC, GFP, CD31) forming lumenized (L) micro-capillaries that are surrounded by perivascular-like cells (PC). TEM micrographs showing that micro-capillaries and perivascular cells are embedded in a dense network of ECM (black arrows). E) Ultrastructural analysis of the perivascular ECM layer by TEM microscopy showing heterogeneous ECM composition including collagen microfibrils (black arrows) and close cell-ECM interaction. Scale bars, 200 nm and 500 nm. F) Representative immunofluorescence images of the perivascular ECM layer by exclusive labeling of extracellular deposited ECM proteins (white) and of micro-capillaries (CD31 in green, F-actin in red). Scale bar: 20 µm. All depicted immunofluorescence images are Z-projections.

Micro-capillaries promote the perivascular commitment of BM-MSCs

Next, using the optimized micro-capillary cultures (1.7% PEG, 50 ng/ml FGF-2), we investigated the changes BM-MSCs undergo in the perivascular microenvironment by unbiased transcriptome analysis (**Fig. 4A**). To retrieve BM-MSC (and derivatives) from micro-capillary networks or monocultures, we digested PEG-hydrogels by collagenase and isolated CD31-negative cells by FACS (**Fig. 4A and Fig. 4B**). Successful cell separation was verified by qRT-PCR for CD31 mRNA expression in isolated populations (**Fig. S3**). In subsequently isolated and sequenced mRNA of BM-MSCs, we detected 16839 transcripts. Among this absolute number of detected transcripts we found 551 to be strongly and significantly up-regulated and 771 down-regulated in micro-capillary network-derived BM-MSCs (**Fig. 4C**). A strong effect was assumed above a $\log_2$-fold change of 1 and significance was accepted below a FDR of 0.01. The 100 most significantly differentially expressed genes (DEG) are displayed as a heatmap in **Figure 4D**. To systematically investigate the relationship of the differentially expressed genes in BM-MSCs we functionally enriched genes within the gene ontology (GO) domain Cellular Component (**Fig. 5**). As a result, Cellular Component terms that are overrepresented (gene-enriched) appear as clusters in the visualization map of **Figure 5A**. To gain deeper insights into the transcriptome changes that BM-MSCs undergo in the perivascular environment, we addressed the most prominent clusters of the gene enrichment **(Fig. 5B)**. Strikingly, the largest changes in perivascular BM-MSCs were related to components of the ECM, as the up-regulation of one big ECM cluster and the down-regulation of another one indicate that BM-MSCs actively participate in the functional reshaping of the perivascular ECM (**Fig. 5B**: clusters 1,2). More specifically, the induced ECM genes included many collagenous and non-collagenous components of the vascular basement membrane (COL4A1-2, COL15A1, COL18A1, NID1, NID2, LAMB3, LAMA4, LAMC1, NTN4) as well as fibrillar collagens (COL1A2, COL3A1, COL5A1-3). Conversely, rather rare collagens (COL11A2, COL17A1, COL8A2, COL28A1) and specialized basement membrane components (COL4A3, COL4A4, LAMA3) were reduced. Other clusters in the GO Cellular Component domain indicate a reorganization of the cell surface including an induction of integrins and ion/voltage-dependent channels (**Fig. 5B**: clusters 3-6). When alternatively enriching the differentially expressed genes in the GO domain Biological Process, we detected prominent clusters of blood vessel regulation and vasoconstriction, cell-matrix interactions and metal and ion homeostasis, all pointing towards a contractile phenotype of perivascular BM-MSCs (**Fig. S4**).

Interestingly, we also found many components and target genes of the Notch signaling pathway to be induced in perivascular BM-MSCs (**Fig. S5**). Therefore, we next examined the induction of basement membrane genes as well as components and targets of the Notch pathway (NOTCH3, JAG1 and PDGFRB) in BM-MSCs by qRT-PCR and could confirm the expression pattern seen in the RNA-seq analysis (**Fig. 6A**).

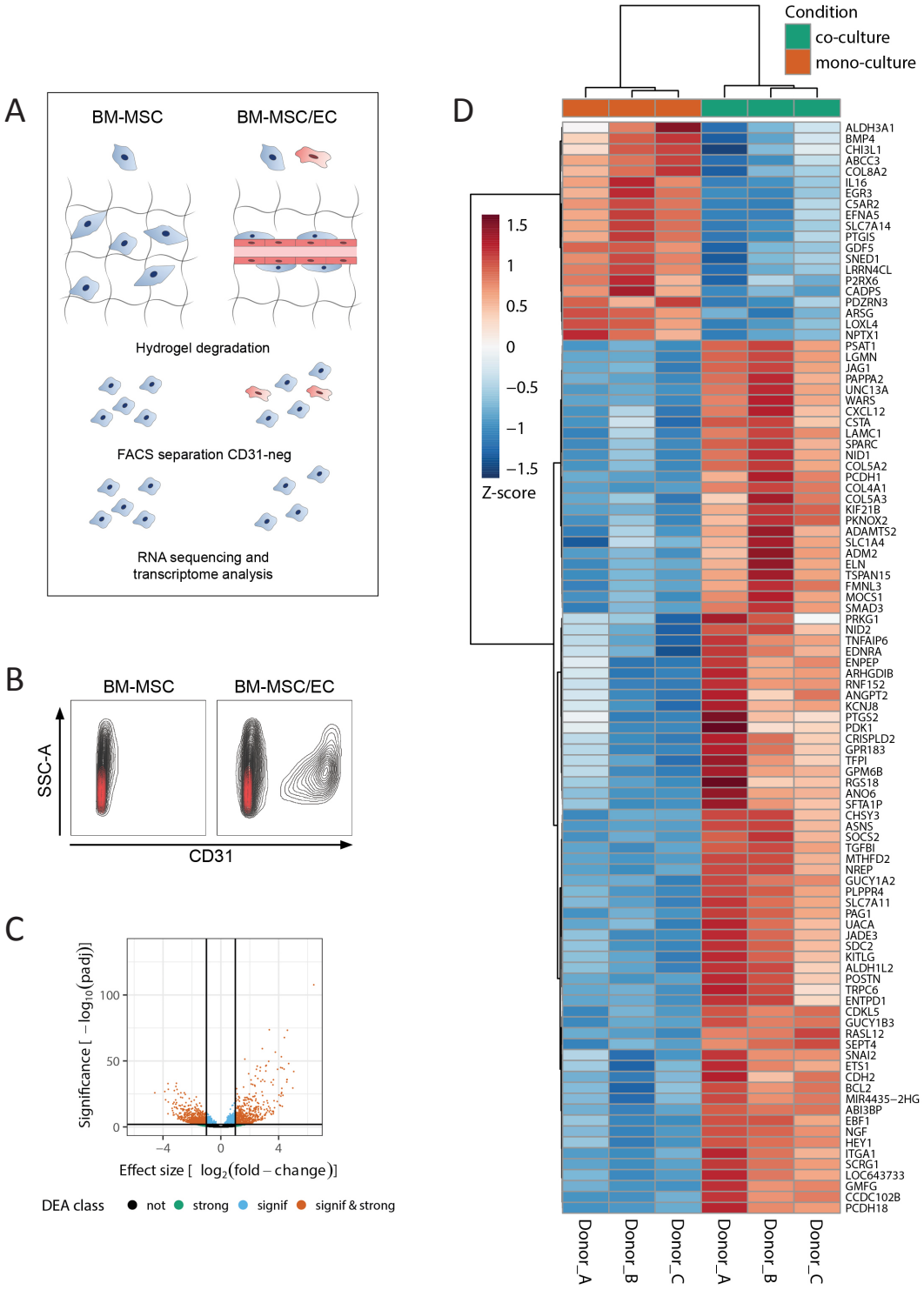

Figure 4: Genome-wide transcriptional analysis of perivascular BM-MSCs. A) Schematic of experimental workflow. BM-MSC (n = 3 donors) were cultured alone or in micro-capillary co-cultures with endothelial cells (EC). After 7 days, cells were retrieved from PEG-hydrogels and BM-MSC (and derivatives) were isolated by FACS-sorting for non-endothelial (CD31-negative) cells. BM-MSC isolated RNAs were analyzed by next-generation sequencing and differential gene expression. B) FACS separation of BM-MSC and ECs by means of CD31-staining. Black represents the full cell population of beforehand as single and live determined cells. Red represents the staining pattern of the isotype control antibody. C) Volcano plot of differentially expressed genes between mono- and co-cultured BM-MSCs. The horizontal line corresponds to a FDR = 0.01 and genes below this line are considered as not significant (not) while genes above are considered as significant (singif). The two vertical lines correspond to a $\log_2$-fold change of 1 in expression and genes outside this range are considered as strongly affected (strong; signif & strong). D) Heatmap of gene expression by BM-MSC monocultured or cultured in the perivascular microenvironment. Depicted are the 100 most significantly changed genes due to culture in the perivascular microenvironment. Hierarchical clustering separates genes with positive $\log_2$ fold change from negative change, red and blue respectively.

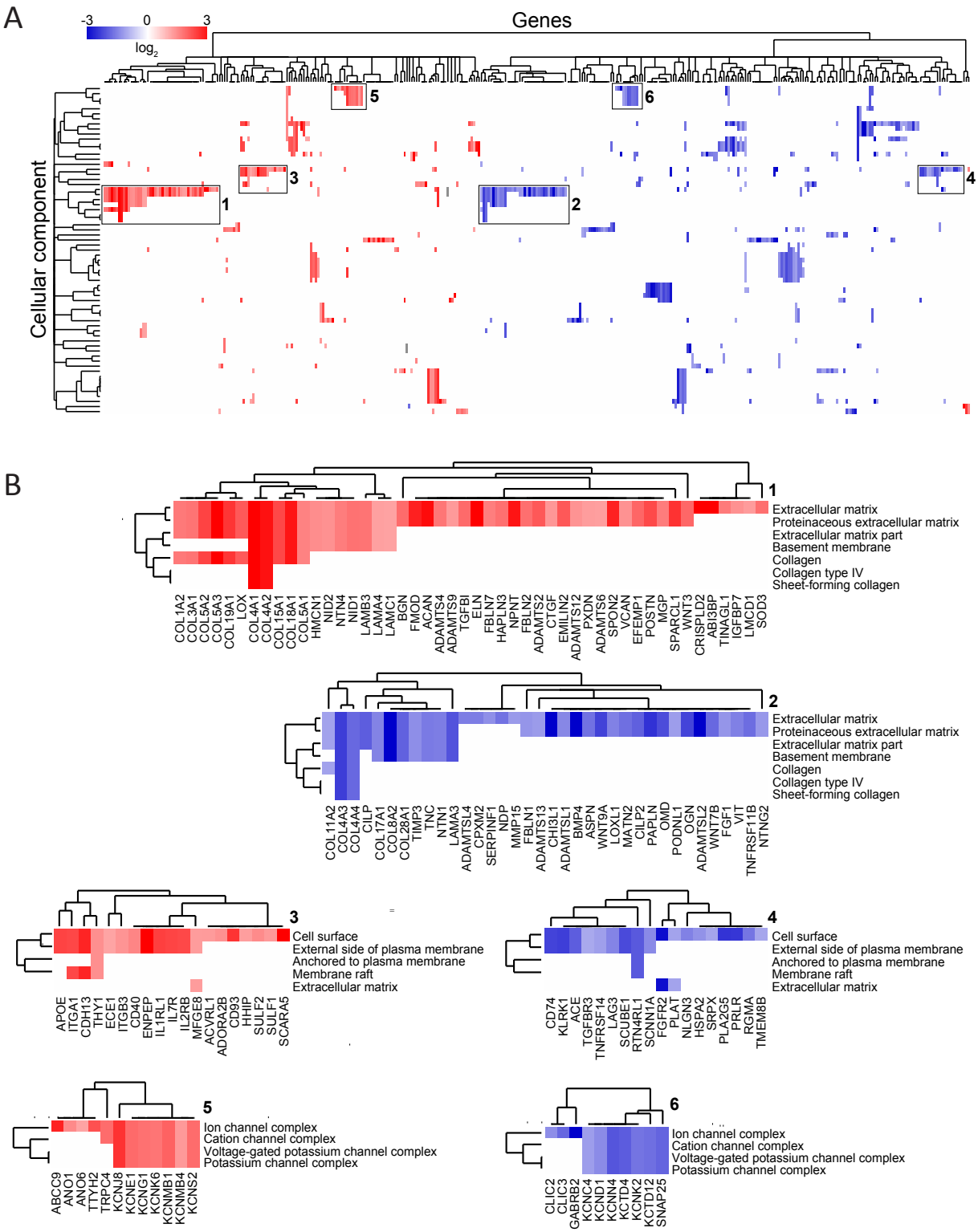

Figure 5: **Functional enrichment map of differentially expressed genes (DEG) in perivascular BM-MSCs.** A) Genes identified as DEG following transcriptome analysis are enriched and clustered by the gene ontology domain GO Cellular Component. Up- and downregulated genes in perivascular BM-MSC are displayed in red and blue, respectively. B) Strongly represented GO Cellular Component clusters show a strong rearrangement of the ECM including the basement membrane (1, 2), the rearrangement of matrix interaction partners and receptors on the cell-surface (3, 4) as well as of membrane ion channel complexes (5, 6).

Perivascular microenvironment-mediated commitment of MSCs is not cell source dependent

We next asked whether the induced expression of basement membrane ECM and Notch components are cell source dependent. To address this question we used mesenchymal progenitor cells from human adipose tissue, which are adipose-derived stromal cells (ASCs), and we performed 3D co-cultures of ASCs and HUVEC. ASCs support micro-capillary formation in PEG-hydrogels under identical conditions as for BM-MSCs and reside in the perivascular microenvironment of micro-capillaries (data not shown). Hence, we isolated ASCs from engineered micro-capillary networks and compared their gene expression to monocultured ASCs by qRT-PCR (**Fig. 6B**). Similar to what was observed for BM-MSCs, basement membrane ECM components and Notch target genes (NOTCH3, JAG1, PDGFRB) are induced in vascular ASCs. Specifically, COL4A1, COL4A2, COL18A1, COL5A3, NOTCH3 and JAG1 were the 6 most induced genes in both MSC types. To further investigate if the induced expression pattern in MSCs is dependent on the endothelia cell type we formed micro-capillary networks with human ASCs and human endothelial progenitor cells from the umbilical cord blood, also known as endothelial colony forming cells (ECFCs) (**Fig. 6C)**. We found that ASCs from micro-capillaries compared to ASCs from monocultures within the investigated gene subset upregulated the same top 6 genes as BM-MSCs and ASCs when co-cultured with HUVECs. In sum, our data show that mesenchymal progenitor cells from bone marrow and adipose tissue up-regulate components of the basement membrane ECM when cultured together with endothelial cells (HUVECs or ECFCs) in PEG-hydrogels. Furthermore, we found that in all three applied cell combinations the Notch pathway was affected in MSCs.

Jagged1-modified PEG-hydrogels induce a perivascular MSC phenotype

Jagged1 is a cell-surface protein exposed on endothelial cells, and is able to trigger the Notch pathway in receiving cells **(Fig. 6D)**. In perivascular cells, Jagged1 is a target of the Notch pathway and able to establish an autoregulatory loop[176]. We therefore reasoned that in our perivascular microenvironments endothelial Jagged1 could be an important factor to control the observed expressional changes in MSCs. Thus, we sought to engineer microenvironments that mimic endothelial cell-derived cell-cell interactions by immobilized Jagged1 **(Fig. 6D)**. Since herein used PEG-hydrogels are of modular design we made use of an earlier described protein A-based linker (Gln-ZZ), which via ZZ-domain binds Fc-tagged proteins with high affinity and via Gln-domain is covalently tethered to PEG-hydrogels[177]. Hence, the pre-incubation of Gln-ZZ with Jagged1-Fc or IgG-Fc leads to the formation of stable protein complexes that are immobilized to PEG-hydrogels by Factor XIIIa. Next, we examined whether monocultured BM-MSCs induce the vascular basement membrane and the Notch pathway in Jagged1-modified 3D microenvironments compared to IgG control-modified microenvironments. To do so we cultured BM-MSCs in the same conditions as above for endothelial co-cultures, we retrieved cells from PEG-hydrogels and assessed target genes by qRT-PCR (**Fig. 6E**). In fact, matrix immobilized Jagged1 did successfully induce the Notch pathway in BM-MSCs as shown by induction of NOTCH3, JAG1 and PDGFRB. Moreover, all tested basement membrane ECM genes that were induced in BM-MSCs by endothelial cells were also induced in BM-MSCs by the matrix immobilized Jagged1.

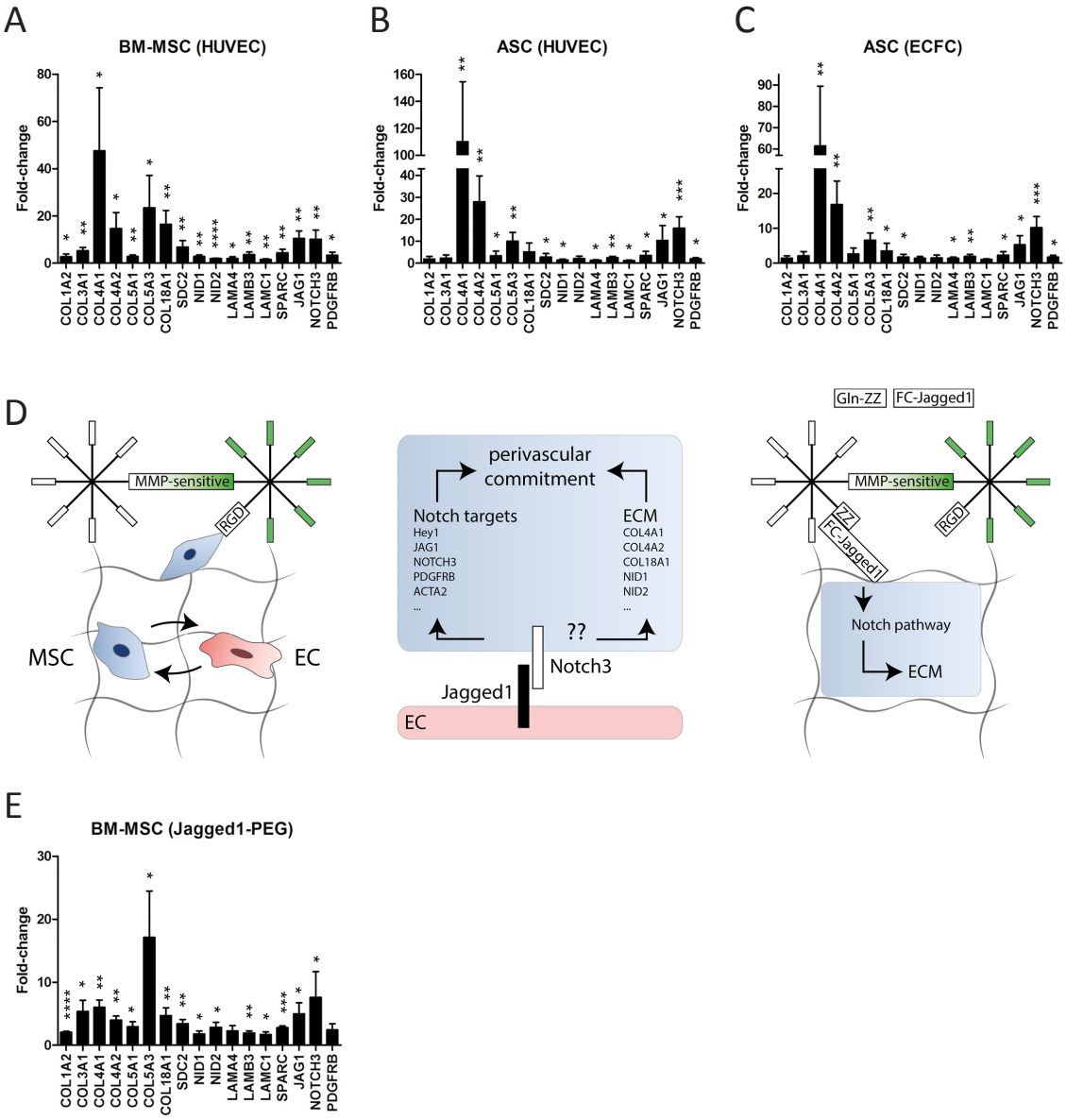

Figure 6: Jagged1-functionalized hydrogels recapitulate perivascular microenvironment promoted expression of basement membrane ECM and Notch-target genes. A - C) Induction of gene expression in MSCs after 7 days of participation in 3D micro-capillary networks versus MSCs monocultured in PEG-hydrogels. A) BM-MSCs isolated from co-cultures with HUVECs (n = 5 donors). B) ASC isolated from co-cultures with HUVECs (n = 6 donors). C) ASC isolated from co-cultures with ECFCs (n = 6 donors). D) Schematic showing the concept of endothelial cell-interaction mimicking Jagged1-functionalized synthetic matrices. In optimized synthetic hydrogel-based co-cultures endothelial cells, by direct Jagged1-Notch3-mediated cell-cell interaction promote the upregulation of ECM and Notch-target genes in MSCs and thereby govern their perivascular commitment. Modular designed synthetic hydrogels, which in addition to the integrin ligands RGD and MMP-sensitive sites contain immobilized Jagged1 induce the perivascular commitment of MSCs in absence of endothelial cells. E) BM-MSCs after 7 days of mono-culture in Jagged1-functionalized PEG-hydrogels (n = 4 donors). Data are displayed as relative fold-changes compared to MSCs monocultured in unmodified (for Figures A – C) or with control IgG functionalized PEG-hydrogels (D). Gene expression was analyzed by qRT-PCR and normalized on 3 reference genes (GAPDH, YWHAZ, EEF1A1). Bars represent mean values ± SD, one-sample t tests address the significance of the induction: * $p < 0.05$, ** $p < 0.01$, *** $p < 0.001$,**** $p < 0.0001$.

Discussion

Here, we describe a model to study MSCs in a perivascular microenvironment re-created in biomimetic PEG-hydrogels. Using this synthetic and readily tunable model, we screened the expression profiles of MSCs and identified a switch in vascular basement membrane ECM and alterations in Notch pathway target genes as novel characteristics of perivascular MSCs. By applying this novel biological stem cell knowledge to the engineering of materials-based microenvironments, we were able to hypothesize and verify that substitution of endothelial capillaries with the immobilized Notch-activator Jagged1 in PEG-hydrogels leads to activation of Notch signaling and ECM remodeling. These results show that biomaterials-based tissue mimetics serve to study biological processes, which immediately reinstruct the design of innovative materials for the reconstruction of tissues and microenvironments with increasing physiological relevance and complexity.

In contrast to naturally derived ECM polymers such as collagen, fibrin or the tumor-derived matrigel, synthetic materials allow for the engineering of defined 3D cell microenvironments under fully controlled conditions. In such synthetic ECM-mimics the researcher determines the cellular microenvironment by engineering the signals of choice. However, interactions between the engineered material and the embedded cells are reciprocal and result in the modification of the synthetic material by deposited cell-derived ECM. Surprisingly, such cell-derived ECM deposition is an often neglected phenomenon, but likely contributes or even drives the outcome of synthetic 3D materials-based cultures. Here, we could evaluate the contribution of BM-MSC-derived ECM to altering their own microenvironment. We show that the deposition of cellular ECM into PEG-hydrogels starts immediately after cell embedding and within the adaption phase of cellular spreading and cell-matrix interaction. Intriguingly, the presence of the adhesion-ligand RGD was beneficial but not required for cell spreading, indicating that cell-derived ECM facilitates cell spreading. Indeed, by silencing the very early appearing, tissue-templating ECM protein fibronectin we show to our knowledge for the first time that the cell-derived ECM facilitates cell spreading in synthetic 3D hydrogel materials. However, whether and how these findings relate to cultures with other cell types remains to be investigated. Similarly, it needs to be determined how the cell-derived ECM might influence the recognition of cell-instructive growth factors and ligands presented by engineered biomaterials.

Earlier studies made use of the endothelial cell supporting function of mesenchymal lineage cells to focus on the formation of micro-capillaries in synthetic or semi-synthetic matrices[78, 85, 91, 93, 94, 124]. Here, we engineered micro-capillary networks to study the fate of MSC in the perivascular microenvironment. By optimizing the physical properties, we found that micro-capillary network formation and material stiffness are negatively correlated, which is in line with previous work showing that capillary formation is favored at low ECM/materials density[85, 91, 93, 103, 104]. Blocking MMP-mediated matrix degradation and cell migration, even in soft matrices, inhibits micro-capillary network formation. Conversely, the well-known pro-migratory and pro-angiogenic factor FGF-2 strongly induces micro-capillary network formation. Hence, it is conceivable that micro-capillary network formation is most efficient if culture conditions best support cell migration and

communication as well as matrix remodeling, all key functions required during native angiogenesis processes. Using optimized culture conditions, we show that engineered micro-capillaries are surrounded by a dense layer of cell endogenous ECM similar to what has been reported previously for micro-capillaries within 3D naturally derived hydrogels[64, 65, 178].

To assess the fate change of BM-MSCs in engineered perivascular microenvironments we performed an unbiased gene expression analysis comparing BM-MSCs isolated from engineered micro-capillaries to BM-MSCs from monocultures. We detected the significant induction of a number of perivascular markers/components that are associated with perivascular cells (PDGFRB, ACTA2, CDH2, GUCY1A2, GUCY1A3, GUCY1B3, MYOCD, KCNJ8, RGS5; **Fig. S6**). Importantly, our transcriptome evaluation unveiled a prominent switch in the expression of ECM components. To our knowledge, we show for the first time that in micro-capillary derived BM-MSCs, components of the general and capillary basement membrane are strongly induced, while specific glomerular, corneal or epidermal basement membrane proteins are downregulated[41, 179-182]. Furthermore, we showed that the induction of vascular basement membrane ECM in perivascular MSCs is not dependent of the cell source of both the receiving MSCs and the triggering endothelial cells, showing that this is a general effect between MSCs and endothelial cells. In two recent studies, the induction of vascular basement membrane components was reported in 3D co-cultures of endothelial cells and pericytes, however, without addressing which cell type is responsible for their expression[124, 183]. In a more detailed study, Stratman et al reported several basement membrane components to be directly induced in bovine pericytes by human endothelial cells when co-cultured in collagen hydrogels[64]. Together, it is conceivable that perivascular lineage commitment is a general feature of MSCs residing in the perivascular niche of different tissues, which is recapitulated in engineered micro-vessels. However, it needs to be determined if the observed perivascular cell commitment of MSCs is involved in the generation of perivascular cells in vivo and what fraction of MSCs undergo commitment.

We also found the triggering of Notch pathway components in perivascular BM-MSCs, which, in the case of Notch3 signaling, has been previously shown to be important for perivascular cell regulation[16, 184-187]. Activation of the Notch pathway in perivascular cells occurs via the cell-surface protein Notch that interacts with endothelial cell surface-presented Jagged1[176, 187-191]. In this regard, it has been demonstrated that endothelial Jagged1 is required for the induction of Notch3 target genes, including NOTCH3 and JAG1 in perivascular cells[176], both of which we found to be induced in perivascular MSCs as well. Furthermore, two other strong hits of our analysis (COL18A1 and COL5A3) were previously induced in dermal fibroblasts by endothelial cells in a Notch-dependent manner[192]. Additionally, MSCs differentiated towards smooth muscle cells when cultured on Jagged1-coated tissue culture plastic (TCP)[193]. Based on these earlier observations and our finding that many Notch target genes are induced in perivascular MSCs, we reasoned that endothelial cells presenting Jagged1 could likely contribute to the perivascular lineage commitment of MSCs. Therefore we hypothesized that Jagged1-presenting hydrogels could substitute endothelial cell-functions of the perivascular microenvironment and allow the design of novel cell-interaction mimicking biomaterials. For this, we took advantage of an earlier developed protein A based linker-peptide (ZZ), which can be used as modular, covalently integrating component of our PEG-hydrogel and enables high affinity binding of Fc-tagged proteins[168, 177]. By using this strategy, we

readily form Jagged1-presenting 3D microenvironments to study the commitment of encapsulated BM-MSCs in the absence of endothelial cells-induced perivascular signals. Indeed, we confirm that vascular basement membrane ECM genes are upregulated in BM-MSCs harvested from Jagged1-engineered hydrogels. Hence, we demonstrate for the first time that Jagged1-engineered hydrogels via Notch pathway stimulate the expression of vascular basement membrane ECM components in MSCs and thereby bypasses the need for endothelial cells in promoting their perivascular lineage commitment.

In future, the use of perivascular cells and endothelial cells from various tissue sources in our synthetic hydrogel-based perivascular microenvironment platform followed by systematic analysis of cellular expression profiles will offer new perspectives to destruct existing complex in vivo perivascular niches. Therefore, we envision that this platform will provide a basis to elucidate the functional and phenotypic relationship of MSCs, pericytes and vascular smooth muscle cells in quiescent physiological vessels as well as their role in healing or diseased tissues. The tuning, integration and interactive manipulation of selected microenvironmental parameters by the use of innovative materials will enable the characterization and testing of new niche and stem cell regulatory signals under controlled in vitro conditions.

Experimental section

Cell culture

Human bone marrow-derived mesenchymal stem cells (BM-MSCs) were isolated as described previously[194] from bone marrow aspirates of healthy donors (n = 6) obtained during orthopedic surgical procedures after informed consent and in accordance with the local ethical committee (University Hospital Basel; Prof. Dr. Kummer; approval date 26/03/2007 Ref Number 78/07). Human adipose-derived stromal cells (ASCs) were isolated as described previously[195, 196] from adipose tissue obtained during routine surgical procedures of healthy donors (n = 6) after informed consent and in accordance with the local ethical committee (Ethikkommission beider Basel [EKKB], Ref Number 78/07). ASCs and BM-MSCs were maintained in MEM alpha (with nucleosides, Gibco) supplemented with FBS (10%, Gibco), penicillin (100 U ml^{-1}, Gibco), streptomycin (100 µg ml^{-1}, Gibco), and FGF-2 (5 ng ml^{-1}, PeproTech). Human umbilical vein endothelial cells (HUVECs, PromoCell) and human endothelial colony-forming cells (ECFCs) isolated from term umbilical cord blood (n=6) as described previously[197] were maintained in EGM-2 (EBM-2 basal medium supplemented with the EGM-2 SingleQuots growth factor kit, both from Lonza) and FCS (10%) in collagen coated flasks (0.15 mg ml^{-1} rat-tail collagen, Corning).

All cells were cultured at 37°C in a humidified atmosphere at 5% CO_2.

TG-PEG matrix formation and culture

1 mL of FXIIIa (200 U ml^{-1}, Fibrogammin, CSL Behring) was activated with 100 µl of thrombin (20

U ml^{-1}, Sigma–Aldrich) for 30 min at 37 °C. Small aliquots of FXIIIa were stored at −80°C for further use. Hydrogels with final dry mass contents of 1 - 3% w/v were prepared by stoichiometrically balanced ([Lys]/[Gln] = 1) precursor solutions of n-PEG-Gln and n-PEG-MMP-sensitive-Lys (previously described[174, 175]) in 50 mM Tris buffer pH 7.6 containing 50 mM $CaCl_2$. Additionally, Lys-RGD to a final concentration of 50 μM and cells to final concentrations 3 Mio ml^{-1} for co-cultures (1.5:1.5 Mio ml^{-1}) and 1, 1.5 or 3 Mio ml^{-1} for MSC monocultures were added. Subsequently, PEG cross-linking was initiated by addition of 10 U ml^{-1} FXIIIa and disc-shaped matrices were prepared between hydrophobic glass slides (treated with SigmaCote, Sigma-Aldrich). Final hydrogels were cultured in medium containing MEM alpha, FCS (10%), penicillin (100 U ml^{-1}), streptomycin (100 μg ml^{-1}) and human recombinant FGF-2 (0-100 ng ml^{-1} as indicated in the results, Prepotech) at 37°C in a humidified atmosphere at 5% CO_2 for time periods such as indicated in the results. Medium was replaced after 4 days.

For MMP inhibition experiments 1.7% TG-PEG hydrogels were cultured for 7 days in full medium containing 50 ng ml^{-1} FGF-2 and the following chemical MMP-Inhibitors at 10 or 100 μM: GM6001 (Calbiochem, 364206), MMP-2 Inhibitor III (Calbiochem, 444288), MMP-9 Inhibitor I (Calbiochem, 444278).

Characterization of hydrogel stiffness by in situ rheometry

Hydrogel gelation was analyzed on a rheometer (MCR 301, Anton Paar) equipped with 20 mm plate–plate geometry (PP20, Anton Paar) at RT and under humidified atmosphere. After adding FXIIIa to a reaction of 100 μl, containing precursors in stoichiometrically balanced amounts (8-PEG-Gln and 8-PEG-MMP-sensitive-Lys, 1 - 3% w/v), the mixture was quickly vortexed and precisely loaded onto the center of the bottom plate. The upper plate was lowered to a measuring gap size of 0.2 mm, ensuring proper loading of the space between the plates according to DIN 51810-1 and the dynamic oscillating measurement was started. The evolution of storage and loss moduli at a constant angular frequency of 0.5 rad/s and constant shear strain of 0.1% was recorded for 30 min.

Immunofluorescence and confocal laser scanning microscopy (CLSM)

For immunofluorescence staining of ECM components, primary antibodies were added directly to the medium of cultures and incubated for 4 hours at growth conditions. Afterwards, hydrogels were washed twice with PBS followed by fixation in 4% PFA for 30 min at RT. Next, gels were washed for 1 hour with PBS and incubated with the corresponding secondary antibodies and with Rhodamine phalloidin (Molecular Probes 1:500) in PBS containing 1% BSA (Albumin Fraction V, AppliChem) for 4 hours at RT.

For immunofluorescence staining of CD31, hydrogels were washed once with PBS followed by fixation in 4% PFA for 30 min at RT. Fixed gels were washed twice with PBS and permeabilized in 0.3% Triton X-100/PBS (Sigma) containing 1% BSA (Albumin Fraction V, AppliChem) for 30 min at RT. Afterwards, hydrogels were incubated with a primary antibody to CD31 in 1% BSA/PBS

over night at 4°C. Next, gels were washed 1 hour with PBS and incubated with the corresponding secondary antibody and with Rhodamine phalloidin (1:500) in PBS containing 1% BSA (Albumin Fraction V, AppliChem) for 4 hours at RT.

For co-stains of ECM components and CD31, primary antibodies to ECM components were added directly to the medium of cultures and incubated for 4 hours at growth conditions. Afterwards, hydrogels were washed twice with PBS followed by fixation in 4% PFA for 30 min at RT. Fixed gels were washed twice with PBS and permeabilized in 0.3% Triton X-100/PBS (Sigma) containing 1% BSA (Albumin Fraction V, AppliChem) for 30 min at RT. Afterwards, hydrogels were incubated with a primary antibody to CD31 in 1% BSA/PBS over night at 4°C. Next, gels were washed 1 hour with PBS and incubated with the corresponding secondary antibodies and with SiR-Actin (Spirochrome 1:1000) in PBS containing 1% BSA (Albumin Fraction V, AppliChem) for 4 hours at RT. Finally, stained hydrogels were washed with PBS for 3 h prior to image acquisition. Confocal images were acquired by an inverted laser-scanning microscope (TCS SP5, Leica). Images were processed with ImageJ software (Fiji version 1.48.u, April 2014) and are depicted as projections of Z-stacks. To quantify the overall length of CD31-positve structures 100 μm Z-stacks were taken by recording 25 planes at 4 μm Z-steps. Images were Z-projected and measured by the AngioQuant tool[198] in Matlab (version R2013b, MathWorks Inc, USA). The overall length of CD31-positive structures was normalized on the image area (mm mm^{-2}). Mean values were compared by one-way analysis of variance (ANOVA) using GraphPad Prism (GraphPad software version 5.04, San Diego California, USA) followed by Bonferroni's post hoc test to judge statistical significance. Statistical significance was accepted for $p < 0.05$.

Fibronectin knockdown experiments

BM-MSC were seeded in MEM alpha supplemented with FBS, penicillin, streptomycin at 50000 cells per 12-well. 24 hours post seeding, knockdown was initiated following the standard protocol of lipofectamin RNAiMAX (Invitrogen): 20 pmol siRNA were premixed for 5 min with 3 μl lipofectamine in 100 μl OptiMEM (Invitrogen) and added to cells for a final concentration of 20 nM. The following silencer select siRNAs were used: Negative control No 1 siRNA (4390843, Ambion), FN1 siRNA: A (ID: s223585, 4427037, Ambion), B (ID: s223586, 4427037, Ambion), C (ID: s5321, 4427037, Ambion).

After 48 hours of incubation, the knockdown efficiency was evaluated by Western blot analysis. The fibronectin signal intensities were quantified by the *gels* tool of ImageJ software (Fiji version 1.48.u, April 2014) and normalized to tubulin signal intensities. For spreading experiments, knockdown and control cells were obtained after 48 h of knockdown and embedded in 1.7% TG-PEG hydrogels containing 0 or 50 μM RGD at a cell concentration of 1 Mio ml^{-1}. After 3 days of culture hydrogels were immunostained for FN and F-actin as described above. To quantify the cellular spreading 100 μm Z-stacks of F-actin stainings were taken by recording 10 planes at 10 μm Z-steps. Images were Z-projected, binarized and automatically measured by the *analyze particles* tool of ImageJ software (Fiji version 1.48.u, April 2014). The spreading index is the inversion of cell circularity = 1-circularity ($4pi(area/perimeter^2)$); a value of 0 indicates a perfect circle, a value

of 1 indicates an increasingly elongated shape.

Transmission electron microscopy (TEM)

For TEM microscopy, hydrogels were washed once with PBS followed by fixation in 2.5% glutaraldehyde in 0.1 M sodium cacodylate buffer (pH 7.4, 540 mOsmol kg^{-1} H_2O). Hydrogels were washed 3 times in 0.1 M sodium cacodylate buffer (pH 7.4, 340 mOsmol kg^{-1} H_2O) and postfixed in 1% OsO_4 (in 0.1 M sodium cacodylate buffer pH 7.4, 340 mOsmol kg^{-1} H_2O). Hydrogels were again washed 3 times in 0.1 M sodium cacodylate buffer (pH 7.4, 340 mOsmol kg^{-1} H_2O) and subsequently gradually dehydrated by an increasing concentration series of ethanol as follows: 70%, 80%, 90%, 96% for 30 min and finally twice in 99% and 100% for 15 min. Last, ethanol was replaced by 100% acetone. Finally, specimens were embedded in epoxy resin. Ultrathin sections were obtained at 70 nm thickness on a microtome (Ultracut S, Reichert) and images were obtained using an electron microscope (EM 400T, Philips) and Morada Soft Imaging System (Olympus).

FACS separation, RNA-Sequencing and DEG Analysis

BM-MSCs from 3 different donors were encapsulated in monoculture (1.5 Mio ml^{-1}) or 1:1 co-culture with HUVEC (1.5:1.5 Mio ml^{-1}) within 1.7% TG-PEG hydrogels and cultured in medium containing MEM alpha, FCS (10%), penicillin (100 U ml^{-1}), streptomycin (100 μg ml^{-1}) and human recombinant FGF-2 (50 ng ml^{-1}) at 37°C in a humidified atmosphere at 5% CO_2 for 7 days. Medium was exchanged after 4 days. To retrieve BM-MSC, hydrogels were degraded in 0.5 mg ml^{-1} collagenase A (Sigma, 11088793001) at 37 °C for 60-90 min. Next, cells were washed once in FACS buffer (PBS, 1 mM EDTA, 2% FCS) and incubated for 2 min in trypsin-EDTA (Gibco, 25300062) at 37°C. Cells, were washed twice in FACS buffer and stained with a monoclonal PE-labeled CD31-antibody for 45 min at 4 °C. Cells were washed twice and resuspended in FACS buffer. Cell viability was assessed by SYTOX blue and red stain (Molecular Probes, 1:1500). CD31-positive and CD31-negative cells were separated by the cell sorter BD FACSAria III (BD Bioscience). CD31-negative cells were collected, washed once in PBS and lysed in the RLT-buffer from RNeasy Micro Kit (Qiagen). Subsequently, total RNA was isolated from cells following the manufacturer's instructions.

Next, quality of the RNA was assessed with the Agilent TapeStation 4200. Concentration was determined with RiboGreen (Life Technologies) and measured on the Infinite M1000 Pro plate reader (Tecan). 200 ng total RNA were used for RNA-seq library prep with the TruSeq Stranded mRNA Library Prep Kit (Illumina) according to manufacturer's specifications. Libraries were pooled and sequenced SR81 with the Illumina NextSeq 500 system using the High Output Kit v2 (75 cycles). Primary data analysis was performed with the Illumina RTA version 2.4.11, bcl2fastq v2.18.0.12.

Starting from the raw .fastq files the reads were mapped against the human reference genome and simultaneously soft-clipped using the STAR aligner (version 2.4.0). Standard quality control (Picard, RSeQC, QoRTs) was run to assess the quality of the resulting alignments. Subsequently, strand-specific (reversely stranded) read counting was performed using featureCount (subread,

version 1.5.0). To avoid technical artifacts the data were filtered such that genes where the average over all samples was less than 5 counts were removed. This resulted in 40980 transcripts removed out of 57825 in total, leaving 16845 transcripts for further analysis. Transcripts were mapped to HGNC symbols and ENTREZID's using the org.Hs.eg.db package version 3.4.0. Differential expression was modeled using generalized linear regression of the negative binomial family, as implemented in the DESeq2 package[199] of the R environment for statistical computing[200]. A list of differentially expressed genes (DEG) was compiled with identified genes having a false discovery rate less than 0.01. and fold change of more than of 2.

Functional enrichment maps were generated as described previously[201, 202]. Over-representation of gene ontology terms was calculated for the list of DEG using High-Throughput GoMiner[203]. One thousand randomizations were performed and data were thresholded for a 0.05 false discovery rate. Over-represented terms with ≥5 and ≤500 assigned genes were reported. Fold change values were mapped onto genes assigned to each over-represented term, and the data matrix was subjected to hierarchical clustering analysis on the basis of uncentred Pearson correlation and a complete-linkage matrix using Cluster 3.0[204]. Clustered data were visualized using Java TreeView[205].

Quantitative real-time PCR (qRT-PCR)

BM-MSCs or ASCs in monoculture (1.5 Mio ml^{-1}) or 1:1 co-culture with HUVECs or ECFCs (1.5:1.5 Mio ml^{-1}) were encapsulated in 1.7% TG-PEG hydrogels and cultured in medium containing MEM alpha, FCS (10%), penicillin (100 U ml^{-1}), streptomycin (100 μg ml^{-1}) and human recombinant FGF-2 (50 ng ml^{-1}) at 37°C in a humidified atmosphere at 5% CO_2 for 7 days. Medium was exchanged after 4 days. RNA from retrieved and separated BM-MSC or ASC was obtained as described above. For quantitative real-time PCR (qRT-PCR) 300 ng RNA were converted into 80 ul cDNA by means of the High-Capacity cDNA Reverse Transcription Kit (Applied Biosystems). qRT-PCR was carried out using 1.5 ul cDNA template, the TaqMan Universal PCR Master Mix (Applied Biosystems) and the Viia 7 Real-Time PCR System (Applied Biosystems). The following TaqMan primer/probe sets were used for gene expression tests: Hs00266237_m1 (COL4A1), Hs01098873_m1 (COL4A2), Hs00181017_m1 (COL18A1), Hs00609133_m1 (COL5A1), Hs01555669_m1 (COL5A3), Hs01081432_m1 (SDC2), Hs00915875_m1 (NID1), Hs00201233_m1 (NID2), Hs01128537_m1 (NOTCH3), Hs00943809_m1 (COL3A1), Hs00169777_m1 (PECAM1), Hs00164099_m1 (COL1A2), Hs00234160_m1 (SPARC), Hs00165078_m1 (LAMB3), Hs00267056_m1 (LAMC1), Hs00935293_m1 (LAMA4), Hs01019589_m1 (PDGFRB), Hs01070032_m1 (JAG1). Data were normalized on the expression of the following genes Hs02758991_g1 (GAPDH), Hs03044281_g1 (YWHAZ) and Hs00265885_g1 (EEF1A1) relative gene expression was calculated by the comparative Ct method.

Jagged1 modified PEG-hydrogels

Recombinant human Jagged1-Fc Chimera (R&D Systems, 1277-JG-050 FC-IgG) or control IgG1 Fc-fragment (R&D Systems, 110-HG-100 FC-IgG) were immobilized to TG-PEG hydrogels to a final

molar concentration of 70 nM by a 30 min pre-incubation step with 5 μM (final molar concentration) of Gln-ZZ protein (previously characterized[177]). ZZ is a synthetic protein A analogue with super high affinity to the Fc-fragment of immunoglobulins. The FXIIIa mediated immobilization of the Gln-ZZ-Fc-Jagged1 protein complex to TG-PEG leads to the presentation Jagged1 within hydrogels. BM-MSCs were encapsulated at 3 Mio ml^{-1} in Jagged1 or IgG modified TG-PEG hydrogels (1.7% w/v, 50 μM RGD) and cultured in medium containing MEM alpha, FCS (10%), penicillin (100 U ml^{-1}), streptomycin (100 μg ml^{-1}) and human recombinant FGF-2 (50 ng ml^{-1}) at 37°C in a humidified atmosphere at 5% CO_2 for 7 days. Medium was exchanged after 4 days. RNA extraction and qRT-PCR were done as described above.

Antibodies

Antibody	Application/Dilution	Catalog Number
Mouse anti-CD31	ICC 1:150	BD Bioscience 555444
Rabbit a-CD31	ICC 1:50	Abcam ab28364
Mouse a-FN (IST9 to the ED-A domain present in cellular FN)	ICC 1:300	Santa Cruz sc59826
Mouse a-Col1	ICC 1:150	Abcam ab90395
Rabbit a-Col3	ICC 1:150	Abcam ab7778
Mouse a-Col4	ICC 1:150	Abcam ab6311
Mouse a-HSPG-2	ICC 1:200	Abcam ab23418
Rabbit a-Laminin 1+2	ICC 1:150	Abcam ab7463
Goat a-mouse-488	ICC 1:200	Abcam ab150113
Goat a-rabbit-488	ICC 1:200	Abcam ab150077
Goat a-rabbit-568	ICC 1:200	Abcam ab175471
Goat a-mouse-555	ICC 1:200	Biolegend 405324
Mouse a-alpha-Tubulin	WB: 1:2000	Sigma T-5168
Mouse a-FN (IST4)	WB 1:1000	Sigma F-0916
Goat a-mouse-HRP	WB 1:2000	DAKO P0447
Mouse a-CD31-PE	Flow cytometry 1:50	BD Bioscience 560983
Mouse IgG1, k isotype control-PE	Flow cytometry 1:50	BD Bioscience 556650

Acknowledgments

We would like to thank Marcy Zenobi-Wong (ETH Zurich) and Philipp Fisch (ETH Zurich) for support with rheology measurements, Christian Beisel (Genomics Facility Basel, ETH Zurich) for support on RNA sequencing, Michael Prummer (NEXUS, ETH Zurich) for differential gene expression analysis, Werner Graber (University of Bern) for TEM microscopy and Anette Schütz (Flow Cytometry Core Facility Zurich) for cell sorting. This work has been supported by the European Union's Seventh Framework Programme (iTERM grant agreement No. 607868) and by the Swiss National Science Foundation (310030-169808/1).

Supporting figures

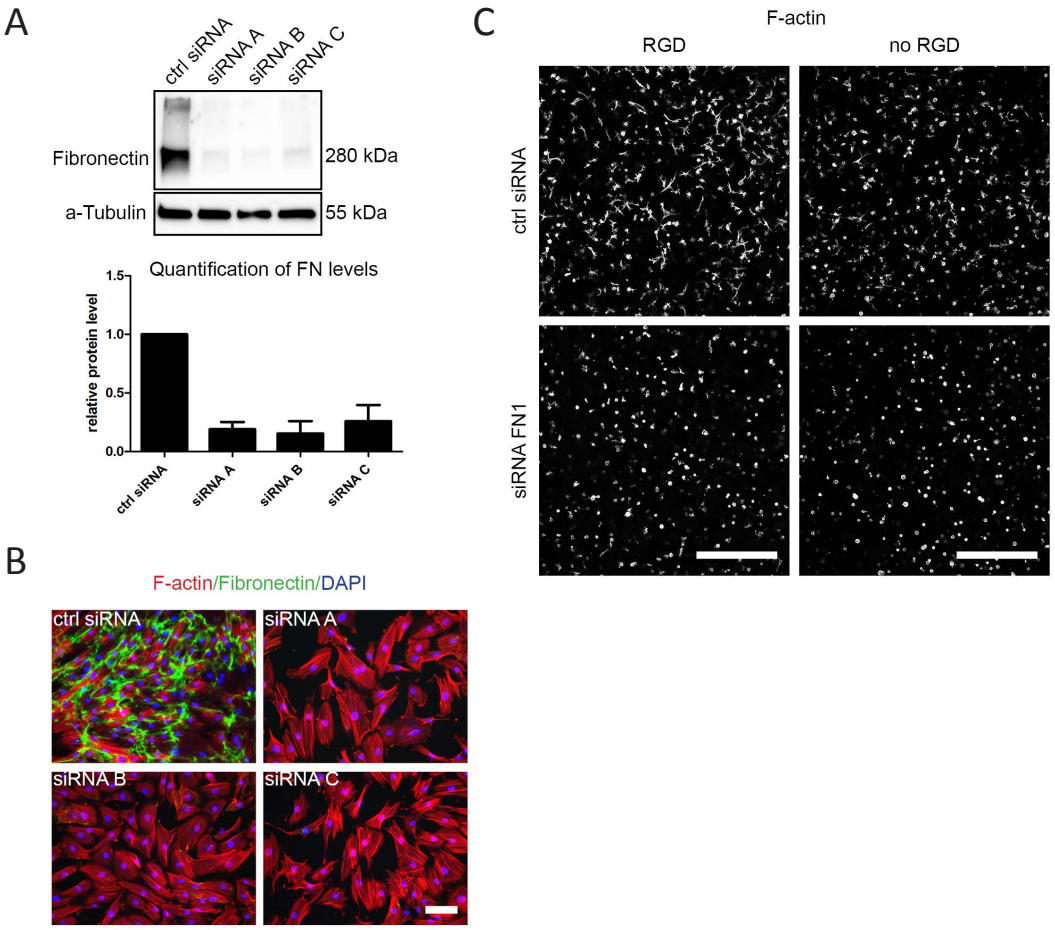

Figure S1: Fibronectin is knocked-down in BM-MSC by siRNA gene silencing. A) Efficiency of siRNA caused fibronectin knockdown in BM-MSC analyzed by Western Blot analysis 48h after knockdown initiation. Quantification shows the western blot signal intensity of fibronectin normalized to a-tubulin. (mean ± SD; n= 4 donors). B) Absence of cellular fibronectin networks analyzed by immunofluorescence of cell-derived fibronectin 3 days after knockdown. Scale bar, 100 μm. C) Representative image as used for quantification of spreading of control siRNA and fibronectin knockdown BM-MSCs within RGD-modified and RGD-free TG-PEG hydrogels after 3 days of culture. Images display projections of 100 μm Z-stacks of F-actin stained samples. Scale bar, 500 μm.

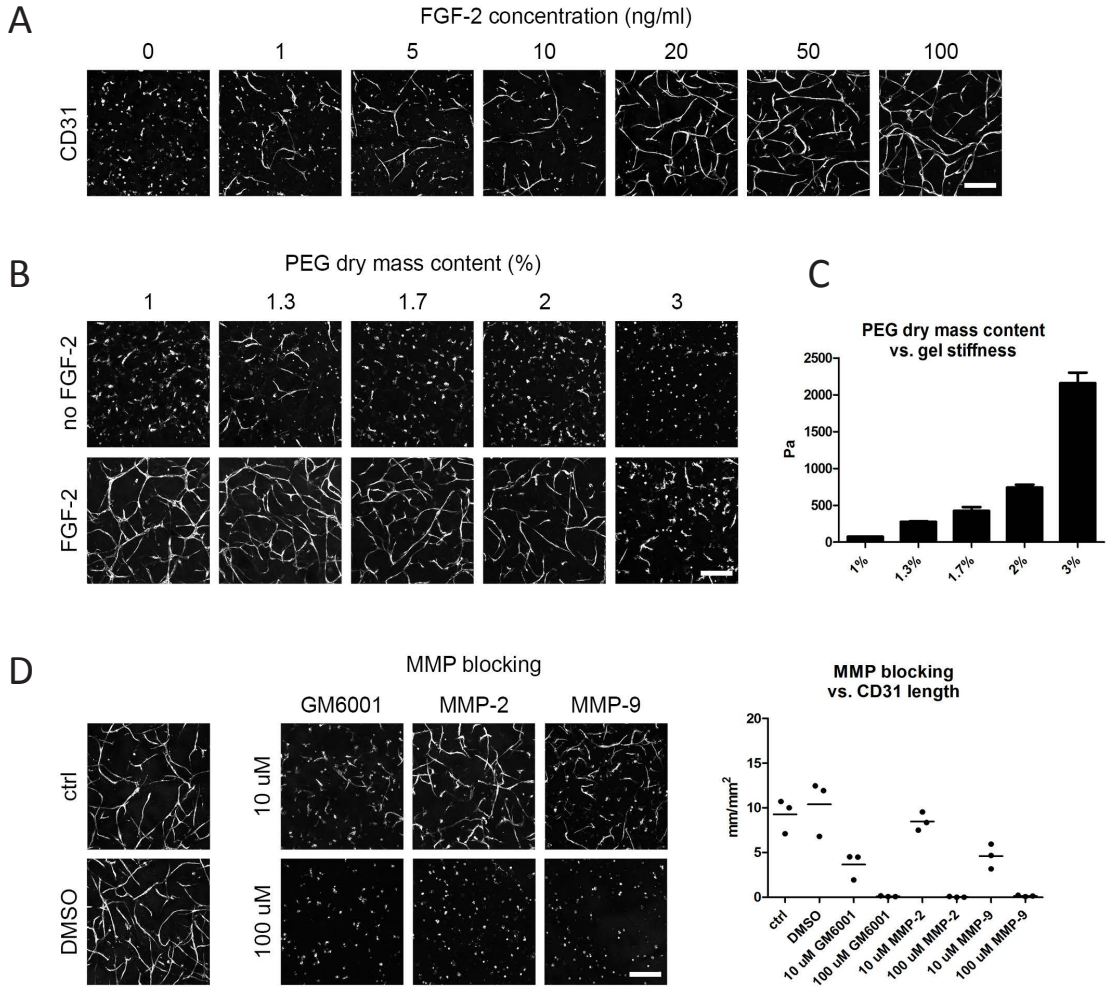

Figure S2: 3D micro-capillary network formation in PEG-hydrogels is FGF-2-, matrix stiffness- and MMP-dependent. Representative images of CD31-immunostained micro-capillary networks. All images depict Z-projections of 100 µm Z-stacks and are obtained after 7 days of culture. Scale bars, 200 µm. Impact of A) FGF-2 concentration (ng/ml) in the medium, B) physical matrix properties and D) MMP-activity on micro-capillary network formation in ECM mimics. C) Correlation of PEG dry mass content and matrix stiffness assessed by rheological measurement of the corresponding storage moduli. (Bars represent mean values ± SD of n = 3 experiments). D) Quantitative analysis of the MMP-inhibition effect on the absolute length of CD31-positve micro-capillary networks. Individual data points and mean (line), n = 3 samples from 3 donors. ANOVA with Bonferroni's post hoc test: All MMP-blocking conditions except 10 µM MMP-2 are significantly reduced compared to control and DMSO control groups.

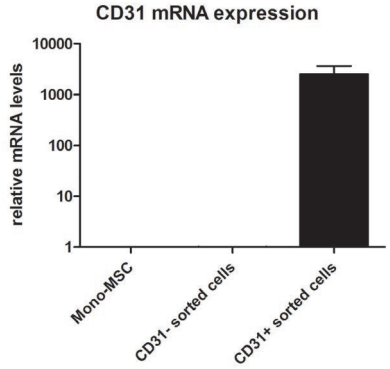

Figure S3: **CD31 mRNA expression (qRT-PCR) of monocultured BM-MSC, CD31-negative and CD31-positive isolated cells from FACS sorting.** CD31 mRNA expression in FACS separated cell populations after 7 days of culture in PEG-hydrogels. Bars represent mean values ± SD of n = 3 donors. ANOVA with Bonferroni's post hoc test: CD31-positive sorted cells are significantly different from both other conditions with ** $p < 0.01$.

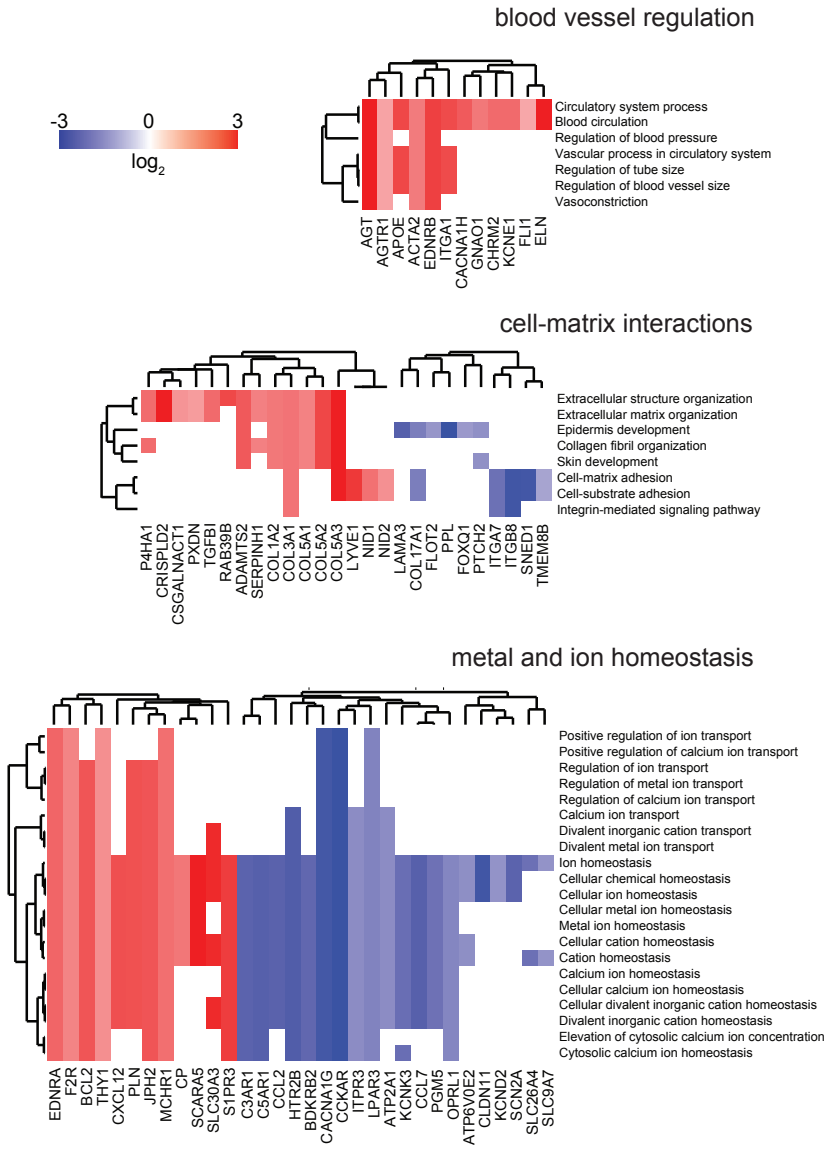

Figure S4: Functional enrichment map of differentially expressed genes (DEG) in perivascular BM-MSCs. Genes identified as DEG following transcriptome analysis are enriched and clustered by the gene ontology domain GO Biological Process. Up- and downregulated genes in perivascular BM-MSC are displayed in red and blue, respectively. GO Biological Process clusters show clusters of blood vessel regulation, cell-matrix interactions and metal and ion homeostasis.

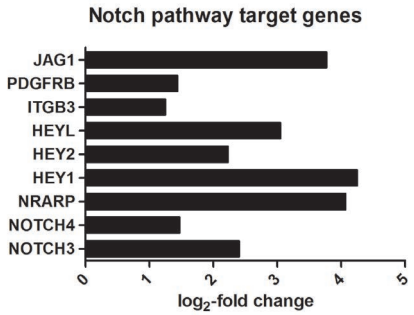

Figure S5: Induction of Notch pathway target genes in perivascular BM-MSCs. Genes identified by transcriptome analysis as differentially expressed genes in perivascular BM-MSCs compared to monocultured BM-MSCs.

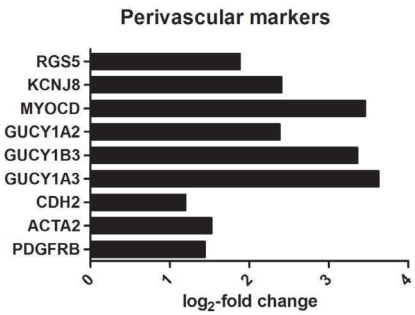

Figure S6: Induction of perivascular marker genes in perivascular BM-MSCs. Genes identified by transcriptome analysis as differentially expressed genes in perivascular BM-MSCs compared to monocultured BM-MSCs.

Chapter III:

Dual role of mesenchymal stem cells allows for micro-vascularized bone tissue-like environments in PEG hydrogels

The content of this chapter is published as full article: U. Blache, S. Metzger, Q. Vallmajo-Martin, I. Martin, V. Djonov and M. Ehrbar (2016): Dual role of mesenchymal stem cells allows for micro-vascularized bone tissue-like environments in PEG hydrogels; *Advanced Healthcare Materials* 5 (4): 489-498

Abstract

In vitro engineered tissues, which recapitulate functional and morphological properties of bone marrow and bone tissue, would be desirable to study bone regeneration under fully controlled conditions. Among the key players in the initial phase of bone regeneration are mesenchymal stem cells (MSCs) and endothelial cells (ECs) that are in close contact in many tissues. Additionally, the generation of tissue constructs for in vivo transplantations has included the use of ECs since insufficient vascularization is one of the bottlenecks in (bone) tissue engineering. Here we show that 3D co-cultures of human bone marrow derived MSCs (hBM-MSCs) and human umbilical vein endothelial cells (HUVECs) in synthetic biomimetic poly(ethylene glycol) (PEG)-based matrices can be directed towards vascularized bone mimicking tissue constructs. In this environment, bone morphogenetic protein-2 (BMP-2) or fibroblast growth factor-2 (FGF-2) promotes the formation of vascular networks. However, while osteogenic differentiation is obtained with BMP-2, the treatment with FGF-2 suppressed osteogenic differentiation. Thus, our study shows that co-cultures of hBM-MSCs and HUVECs in biological inert PEG matrices can be directed towards bone and bone marrow-like 3D tissue constructs.

Introduction

Despite the regeneration and self-healing capacity of bone tissue 5-10% of all bone fractures do not heal properly and lead to delayed unions or nonunions[206]. Moreover, the regeneration of bone tissue can be impaired due to pathological reasons such as infections, tumors or necrosis[207]. Thus, osteogenic grafts, which could replace missing or defective bone tissue, have been generated by combining mesenchymal stem cells (MSCs) with 3-dimensional (3D) biomimetic materials. To accelerate the engraftment and improve the survival of such engineered bone tissues, the focus has recently been directed towards their pre-vascularization[208-214]. Additionally and equally important, the acquiring of knowledge on vascularization of bone mimicking tissues in combination with novel tailorable biomaterials and advanced 3D manufacturing processes will make the creation of physiologically relevant in vitro bone models become tangible. Such models would allow for the study and testing of healing inducing treatments under fully defined and reproducible experimental conditions.

Bone is a highly vascularized tissue whose development and regeneration is tightly regulated by the presence of vascular structures. Moreover, MSCs have been shown to reside in the perivascular niche[19, 22]. This indicates that the vascular microenvironment influences the mobilization and differentiation behavior of MSCs and serves as a repository for mesenchymal tissue forming cells, which is activated during tissue healing processes[215]. Thus due to various reasons bone tissue engineering needs to consider osteogenic and vasculogenic processes in a tightly intertwined fashion[216].

3D bone tissue models should at least partially recapitulate properties of the native tissue microenvironment, which is the sum of cues provided by neighboring cells, extracellular matrix (ECM) signals as well as growth factor presentation and physical cues. These microenvironments have been recapitulated by culturing bone cells in ECM derived hydrogel materials such as collagen, fibrin, matrigel or glycosaminoglycans. However, ECM components, due to their inherent biological signals can either trigger biological or cover cellular responses. Particularly, when focusing on the role of ECM producing cells such as MSCs the use of ECM free hydrogels seems to be appropriate.

Synthetic hydrogels such as poly(ethylene glycol) (PEG) avoid biological interferences and enable the study of cells on a blank slate. As PEG hydrogels are formed under chemically controlled conditions they can readily be modified towards specific requirements[49, 90, 217, 218]. We and others have successfully used mouse or human mesenchymal cells to support the culture of human endothelial cells in synthetic proteolytically-degradable PEG hydrogels[91-93, 219-221]. However, vascularized tissue models that allow for the study of osteogenesis have not been described in PEG hydrogels.

Here, we combine a fully synthetic 3D PEG system with hBM-MSCs and HUVECs towards the establishment of an artificial vascularized bone tissue-like environment. Towards this aim we employ a previously established transglutaminase (FXIII) cross-linked PEG hydrogel that enables cell adhesion by RGD presentation and cell migration by MMP-sensitive cleavage sites[174, 222, 223]. In doing so, we make use of the dual role of MSCs, which is their ability to give rise to osteogenic cells

and their ability to support endothelial cells. We demonstrate that hBM-MSCs enable HUVECs in self-organized co-cultures to build lumenized microvascular structures in synthetic PEG hydrogels. Additionally, we show that at the same time hBM-MSCs in 3D co-cultures can be differentiated towards bone by the bone morphogenetic protein-2 (BMP-2) or prevented from differentiation by the fibroblast growth factor 2 (FGF-2). Hence, by combining MSCs with endothelial cells in a synthetic 3D environment we provide a vascularized tissue-like construct that can be differentiated towards bone or maintained in a non-differentiated state.

Results & Discussion

Mesenchymal stem cells enable microvascular-like structures in synthetic PEG hydrogels

To establish bone tissue-like constructs, fully synthetic, factor XIII polymerized PEG (TG-PEG) hydrogels containing matrix metalloproteinase (MMP) degradable linker sequences were used as blank slate (**Fig. 1**). Together with the immobilized prototypic integrin binding site RGD these low stiffness hydrogels (30-250 Pa) provide minimal requirements for the adhesion, spreading and migration of mesenchymal cells[174, 222, 223].

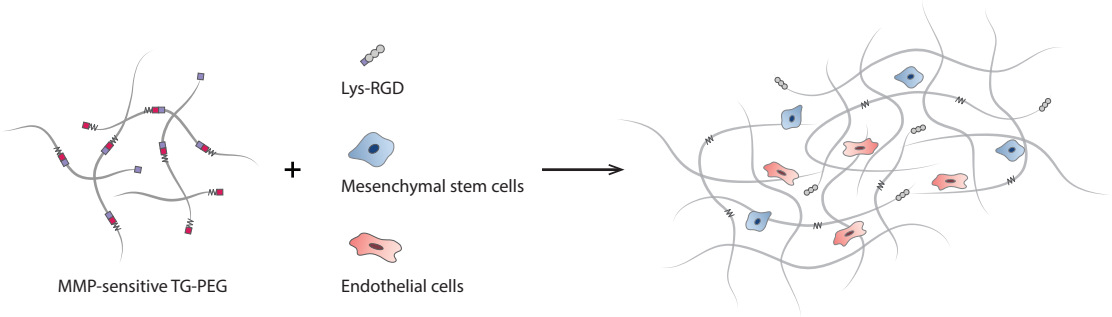

Figure 1: Scheme of the artificial minimal 3D tissue-like environment. TG-PEG hydrogels are formed by the cross-linking of 8-PEG-$MMP_{sensitive}$-Lys and 8-PEG-Gln precursors via FXIIIa transglutamination. The cell adhesion peptide Lys-RGD is cross-linked into the gel at the same time. Endothelial cells and mesenchymal stem cells (MSC) are 3D encapsulated in TG-PEG hydrogels during the gelation process.

To study the interactions of hBM-MSCs and HUVECs within our TG-PEG hydrogels we 3D encapsulated single cell suspensions of both cell types individually or as co-culture in a 1:1 ratio. Cultures were conducted in presence of the pro-vasculogenic and pro-mesenchymal growth factor FGF-2. While the formation of cellular networks was determined after 3 days of culture **(Fig. 2a**), cellular dynamics were continuously evaluated by time-lapse microscopy (**Fig. S1,** supporting figures are found at the end of this chapter and at pages 55-56). In accordance with the study by Moon et al.[91], where a 10-fold higher concentration of cells in a similar MMP-sensitive but UV-cross-linked PEG hydrogel matrix was used, we show that HUVECs in mono-culture do actively migrate in our MMP-sensitive PEG hydrogels for an initial phase of 24 h (**Fig. S1A**). However, in this ECM-free environment HUVECs do not fuse into cord-like structures as shown by F-actin visualization and immunofluorescence staining of the endothelial-specific marker CD31 (**Fig. 2A, upper row**), indicating that in contrast to short-term mono-cultures in collagen[63] matrix related features are missing.

In contrast, hBM-MSCs comparable to other mesenchymal cells start spreading only a couple of

hours after encapsulation and form a stable cellular network when cultured as mono-culture in PEG hydrogels (**Fig. 2A, middle row** and **Fig. S1B**). Furthermore, when hBM-MSCs and HUVECs were co-cultured in a 1:1 ratio a cellular network was formed as well (**Fig. 2A, lower row** and **Fig. S1C**). The contribution of HUVECs to cellular networks in the co-culture can be identified by the endothelial-specific marker CD31 (**Fig. 2A** lower panel). While in hBM-MSC mono-cultures cellular networks are just positively stained for F-actin and are negative for CD31, in co-cultures CD31-positive stained HUVECs are part of the overall cellular network and form cord-like structures. In this way we show that HUVECs indeed fuse and form CD31-positive cord-like structures in the presence of hBM-MSC. Live/Dead staining of corresponding hydrogels support our observations by indicating that the amount of live cells in co-cultures was much higher than in HUVEC mono-cultures (see **Fig. 2B**). This is in agreement with previous studies in semi-synthetic hydrogels (PEG-Heparin, PEG-Collagen, GelMA) where the presence of mesenchymal cells including 10T1/2 cells, human fibroblasts and MSCs[74, 78, 85] supported the formation of microvascular structures by HUVECs or late outgrowth endothelial cells (OECs). Similarly, in fully synthetic hydrogels the presence of mesenchymal lineage cells could stabilize cord-like structures by HUVECs in vitro[91-93, 219-221]. Therefore, the presence of human BM-MSCs was necessary to support EC survival and facilitate the formation of viable microvascular-like structures in fully synthetic PEG hydrogels.

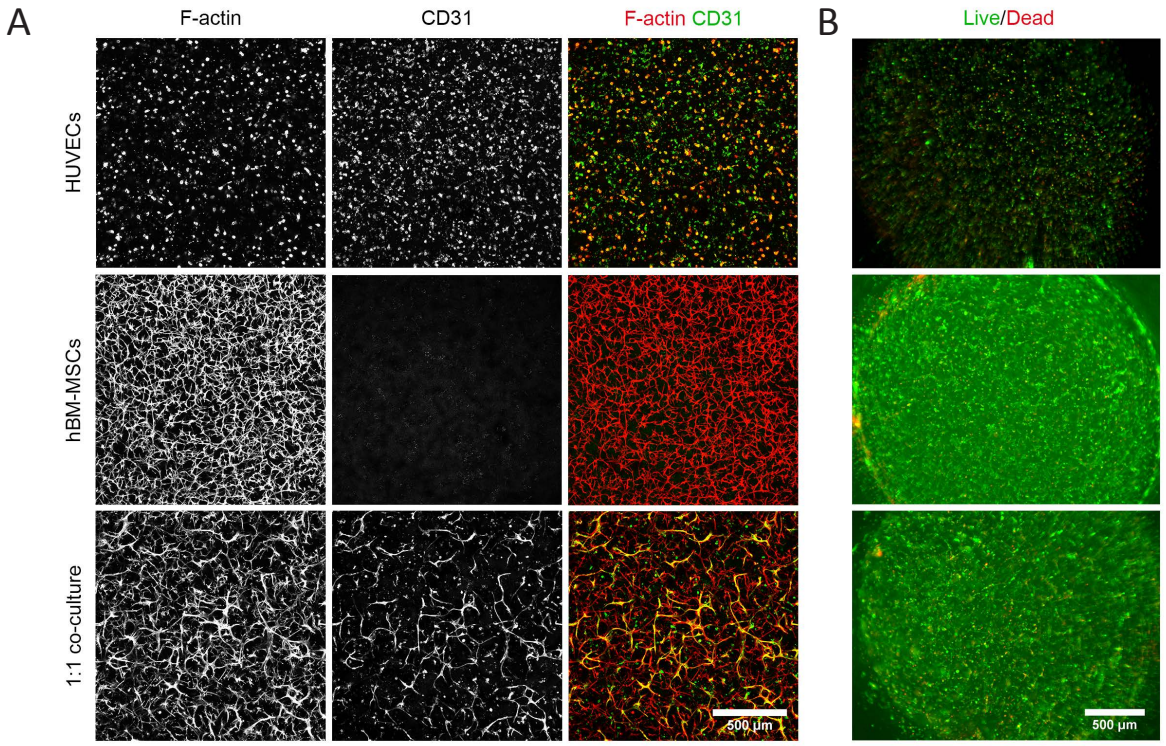

Figure 2: MSCs enable HUVECs to fuse into microvascular-like structures. A) Mono-cultures of HUVECs (upper row), MSCs (middle row) and 1:1 co-culture MSC/HUVEC (lower row) after 3 days of culture in PEG hydrogels. Cells have been stained for F-actin (red) and CD31 (green). Images depict Z-projections of confocal stacks through 150 µm. Scale bar: 500 µm. B) Live/Dead staining of corresponding hydrogels at day 6. Scale bar: 500 µm.

3D MSC mono-cultures can be osteogenically differentiated in synthetic PEG hydrogels

It is generally assumed that MSCs, much like the comparably better characterized hematopoietic stem cells, reside in their niche in an undifferentiated state and become mobilized by growth

factor signals. In the early phase of inflammation, factors such as the platelet derived growth factor (PDGF) are released from alpha granules and have been described to mobilize and attract MSCs[123, 224-226]. Subsequently, mitogenic factors such as FGF-2 encourage MSCs to proliferate. Interestingly, FGF-2 has been described not just to act as mitogenic factor on MSCs but also to maintain their stem cell capacity in vitro by suppressing lineage differentiation[227-231]. Therefore, FGF-2 has been used widely to expand MSCs in vitro. Once MSCs have been recruited to a wound BMP-2 stimulates the osteogenic differentiation of MSCs in the healing process. In order to mimic the differentiation behavior of mobilized MSCs in synthetic PEG hydrogels, mono-cultures of hBM-MSCs were 3D encapsulated and cultured for 14 days in presence of FGF-2 and/or BMP-2. As shown by alkaline phosphatase (ALP) enzyme activity, an early marker of osteogenic differentiation, BMP-2 promotes while FGF-2 does not induce the osteogenic differentiation of hBM-MSCs in hydrogels (**Fig. 3A**). The absence of osteogenic differentiation by FGF-2 was expected but interestingly FGF-2 also interferes remarkably with the BMP-2 induced ALP activity. This indicates that FGF-2 in herein used concentration could efficiently suppress the BMP-2 induced osteogenic differentiation of MSCs when applied simultaneously with BMP-2. These findings are consistent with the known function of FGF-2 to suppress osteogenic differentiation of MSCs in vitro and to maintain their stem cell capacity[228, 232, 233]. To further confirm the growth factor mediated differentiation behavior of hBM-MSCs in our PEG hydrogel we analyzed the mRNA expression levels of osteogenic markers including alkaline phosphatase liver/bone/kidney (ALPL), runt-related transcription factor 2 (RUNX2), osteopontin (SPP1) and osteocalcin (BGLAP) by qRT-PCR (**Fig. 3B**). While indeed all analyzed genes were significantly induced by BMP-2, FGF-2 did not result in any significant change compared to the control. Nevertheless, osteopontin and osteocalcin mRNA levels seem to be slightly increased by FGF-2. Therefore, our measured mRNA expression experiments confirm that the BMP-2 induced expression of the osteogenic markers is counteracted by FGF-2 when both growth factors were present at the same time. This result suggest that to take advantage of both the mitogenic effect of FGF-2 and the differentiation capacity of BMP-2 the sequential availability of FGF-2 and BMP-2 might be required for osteogenic MSC differentation. Indeed, a recent in vitro study showed that the sequential release of FGF-2 followed by BMP-2 from microspheres promoted ALP expression and osteogenic differentiation in low seeding density MSC cultures. In contrast the sequential release of BMP-2 followed by FGF-2 (as well as their parallel release) showed significantly less differentiation[234]. Taken together our results confirm that BMP-2 can stimulate the osteogenic differentiation of hBM-MSCs in fully synthetic PEG hydrogels comparably to what has been observed in other PEG hydrogel matrices[235, 236]. On the other hand, FGF-2 can be used to maintain hBM-MSCs in PEG gels in a non-osteogenic differentiated state. Moreover, while it has been shown that FGF-2 not only suppresses dedifferentiation of hBM-MSCs but also enhances their chondrogenic potential[237-240] we show in **Figure 3C** that 14 days after culture in FGF-2 hBM-MSCs can still be adipogenically and osteogenically differentiated indicating the maintenance of their multipotency.

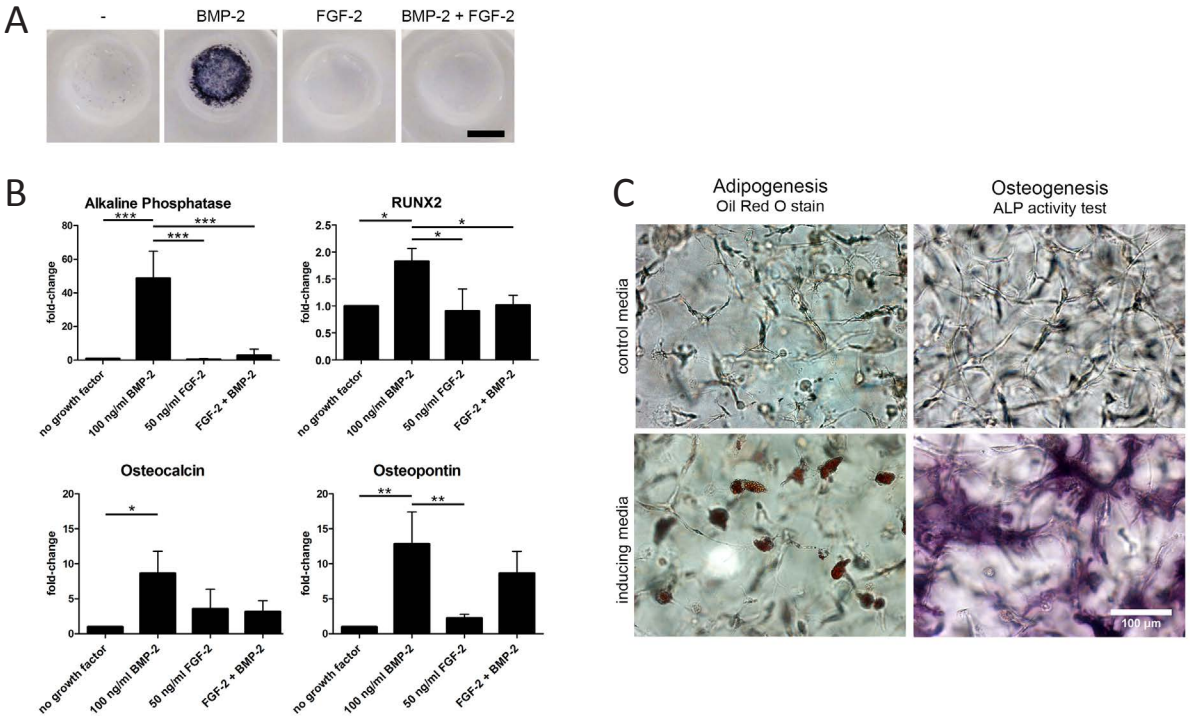

Figure 3: Osteogenic differentiation of MSC mono-cultures in PEG hydrogels. MSCs were cultivated for 14 days inside PEG hydrogels in the presence of BMP-2 (100 ng ml^{-1}) or/and FGF-2 (50 ng ml^{-1}) in the culture medium. A) Whole hydrogels were analyzed for the induction of ALP (purple color indicates ALP enzymatic activity). Scale bar: 3 mm. B) Gene expression of osteogenic markers in PEG hydrogels measured by means of qRT-PCR and normalized on GAPDH expression. Bars represent mean values ± SD, n = 3. One way ANOVAs: Alkaline Phosphatase, p = 0.0002; RUNX2, p = 0.0066; Osteopontin, p = 0.0024; Osteocalcin, p = 0.0172. Bonferroni's post hoc test * $p < 0.05$; ** $p < 0.01$; *** $p < 0.001$. C) After 14 days of FGF-2 culture in PEG hydrogels, MSCs can still be differentiated inside hydrogels. Lipid staining (Oil Red O) and ALP-activity test of control cultured and adipogenic or osteogenic induced hydrogels reveal differentiation capacity after 12 days of differentiation in 3D. Scale bar: 100 µm

MSCs can be osteogenically differentiated in 3D co-cultures with endothelial cells

To establish minimal 3D in vitro bone marrow-like and bone tissue-like environments we aimed to combine the supportive role of hBM-MSCs for ECs to form a vascular network with their potential for osteogenic differentiation (as shown individually in **Fig. 2 and Fig. 3**). Therefore, we established co-cultures consisting of hBM-MSCs and HUVECs and examined them for osteogenic differentiation in PEG hydrogels. Single cell suspensions of hBM-MSC of different donors and HUVECs were 3D encapsulated in hydrogels and cultivated for 14 days in the presence of BMP-2 and/or FGF-2. Subsequently, ALP activity was examined in these co-cultures (see **Fig. 4**). While mono-cultures of hBM-MSC without growth factors did not show ALP activity (**Fig. 3A**) we observed a basal activity of ALP in co-cultures without growth factors (**Fig. 4A**). It has been shown that HUVECs can produce BMP-2[241, 242] and induce ALP activity in BM-MSCs[241, 243], adipose-derived stem cells[242] and osteoblasts [244] when co-cultivated. However, in two of these studies it was also shown that HUVECs themselves have weak but detectable amounts of ALP[242, 243]. Importantly, when we actively differentiated co-cultures by means of BMP-2, ALP was strongly induced (**Fig. 4A**). Similar to our results for mono-cultures the effects of BMP-2 were disabled when co-cultures were simultaneously cultivated with BMP-2 and FGF-2. The opportunity to osteogenically differentiate co-cultures by BMP-2 as well as the counteracting effect of FGF-2 on BMP-2 in 3D co-cultures was

confirmed by quantitatively analyzing ALP activity (**Fig. 4B**). Moreover, we show that the pattern of differentiation by BMP-2 and its prevention by FGF-2 could be followed for 4 weeks of in vitro culture (**Fig. S2**).

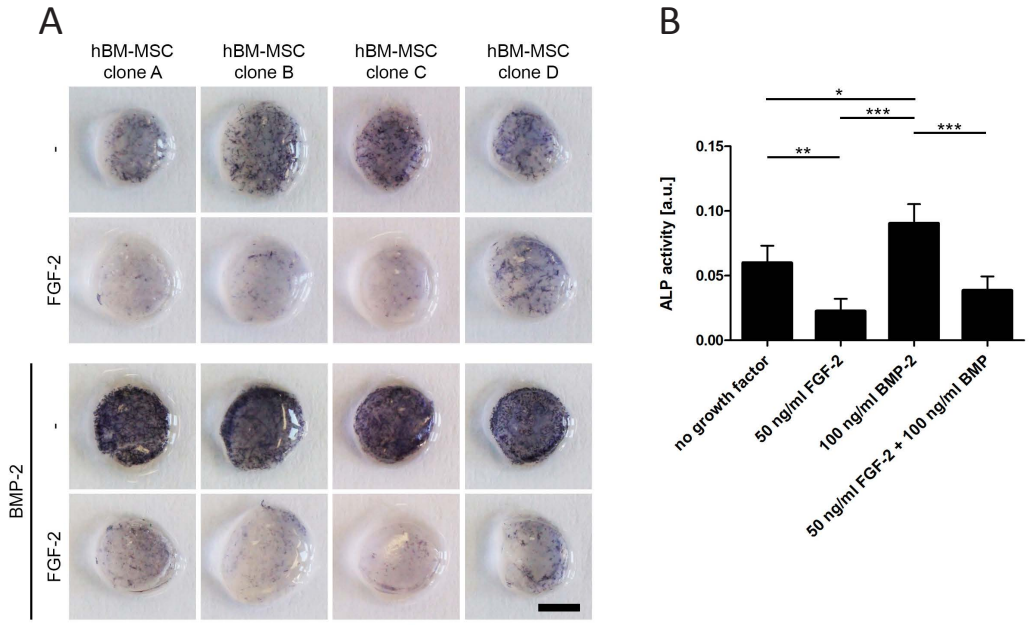

Figure 4: ALP activity of MSC/HUVEC co-cultures in PEG hydrogels. Co-cultures were cultivated for 14 days inside PEG hydrogels in the presence of BMP-2 (100 ng ml^{-1}) and/or FGF-2 (50 ng ml^{-1}) followed by analysis of ALP activity. A) Colorimetric evaluation of ALP induction in MSC/HUVEC 1:1 co-culture (purple color indicates ALP enzymatic activity) using 4 different MSC clones. Scale bar: 2 mm. B) Quantitative ALP activity assay in corresponding co-cultures. ALP activity values were normalized on DNA content of the samples. Bars represent mean values ± SD, n = 4. One way ANOVA p = 0.0001. Bonferroni's post hoc test * $p < 0.05$; ** $p < 0.01$; *** $p < 0.001$.

3D co-cultures can be directed towards osteogenically differentiated or undifferentiated vascularized constructs

In order to evaluate whether microvascular structures are present in our model after 14 days of osteogenic differentiation, co-cultures of hBM-MSCs and HUVECs were 3D encapsulated in PEG hydrogels and cultivated in the presence of BMP-2, FGF-2 or both factors. Subsequently, all cells were visualized by F-actin staining while HUVECs were specifically labeled by CD31. The effects of BMP-2 and FGF-2 on the formation of CD31-positive endothelial structures in 3D co-cultures are depicted as confocal Z-projections (**Fig. 5A)**. Experiments were carried out with different hBM-MSC donors and quantitatively analyzed based on the absolute length of all CD31-positive structures per area (**Fig. 5B**) and the average length of individual CD31-positive structures (**Fig. 5C**). While hydrogels cultivated in the absence of growth factors barely show cord-like structures, BMP-2 and FGF-2 induced the formation of CD31-positive microvascular-like structures. Our data show that BMP-2, similarly to the well-known pro-vasculogenic factor FGF-2, significantly enhances the formation of microvascular-like structures in 3D co-cultures. BMP-2 has previously been shown to promote angiogenesis ex vivo in mouse bones explants[245]. Moreover, in vitro BMP-2 directly activated ECs and promoted migration in transwell and scratch migration assays[246] as well as the formation of microvascular structures on matrigel[247, 248]. However, in our hydrogels the stimulation with BMP-2 or FGF-2 is not sufficient to support the formation of vascular structures by HUVECs in mono-cultures (**Fig. S1A**; data not shown for BMP-2). Thus, besides potential direct effects on

HUVECs, growth factor effects mainly rely on the presence of hBM-MSCs. Since the combination of BMP-2 and FGF-2 does not exert an additive effect concerning microvascularization, it is likely that in response to each factor the MSC-derived cues promote EC functions via similar but here not characterized mechanism. In our study, we show that BMP-2 and FGF-2 have a vasculogenic effect in 14 days old co-cultures. Additionally, we show microvascularization can be easily followed up to 4 weeks in PEG hydrogels (**Fig. S2**).

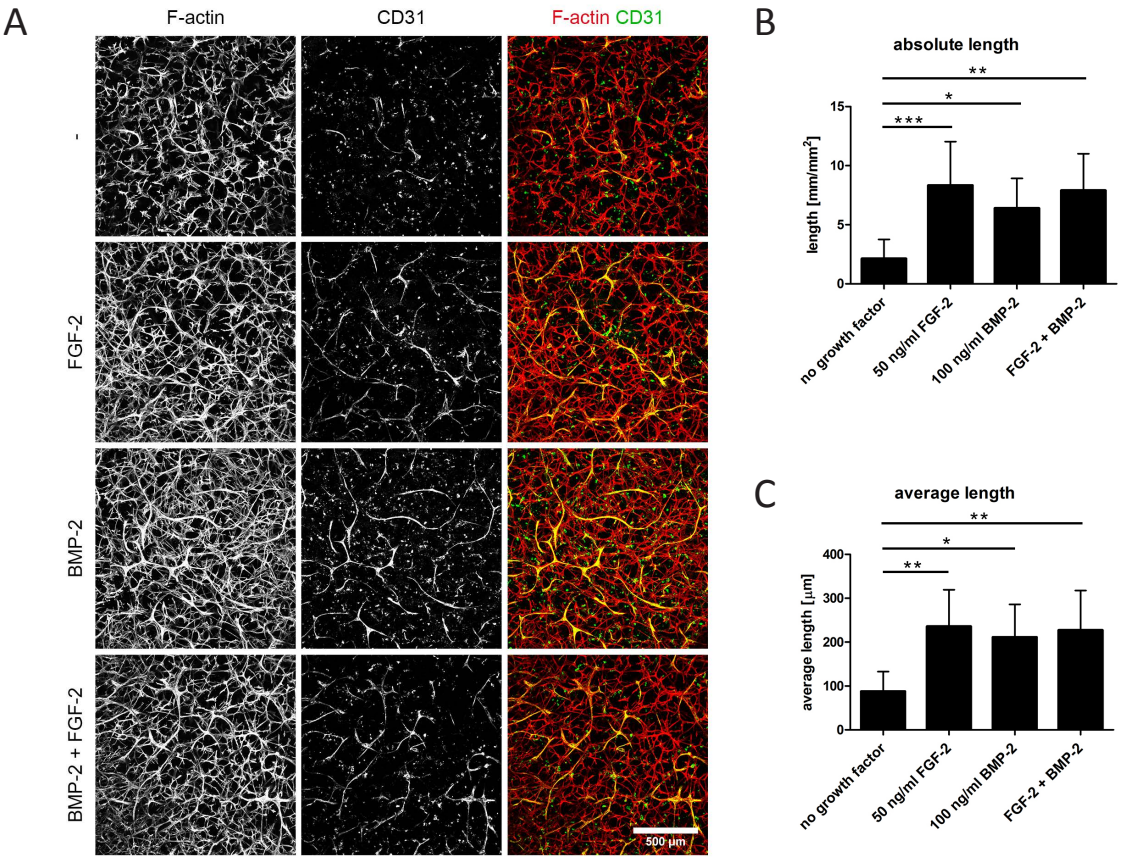

Figure 5: MSC/HUVEC co-cultures form microvascular structures in PEG hydrogels. Co-cultures of MSCs and HUVECs were cultivated for 14 days in the presence of BMP-2 (100 ng ml^{-1}) and/or FGF-2 (50 ng ml^{-1}) followed by F-actin (red) and CD31 (green) labeling. A) Images depict Z-projections of confocal stacks through 150 µm. Scale bar: 500 µm. B) Quantification of the absolute length of all CD31-positive microvascular structures/mm^2. Bars represent mean values ± SD, n = 8. One way ANOVA p = 0.0005. Bonferroni's post hoc test * p < 0.05; ** p < 0.01; *** p < 0.001. C) Quantification of the average length of single CD31-positive microvascular structures. Bars represent mean values ± SD, n = 8. One way ANOVA p = 0.0015. Bonferroni's post hoc test * p < 0.05; ** p < 0.01.

Co-cultures display microvascular-like phenotypes in PEG hydrogels

To gain further insight into established heterocellular interactions in vascularized micro-environments, we assessed the spatial arrangement of hBM-MSCs with respect to HUVECs and show the details of microvascular structures on the cellular level by confocal and transmission electron microscopy (**Fig. 6**). 3D reconstruction of confocal Z-stacks show that in both osteogenic differentiated and FGF-2 maintained cultures CD31-positive endothelial cells have fused into 3D distributed microvascular structures. As revealed by high-resolution confocal images hBM-MSCs align along and spread between the endothelial networks thereby providing support for microvascular structures.

During vasculogenesis and sprouting angiogenesis, newly formed vascular networks need to establish a continuous luminal space. In vitro and in vivo it has been shown that lumen formation in endothelial cells occurs by the generation and fusion of intracellular vesicles[62, 249]. High-magnification confocal images of our 3D co-cultures suggest the formation of lumen in microvascular structures as well as a perivascular localization of hBM-MSCs (**Fig. S3A**). In order to prove real vacuole formation in microvascular structures we further analyzed 3D co-cultures by means of transmission electron microscopy (**Fig. 6**). In fact, co-cultures display a capillary phenotype, including the formation of lumens in endothelial cells, their stabilization by perivascular localized hBM-MSCs, which are only separated by a basal membrane like ECM structure, and the deposition of ECM in the extracellular space (see also **Fig. S3B**). These structures are comparable to those observed when ECs were co-cultured with mesenchymal cells in ECM-derived hydrogels[58, 63, 250].

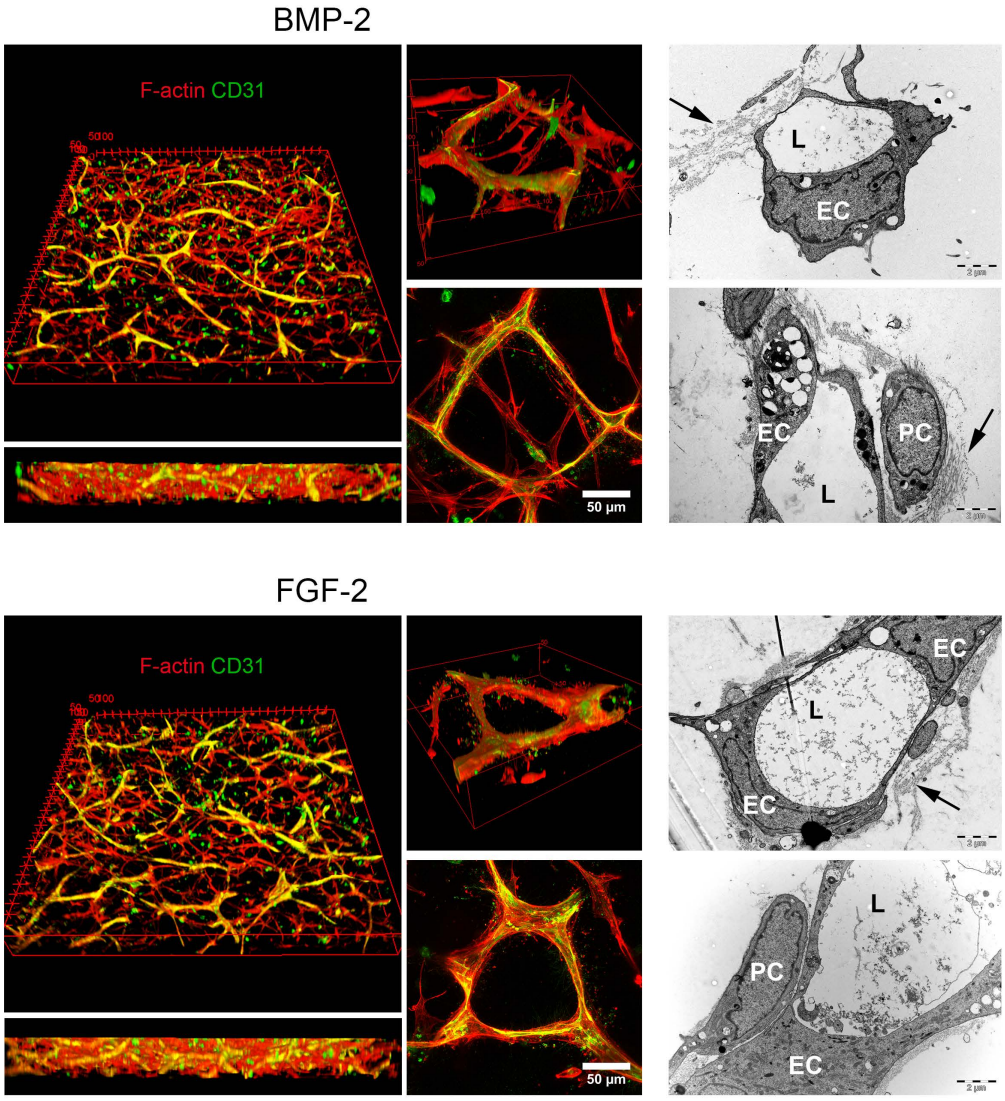

Figure 6: Morphology of microvascular structures in 14 days old co-cultures. Co-cultures have been cultivated in the presence of BMP-2 (upper panel) or FGF-2 (lower panel) and stained for F-actin (red) and CD31 (green). 3D reconstruction of confocal Z-stacks at low magnification (XYZ: 1.5 mm x 1.5 mm x 0.15 mm) and high magnification (XYZ: 246 µm x 246 µm x 50 µm). Lumen formation in microvascular structures and perivascular localization of MSCs are confirmed by transmission electron microscopy (L: Lumen; EC: Endothelial cells; PC: Perivascular cell; Arrows indicate ECM deposition). Scale bar TEM: 2 µm.

Synthetic materials based MSCs and ECs co-cultures as in vitro bone model

Importantly, our co-cultures are based on synthetic materials which do not contain any matrix components and only provide defined integrin signaling cues. Therefore all matrix associated and soluble signals within the system are either cell derived or provided with the cell culture medium. Such a model will clearly help deciphering reciprocal signals between MSCs and ECs as it is amenable to analysis using different approaches. Since cells can easily be harvested by digestion of the hydrogel matrix, the influence of co-culture on cellular phenotypes can be characterized by flow cytometry, RT-PCR or biochemical means. For the evaluation of cell dynamics and positional arrangement of MSCs with different phenotypic or functional properties within the system time-lapse or confocal imaging can be conducted. Therefore our in vitro bone models could be used for higher throughput testing of therapeutic molecules using primary human cells from healthy donors or patients with regenerative disorders under standardized in vitro conditions and without the need of ethically problematic animal trials.

Additionally, the combination of matrices with immobilized microenvironment specific signals with 3D patterning and manufacturing technologies would allow the recreation and specific manipulation of complex vascularized bone models in vitro. In this regard, we have recently established systems for the covalent or affinity based immobilization of growth and differentiation factors as well as strategies to position cells and materials by various manufacturing processes[115, 123, 251]. These approaches can be applied on the here described 3D bone tissue-like constructs to form spatially organized bone models.

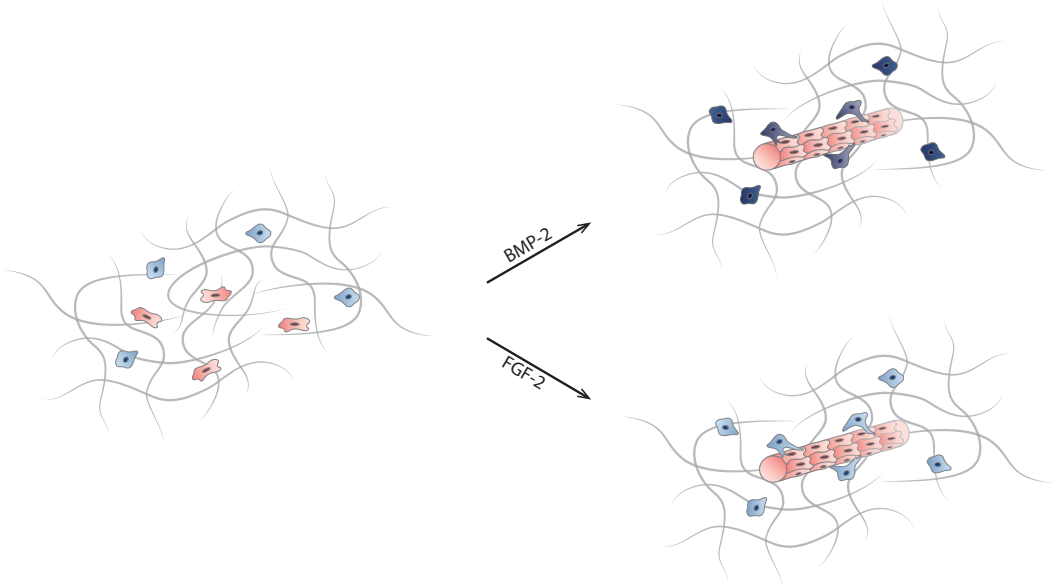

Figure 7: Scheme of the established osteogenic 3D environment. Dual role of MSCs enables the formation of microvascularized osteogenic tissue-like modules in synthetic PEG matrices. Endothelial cells (rose) self-organize into microvascular structures in the presence of hBM-MSCs (blue). Simultaneously, hBM-MSCs can be osteogenically differentiated by BMP-2 (dark blue) or maintained undifferentiated by FGF-2 (light blue).

Conclusion

We have established microvascularized 3D tissue models, in which MSCs support ECs and can be simultaneously osteogenic differentiated or prevented from osteogenic differentiation (**Fig. 7**). Thus we recapitulate some of the features of native bone tissue in an artificial microenvironment by combining vasculogenic and osteogenic processes in PEG hydrogels. These 3D models offer great advantages as they are established under fully defined ECM-free conditions and therefore will allow the deciphering of reciprocal endothelial and mesenchymal cells signals in absence of confounding matrix properties.

Experimental section

Cell Culture

Human bone marrow-derived mesenchymal stem cells (hBM-MSC) were isolated as described previously[194] from bone marrow aspirates of healthy donors (n=4) obtained during orthopedic surgical procedures after informed consent and in accordance with the local ethical committee (University Hospital Basel; Prof. Dr. Kummer; approval date 26/03/2007 Ref Number 78/07). hBM-MSCs were maintained in MEM alpha (with nucleosides, Gibco) supplemented with FBS (10%, Gibco), penicillin (100 U ml^{-1}, Gibco), streptomycin (100 μg ml^{-1}, Gibco), and FGF-2 (5 ng ml^{-1}, PeproTech). Human umbilical vein endothelial cells (HUVEC, PromoCell) were maintained in EGM-2 (EBM-2 basal medium supplemented with the EGM-2 SingleQuots growth factor kit, both from Lonza) and FCS (10%). All cells were cultured at 37°C in a humidified atmosphere at 5% CO_2.

Hydrogel formation and culture

1 mL of FXIIIa (200 U ml^{-1}, Fibrogammin, CSL Behring) was activated with 100 µl of thrombin (20 U ml^{-1}, Sigma–Aldrich) for 30 min at 37 °C. Small aliquots of FXIIIa were stored at −80°C for further use. Hydrogels with a final dry mass content of 1.9% were prepared by stoichiometrically balanced ([Lys]/[Gln] = 1) precursor solutions of n-PEG-Gln and n-PEG-MMP-sensitive-Lys (previously described[174, 222]) in 50 mM Tris buffer pH 7.6 containing 50 mM $CaCl_2$. Additionally, Lys-RGD to a final concentration of 50 μM and cells to final concentration of $3x10^6$ ml^{-1} were added. Subsequently, the cross-linking reaction was initiated by addition of 10 U ml^{-1} FXIIIa. Disc-shaped matrices were obtained by sandwiching the liquid reaction mixtures between hydrophobic glass microscope slides (treated with SigmaCote, Sigma-Aldrich) separated by 0.95 mm thick spacers, clamped with binder clips, and incubated for additional 15 min at 37°C. Finally, hydrogels were released from glass slides and transferred to cell culture plates and cultured at 37°C in a humidified atmosphere at 5% CO_2.

3D mono- and co-cultures were maintained in a combination medium of 4:1 MEM alpha:EGM-2 and FCS (10%), penicillin (100 U ml^{-1}), streptomycin (100 μg ml^{-1}) and FGF-2 (50 ng ml^{-1}).

For osteogenic differentiation experiments, hydrogels containing cells were cultured in the

following medium: MEM alpha (with nucleosides), FCS (10%), penicillin (100 U ml^{-1}), streptomycin (100 μg ml^{-1}), 10 mM HEPES, 1mM sodium pyruvate, 2 mM L-glutamine, L-ascorbic acid (50 μg ml^{-1}) and 10 mM β-glycerol phosphate. The following recombinant human growth factors were used for osteogenic differentiation experiments: BMP-2 (100 ng ml^{-1}, produced as previously described previously[252]), FGF-2 (50 ng ml^{-1}, PeproTech). Medium and growth factors were replaced every 7 days.

Live/Dead staining

The viability of cells in hydrogels was evaluated with the LIVE/DEAD® Viability/Cytotoxicity Kit (Molecular Probes) based on calcein-AM and ethidium homodimer-1 staining. Hydrogels were washed twice with PBS and stained with green-fluorescent calcein-AM (1:2000) and red-fluorescent ethidium homodimer-1 (1:500) for 20 min in serum-free MEM alpha. Subsequently fluorescence images were recorded by an upright fluorescence microscope (DM 5500B, Leica). Images were processed by using ImageJ software (Fiji version 1.48.u, April 2014).

Time-lapse microscopy

After formation, hydrogels were mounted on an inversed microscope (Axiovert 200M, Carl Zeiss) at 37°C in a humidified atmosphere at 5% CO_2 and 20% O_2. Cell performance in hydrogels was followed by acquiring bright field images every 20 min for 72 h. Images were processed and assembled into time-lapse videos by using ImageJ software (Fiji version 1.48.u, April 2014).

Colorimetric staining of alkaline phosphatase and measurement of alkaline phosphatase activity

ALP staining was performed using SIGMA*FAST* BCIP/NBT tablets (Sigma- Aldrich). Medium was removed from cell culture wells and the hydrogels were washed with PBS. To each well 300 μl of ALP substrate solution diluted according to the manufacturer's protocol was added. After 7 min the gels were washed with phosphate buffered saline (PBS) once and hydrogels were fixed by 4% paraformaldehyde (PFA) for 20 min at RT. Whole hydrogels were imaged with a digital camera (HDR XR 500, Sony).

To measure ALP activity, the medium was removed from the wells and the gels were washed with PBS once. Subsequently, gels were digested in 100 μl collagenase A (2 mg ml^{-1}, Roche) for 30 min at 37°C. Next, cells were collected in 500 μl lysis buffer (0.56 M 2-amino-2-methyl-1-propanol, 0.2% Triton X-100, pH 10 in H_2O) and homogenized for 30 sec with a homogenizer (TH220, Omnilab). The cell lysate was centrifuged at 16000 g for 10 min and the supernatant was collected. 50 μl ALP reagent (20 mM 4-nitrophenyl phosphate disodium salt hexahydrate, 4 mM $MgCl_2$ in lysis buffer) was added to 50 μl cell lysate in 96-wells and incubated at 37°C for 10 min before the reaction was stopped by the addition of 100 μl NaOH (1 M). Finally, absorbance was measured at 410 nm with a microplate reader. ALP activity data were normalized on the relative DNA content that

was measured in cell lysates by the CyQuant NF cell proliferation assay kit (C35006, Molecular Probes). Data are shown as mean values ± SD. Mean values were compared by one-way analysis of variance (ANOVA) using GraphPad Prism (GraphPad software version 5.04, San Diego California, USA) followed by Bonferroni's post hoc test to judge statistical significance. Statistical significance was accepted for $p < 0.05$.

Gene expression analysis using qRT-PCR

To measure the expression of osteogenic markers in 3D-PEG gels we encapsulated hBM-MSCs (n=3) in PEG gels at a final concentration of $1.5x10^6$ ml^{-1}. Gels were cultured for 14 days in the presence of BMP-2, FGF-2 or both growth factors. Subsequently, gels (40 µl) were digested in 50 µl collagenase A (2 mg ml^{-1}, Roche) for 30 min on ice. Next, cells were pelleted by a benchtop centrifuge (5415 R, Eppendorf) and total RNA was isolated from the cells by the RNeasy Micro Kit (Qiagen) according to the manufacturer's instructions. For quantitative real-time PCR (qRT-PCR) 200 ng RNA were converted into 40 µl cDNA by means of the High-Capacity cDNA Reverse Transcription Kit (Applied Biosystems). qRT-PCR was carried out using TaqMan Universal PCR Master Mix (Applied Biosystems) and the StepOnePlus Real-Time PCR System (Applied Biosystems). The following TaqMan primer/probe sets were used for gene expression tests: Hs01029144_m1 (ALPL); Hs00959010_m1 (SPP1); Hs01587814_g1 (BGLAP); Hs01047973_m1 (RUNX2). Data were normalized on Hs02758991_g1 (GAPDH) and relative gene expression was calculated by the comparative Ct method.

Multi-lineage differentiation

hBM-MSCs were encapsulated in PEG gels at a final concentration of $1.5x10^6$ ml^{-1} and cultured for 14 days in MEM-alpha (with nucleosides), FCS (10%) with 50 ng ml^{-1} FGF-2. Afterwards differentiation was induced and analyzed as follows: For osteogenic differentiation, gels were cultured in the described osteogenic medium supplemented with 100 ng ml^{-1} BMP-2 and analyzed for ALP activity after 12 days as described above. For adipogenic differentiation, gels were cultured in control medium containing DMEM (low glucose, pyruvate), FCS (10%), penicillin (100 U ml^{-1}), streptomycin (100 µg ml^{-1}) or in adipogenic medium containing DMEM (low glucose, pyruvate), FCS (20%) penicillin (100 U ml^{-1}), streptomycin (100 µg ml^{-1}), 10 µg ml^{-1} insulin (Sigma-Aldrich) 0.5 mM 3-Isobutyl-1-methylxanthin (Sigma-Aldrich), 0.1 mM indomethacin (Sigma-Aldrich) and 1µM dexamethasone (Sigma-Aldrich). After 12 days of adipogenic differentiation, gels were fixed in 4% PFA for 30 min at RT, washed twice by ddH_2O, incubated 10 min in 60% isopropanol and stained for 15 min with Oil Red O (1.8 mg ml^{-1} in 60% isopropanol). Subsequently, gels were washed by tap water and imaged by an inversed microscope (Axiovert 200M, Carl Zeiss).

Immunofluorescence and confocal laser scanning microscopy (CLSM)

For immunofluorescence staining, hydrogels were washed once with PBS followed by fixation in

4% PFA for 30 min at RT. Fixed gels were washed twice with PBS and permeabilized in 0.3% Triton X-100/PBS (Sigma) containing 1% BSA (Albumin Fraction V, AppliChem) for 30 min at RT. Afterwards hydrogels were incubated with mouse monoclonal antibody to CD-31 (555444, BD Biosciences) at 1:150 in 1% BSA/PBS over night at 4°C. Next hydrogels were washed 3 times with PBS and incubated with Alexa Fluor 488-conjugated goat polyclonal anti-mouse antibody at 1:300 (150113, Abcam) and with Rhodamine phalloidin at 1:500 (R415, Molecular Probes) in 1% BSA/PBS over night at 4°C. Stained hydrogels were washed with PBS for 3 h prior to image acquisition.

Confocal images were acquired by an inverted laser-scanning microscope (TCS SP5, Leica). If not differently indicated Z-Stacks with a height of 150 µm were taken by recording 50 planes at 3 µm Z-steps. Images were processed with ImageJ software (Fiji version 1.48.u, April 2014) and depicted as Z-projections. The overall length of microvascular structures per mm^2 and the average length of individual microvascular structures were measured by the AngioQuant tool[253] in Matlab (version R2013b, MathWorks Inc, USA). All data are shown as mean values ± SD. Mean values were compared by one-way analysis of variance (ANOVA) using GraphPad Prism (GraphPad software version 5.04, San Diego California, USA) followed by Bonferroni's post hoc test to judge statistical significance. Statistical significance was accepted for $p < 0.05$.

Transmission electron microscopy (TEM)

For TEM microscopy, hydrogels were washed once with PBS followed by fixation in 2.5% glutaraldehyde in 0.1 M sodium cacodylate buffer (pH 7.4, 540 mOsmol kg^{-1} H_2O). Hydrogels were washed 3 times in 0.1 M sodium cacodylate buffer (pH 7.4, 340 mOsmol kg^{-1} H_2O) and postfixed in 1% OsO_4 (in 0.1 M sodium cacodylate buffer pH 7.4, 340 mOsmol kg^{-1} H_2O). Hydrogels were again washed 3 times in 0.1 M sodium cacodylate buffer (pH 7.4, 340 mOsmol kg^{-1} H_2O) and subsequently gradually dehydrated by an increasing concentration series of ethanol as follows: 70%, 80%, 90%, 96% for 30 min and finally twice in 99% and 100% for 15 min. Last, ethanol was replaced by 100% acetone. Finally, specimens were embedded in epoxy resin. Ultrathin sections were obtained at 70 nm thickness on a microtome (Ultracut S, Reichert) and images were obtained using an electron microscope (EM 400T, Philips) and Morada Soft Imaging System (Olympus).

Acknowledgments

We thank Franz Weber (University Hospital Zurich) for the provision of BMP-2 and Werner Graber (University of Bern) for processing and imaging of hydrogels by TEM microscopy. This work has been supported by the European Union's Seventh Framework Programme (iTERM grant agreement No. 607868) and by the Swiss National Science Foundation (310000-116240).

Supporting figures

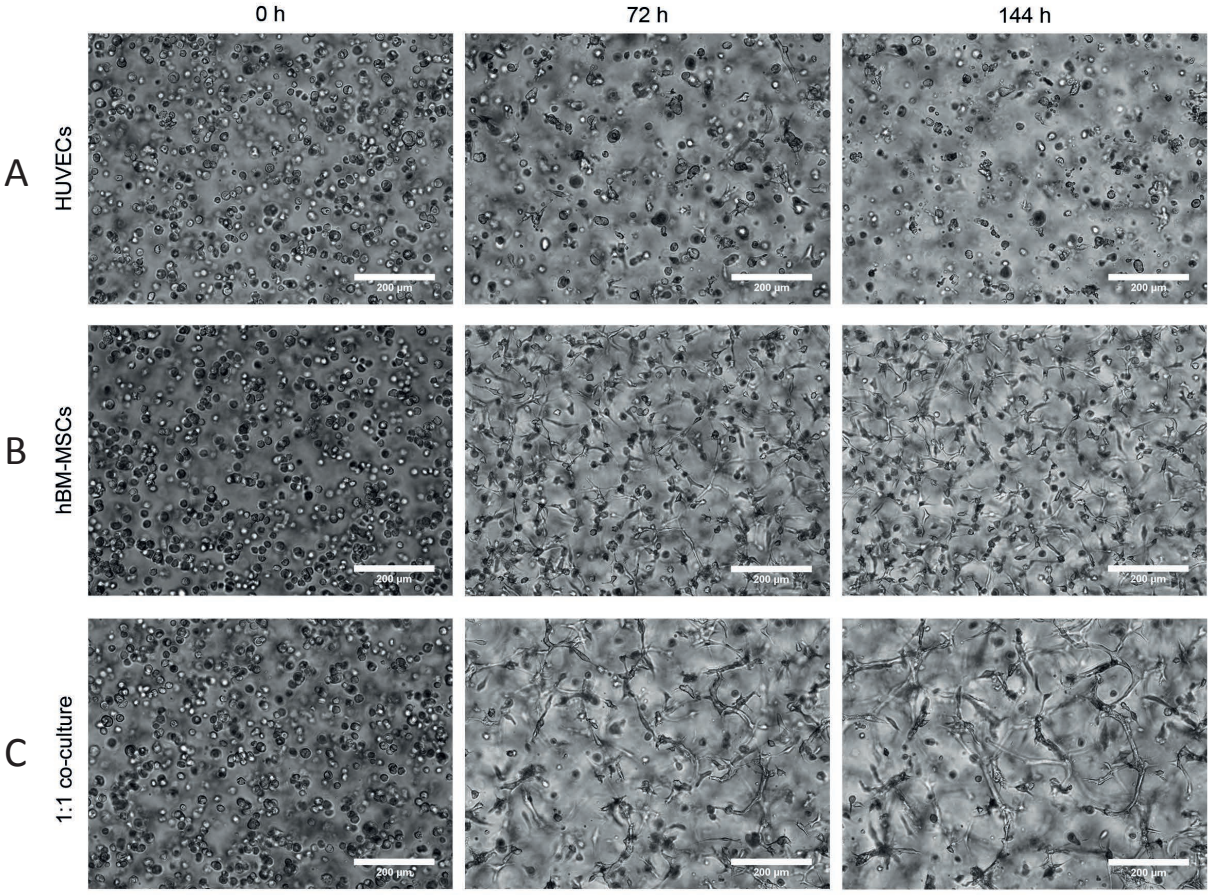

Figure S1: Behavior of HUVEC and MSC mono-cultures or MSC/HUVEC co-cultures in PEG hydrogels visualized by time-lapse microscopy. Cells were 3D encapsulated in hydrogels at a cell concentration of 3 Mio/ml and cultivated for 3 days in the presence of FGF-2 (50 ng ml^{-1}). Images were taken every 20 min. Displayed here are images after 0, 72 and 144 h of culture. Scale bars: 200 µm. A) HUVEC mono-culture. B) MSC mono-culture. C) 1:1 MSC/HUVEC co-culture.

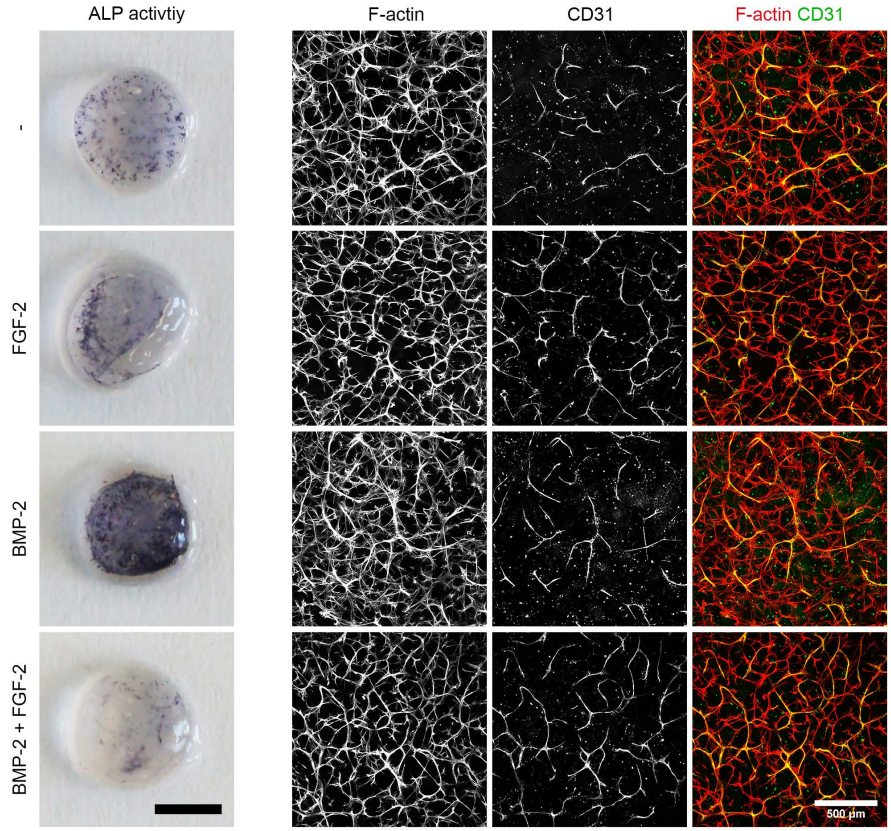

Figure S2: Microvascularization and differentiation pattern in co-cultures are stable for 4 weeks. Co-cultures were cultivated for 28 days inside PEG hydrogels in the presence of BMP-2 (100 ng ml^{-1}) and/or FGF-2 (50 ng ml^{-1}) followed by analysis of ALP activity (scale bar: 2 mm) and evaluation for microvascularization by CD31/F-actin immunofluorescence. Confocal images depict Z-projections of confocal stacks through 150 µm. Scale bar: 500 µm

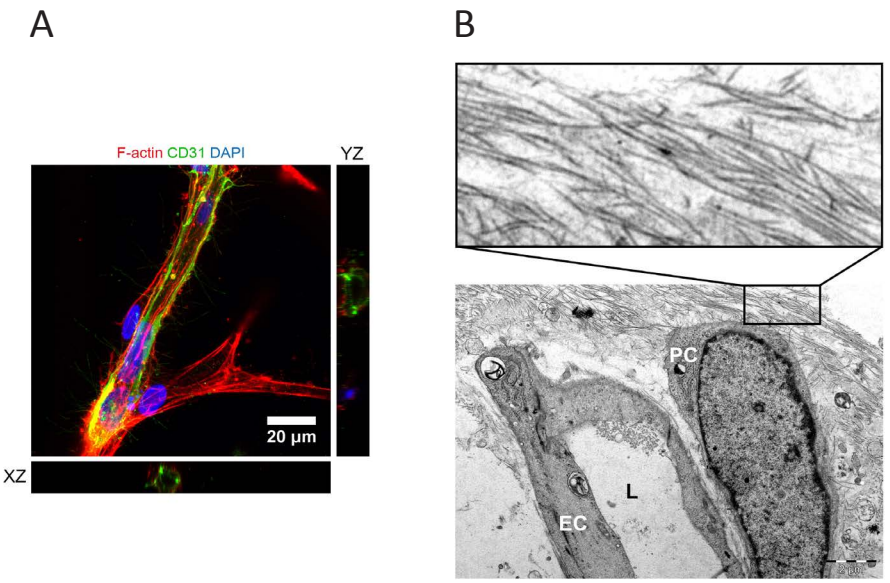

Figure S3: Lumen formation in microvascular structures, perivascular localization of BM-MSCs and fibrillary ECM in 14 days old co-cultures. A) F-actin cytoskeleton (red), CD31 (green) and nuclei (blue) were visualized by confocal microscopy. Scale bar: 20 µm. B) L: Lumen; EC: Endothelial cell; PC: Perivascular cell. Visualized by transmission electron microscopy (TEM). Scale bar: 2 µm.

Chapter IV:

Synthesis, Conclusions and Outlook

Micro-capillary networks engineered in synthetic ECM-free hydrogels

The presented thesis is directed towards the development of vascularized tissue mimics in fully synthetic materials. Consequently, the centerpiece of this thesis is the establishment of artificial blood vessel capillaries in ECM-free 3D scaffolds. Since the late 1980s, myriads of studies have used fibrin and collagen type 1 hydrogels as scaffolds to engineer 3D capillary networks. To date, these two ECM proteins are still the basis for the vast majority of vascular engineering studies, regardless of whether for in vivo or in vitro applications. Especially for 3D in vitro assays, fibrin and collagen type 1 hydrogels are the superior materials as stated by the American Heart Association in 2015[122]. Although ECM hydrogels have provided invaluable insight into basic vascular biology, they possess several drawbacks including batch-to-batch variability, inherent unwanted biological properties, low levels of design freedom and the animal/human origin. These drawbacks not only impede the applicability of ECM hydrogels for tissue models, but also as matrices to elucidate niche signals and cell-matrix interactions involved in vascular biology. In contrast, fully synthetic, ECM mimetic hydrogel materials are flexible in design, biologically inert and chemically defined. These material features facilitate the application of materials engineering, but they also make biological modifications necessary to render synthetic hydrogels biocompatible. Furthermore, as they are produced from scratch, synthetic hydrogels are free of animal products and biological confounding signals, which is important for the reproducibility and medical relevance of tissue models. Not just produced synthetically but also free of any ECM components, poly(ethylene glycol) (PEG) hydrogels are inert matrices that facilitate the study of cells in specifically engineered microenvironments.

In this thesis, we successfully established 3D micro-capillary networks in PEG-hydrogels, which are biologically modified by the fibronectin-derived adhesion peptide RGD and by MMP-sensitive peptide sequences. These two minimal modifications are sufficient for the cell-autonomous arrangement of endothelial and perivascular support cells into micro-capillaries. It is important to visualize that a) the self-assembly of monodispersed, hydrogel-embedded cells into capillary networks necessarily requires 3D cell migration and that b) the pore size of the cross-linked PEG matrix is a magnitude of order smaller than a cell itself. Hence, the locally MMP-mediated degradation of PEG-hydrogel is vital for capillary formation, and such is the case for all morphogenic events that require cell migration. Consequently, blocking MMPs resulted in failed capillary network formation. We further found that higher PEG material density (equivalent to higher cross-linking density and stiffer PEG-hydrogels) adversely affects capillary formation. However, it is not well understood whether the denser matrix itself or the corresponding higher material stiffness is responsible for the inhibition of capillary formation. Interestingly, the pro-migratory factor FGF-2 strongly induced micro-capillary network formation, which supports the observation that capillary

formation is most efficient if culture conditions best support cell migration. In our experiments, we engineered capillary networks by co-culturing endothelial cells with mesenchymal lineage cells. It is important to keep in mind that even though FGF-2 has known effects on both cell types, the question of which cell type is more heavily influenced remains unanswered. Furthermore, the effect of FGF-2 seems to be rather unspecific since other pro-vascular growth factors (GF) can also induce the formation of micro-capillary networks in PEG-hydrogels (**Fig. 1**). The observation that

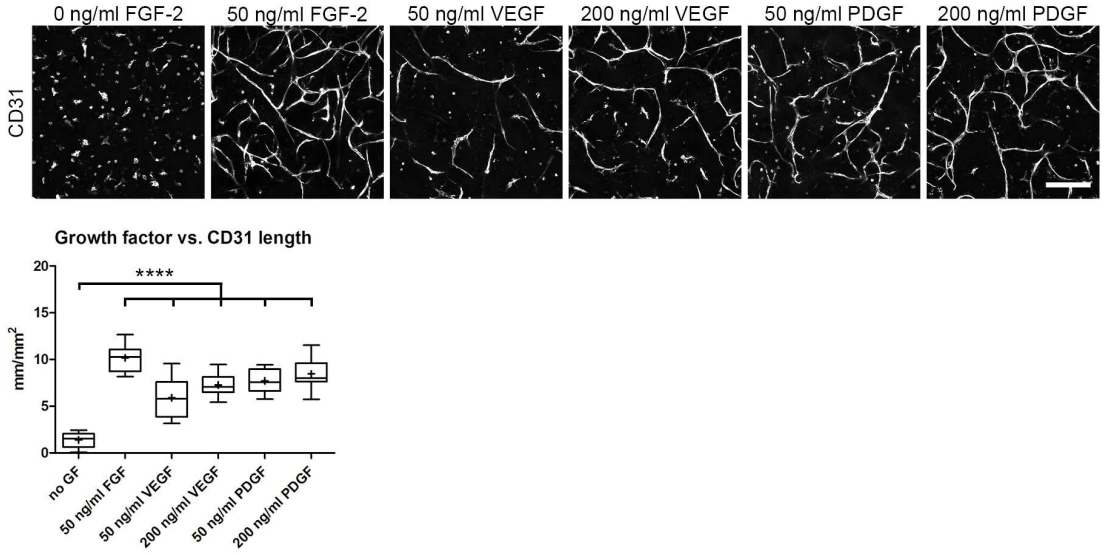

Figure 1: 3D micro-capillary network formation in PEG-hydrogels as function of growth factor stimulation. Representative images of CD31-immunostained micro-capillary networks. All images depict Z-projections of 100 μm Z-stacks and are obtained after 7 days of culture. Scale bar, 200 μm. Cultures were conducted using indicated concentrations of FGF-2, $VEGF_{165}$ or PDGF-BB. Quantitative analysis of the absolute length of CD31-positve networks depending on growth factor stimulation (n = 8 samples from 4 donors. ANOVA with Bonferroni's post hoc test **** $p < 0.0001$; Box plots show 25th and 75th percentiles with whiskers at 5th and 95th percentiles, median (line) and mean (+)). *Experimental conditions and read-out details are same as for Figure 3A of Chapter 2*.

both a mesenchymal cell activating GF (PDGF-BB) as well as an endothelial cell activating GF (less efficient, $VEGF_{165}$) support capillary formation suggests that a general activation of the system might be more important than very specific growth factor effects. Hence, the use of pro-vascular GFs might become less essential if the culture conditions would be adjusted towards a more rapid/easy cell-cell assembly. One way to achieve such conditions would be to uncouple cell migration from (MMP-mediated) matrix degradation by e.g. a matrix pore size that is the same order of magnitude as cells. However, this approach would involve the development of a completely new PEG-hydrogel system. A less arduous way to facilitate a more rapid cell-cell assembly is to initially bring cells closer together by increasing their embedding density. While this approach is feasible, it has not been chosen in the presented thesis since high cell densities markedly impaired the quality of whole mount confocal microscopy in the Z-direction. Besides adjusting the cell density or using other pro-vascular GFs, the initial endothelial/mesenchymal cell ratio could also be modified. In our experiments we chose a ratio of 1:1 since it worked well and was sufficient to adequately monitor events in both cell types. Varying this cell ratio mildly in both directions would still allow for the formation of micro-capillary networks. However, a strong excess of mesenchymal cells will not lead to capillary network formation due to little numbers of endothelial cells, which could be solved by a higher total cell density. Vice versa, strongly increasing the ratio towards endothelial cells will also inhibit capillary formation due to missing vessel maturation signals

from the mesenchymal cells, which are especially important in our MMP-sensitive assay to calm the proteolytic overshoot of endothelial cells. While this is a strong limitation of our PEG system, it is also generally true that 3D in vitro assays with endothelial monocultures are not capable of forming stable capillaries. Hence, without such monoculture control groups it remains difficult to e.g. decipher the actual effect of pro-vascular GF activities in complex, multicellular cultures or tissue models. On the other hand, the fact that capillary formation strongly depends on mesenchymal support cells emphasizes their importance in vascular biology.

In summary, we show that PEG-hydrogels can be used as a robust tool for micro-capillary network engineering. Although we unfortunately did not directly compare them to natural ECM hydrogels, we believe that synthetic PEG-hydrogels have the potential to replace ECM hydrogels for 3D in vitro vascular biology assays if needed.

Perivascular fate and ECM switch of MSCs in micro-capillary networks

Endothelial capillary formation and stabilization depend on support cells from the mesenchymal lineage. In vivo, perivascular cells being pericytes or vascular smooth muscle cells (VSMCs) represent these support cells. However, the functions of perivascular cells are versatile and probably include more than cell assistance and contractile regulation. In this regard, it is suggested that perivascular cells might have mesenchymal tissue progenitor functions. This assumption is based on the two facts that a) in vivo mesenchymal stem cells (MSCs) reside in the perivascular environment of blood capillaries and that b) in vitro MSCs can functionally behave as perivascular-like cells. However, the actual relationship between perivascular cells and MSCs is constantly debated and remains elusive. In the presented thesis, we took advantage of the perivascular-like capacity of BM-MSCs to engineer micro-capillary networks. In contrast to other studies following a similar concept we did not primarily focus on the endothelial component of these capillary networks, but rather on the fate that BM-MSCs undergo in the perivascular microenvironment. To do so we isolated BM-MSC from engineered micro-capillary networks and compared their gene expression to monocultured BM-MSCs. Our results show that BM-MSCs from co-cultures underwent transcriptome changes towards the perivascular lineage. Besides several perivascular markers, we found a prominent switch in ECM gene expression towards a vascular basement membrane phenotype within BM-MSCs. It is important to note that we do not know whether this switch is MSC-specific or universal for cells in contact with endothelial capillaries since we did not carry out control experiments with other perivascular cell types (pericytes, VSMCs or fibroblast). However, we showed that the ECM switch is dependent upon neither the source of MSCs nor the source of endothelial cells, which suggests that a rather general mechanism is behind it. In line with this, it was previously shown that bovine pericytes increased the expression of a subset of basement ECM genes when co-cultured with endothelial cells[64]. Although the specificity and mechanism behind the ECM switch cannot be conclusively clarified, we found good indications that cell-cell contacts play an important role in the BM-MSC regulation since the Notch pathway is involved. More specifically, we found many target genes of the Notch pathway to be strongly induced in BM-MSCs isolated from micro-capillary networks. Notch signaling in general depends

on the activation of membrane-bound Notch proteins by Notch-ligands that are presented on the surface of other cells. As a result, the intracellular domain of Notch proteins is cleaved from the membrane and activates the expression of target genes in the nucleus. In the case of perivascular cells, it is known that Notch family member Notch3 is activated by the Notch-ligand Jagged1, which is presented on the surface membrane of endothelial cells. Since the Jagged1/Notch3 axis is important for perivascular cell differentiation and regulation we asked whether the Notch pathway and the ECM switch are intertwined in BM-MSCs. To address this hypothesis we took advantage of the modular design of our PEG-hydrogel system and indirectly immobilized Jagged1 into 3D hydrogels. By presenting Jagged1 to BM-MSC monocultures we confirmed our hypothesis and for the first time showed that the basement membrane ECM is induced via the Notch pathway. Although only addressed in BM-MSCs, this mechanism may also play a role in pericytes, VSMCs or in completely different cells of other tissue compartments that have a basement membrane ECM. However, even for the investigated BM-MSC we cannot say with absolute certainty that in our micro-capillary assays the Notch pathway is indeed responsible for the observed ECM switch. In this regard, it is conceivable that the Jagged1-induced ECM switch in monocultured MSCs only phenocopies our observation from co-cultured MSCs. To prove that the Jagged1/Notch3 axis is actually causing the ECM switch in co-cultures, depletion or silencing experiments of Jagged1 in endothelial cells and Notch components in MSCs are required. Additionally, chemical disruption or blockage of the Notch pathway in BM-MSCs could validate our findings.

Taken together, we found that MSCs in the perivascular microenvironment undergo perivascular commitment including the induction of basement membrane ECM genes. Hence, MSCs likely contribute in a direct manner to the establishment of the vascular basement membrane ECM, which seems obvious but has not been shown thus far. Additionally, we found that MSCs reorganize their ion channel complexes, which suggests an adaption into a contractile cell phenotype. Although, it cannot be answered whether MSCs differentiate towards pericytes or VSMCs, the increased markers rather point to VSMCs. However, it is also possible and even likely that in our co-culture system MSCs differentiate into various cell types, which cannot be discriminated in the transcriptome analysis due to its averaging approach of the whole non-endothelial (CD31-negative) cell population. To more deeply analyze the fate of MSCs in the perivascular microenvironment, single cell transcriptome analysis, protein levels and in situ immunofluorescence analysis on the cellular level are required. Moreover, it would be extremely interesting to investigate how the tissue progenitor potential of MSCs is affected by their perivascular adaption. Have they lost their multipotent differentiation capacity in capillary networks? Or do they possess an increased differentiation capacity?

Towards vascularized tissue models in synthetic ECM-free hydrogels

In the last part of this thesis, we implemented the idea to build a vascularized model of osteogenic tissue. Our idea was to combine the tissue progenitor and the pro-vascular properties of BM-MSCs. We further aimed to osteogenically differentiate BM-MSCs while simultaneously using them as perivascular support cells. To achieve the differentiation of BM-MSCs we used the bone

morphogenetic protein 2 (BMP-2), which shows both osteogenic and pro-vascular effects in co-cultures of BM-MSCs and endothelial cells. As discussed above we cannot answer whether the pro-vascular effect of BMP-2 occurred directly in endothelial cells or indirectly via modulating BM-MSCs. The next conclusion arises from the idea of boosting micro-capillary network formation by adding FGF-2 in addition to BMP-2. Although slightly increasing the overall length of the micro-capillary networks, the combination of BMP-2 and FGF-2 markedly impaired the osteogenic differentiation of BM-MSCs in co- and monocultures. In fact, it is actually plausible that an osteogenic and a mitogenic GF (BMP-2 and FGF-2, respectively) interfere with each other since stem cells can either differentiate or self-renew. In this regard, very similar results were obtained by observing that the addition of PDGF-BB or EGF to BMP-2 prevents the BMP-2 mediated osteogenic differentiation of BM-MSCs as well (**Fig. 2**). Such crosstalk illustrates the importance of sophisticated GF-presentation strategies that allow the spatially separated presentation of multiple signaling cues. In contrast to many other materials, synthetic hydrogels have the potential to be tailored towards this direction. In this regard, our lab has previously developed several linker tools to immobilize GFs into 3D PEG-hydrogel[115, 123, 177, 254]. Although some of these tools have been applied for the localized presentation of GFs, the spatial resolution is low. Moreover, the simultaneous immobilization of two or more GFs, as it would be required for structured tissue, have yet to be established. Despite these current limitations, it would be interesting, for instance, to develop structured bone and bone marrow like tissues by e.g. antagonizing GF-gradients of BMP-2 and FGF-2.

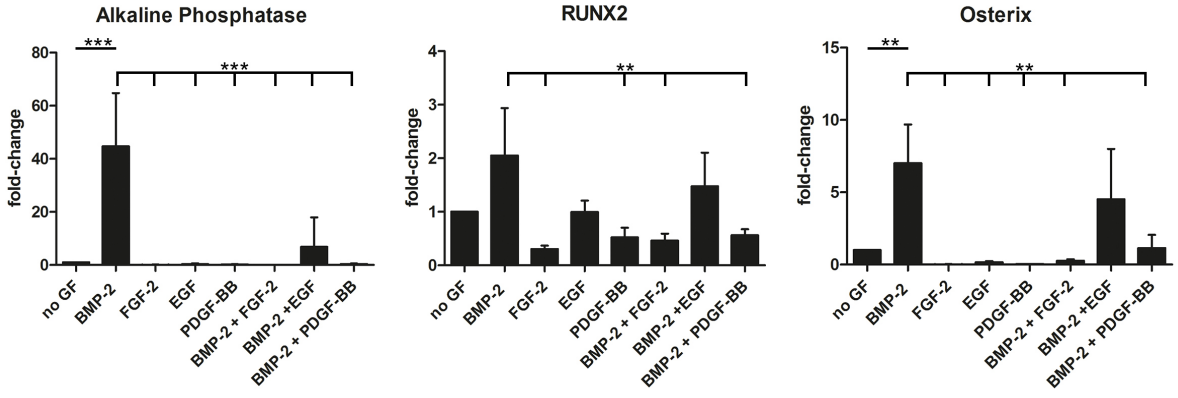

Figure 2: Osteogenic differentiation of MSC mono-cultures in PEG hydrogels. MSCs were cultivated for 10 days inside PEG hydrogels in the presence of no growth factor, BMP-2 (100 ng ml^{-1}) or/and FGF-2, EGF, PDGF-BB (each 50 ng ml^{-1}) in the culture medium. Gene expression of osteogenic markers in cells retrieved from PEG hydrogels measured by means of qRT-PCR and normalized on GAPDH expression. Bars represent mean values ± SD, n = 3. One way ANOVAs: Alkaline Phosphatase (ALPL), p = 0.0001; RUNX2, p = 0.0009; Osterix, p = 0.0003. Bonferroni's post hoc test ** p < 0.01; *** p < 0.001. *Experimental conditions and read-out details are same as for Figure 3B of Chapter 3 except for the readout time point*.

The next conclusion is that fully exploiting the capacity of multipotent MSCs can indeed be beneficial for vascularized tissue models as it replaces the need of adding further perivascular cells. In theory, it would be even simpler to generate hetero-cellular tissue models by using induced pluripotent stem cells (iPSCs) instead of multipotent MSCs. In this case, the same original cell type could give rise to endothelial, perivascular, osteoblastic and other desired cells. While this approach would simplify the cellular conditions, the material challenges would be more demanding since the generation of different cell types from iPSCs requires the spatiotemporal presentation of differentiation cues. Although such 4-dimensional (4D) conditions are certainly

the key to dynamic 3D microenvironments and next-generation tissue models, they are still far away from current standards. The temporal component in 4D models is especially difficult to achieve and to date only light- and temperature-inducible system with low 3D resolution are available to release GFs on external demand.

Besides the randomly organized architecture, the main limitation of our vascularized tissue model is clearly the lack of perfusion. Vascularized tissue models ideally involve the perfusion of engineered blood vessels. To date several perfused, endothelialized tissue models exist thanks to microfluidics techniques. A feature that all these perfused vascular models have in common is the existence of micro-manufactured channels that can be connected to microfluidic systems and mimic large vessels. Therefore, the critical point when aiming for the perfusion of engineered micro-capillaries is their connection to big channels. All existing models that reach this level of complexity are engineered by using ECM hydrogels. However, since the fabrication of big channels is possible in PEG-hydrogels[123, 251] the generation of perfused, endothelialized tissue models within synthetic materials is within reach.

In addition to the discussed tuneability, synthetic hydrogels are free of any naturally occurring ECM components, which has two great benefits: 1) it allows the precise investigation of cells in conditions that are free of biological confounding signals and 2) tissue models can be established without animal derived products and therefore without raising ethical issues. Although our tissue cultures are engineered in fully synthetic PEG-hydrogels, it is important to note that they are free neither of animal products nor of ECM components. By supplementing our cell culture medium with fetal bovine serum (FBS) we do use animal products that furthermore contain soluble ECM proteins such as plasma fibronectin and vitronectin. In future experiments, the usage of FBS could be avoided by using recombinant GF-cocktails. Alternatively, FBS could be replaced by human platelet-rich plasma, which still consists of ECM components but not of animal derived products. In addition to the FBS delivered ECM components, also endogenous, cell-derived ECM is obviously part of our cultures. We are convinced that the endogenously deposited ECM should not be considered as a limitation since it belongs to the inherent response of our system. Moreover, it is conceivable that synthetic hydrogels actually provide promising platforms for 3D tissue models because of the cell-derived ECM. However, the endogenous ECM is an often neglected feature of synthetic materials and needs to be taken into consideration as it might compete or interfere with engineered material features. In fact, we have shown by investigating fibronectin-depleted BM-MSC monocultures that the endogenous ECM deposition does influence the outcome of synthetic hydrogel cultures. However, we have only touched on this point and the role of the endogenous ECM in synthetic hydrogel cultures largely remains a black box. In the future, it would be interesting, for instance, to investigate whether the BM-MSC derived ECM is a necessary condition for endothelial support and micro-capillary network formation in PEG-hydrogels.

Vision: Towards complexity or simplicity?

Tissue models are developed to study biological processes or to conduct drug screenings under defined ex vivo conditions. To make outcomes as valuable as possible, engineered in vitro tissues need to closely resemble in vivo tissues and consequently should include the vasculature if they aim to mimic vascularized tissues. In our developed model, we have established primitive micro-capillary networks. Although this model could certainly be applied to test pro- and anti-vascular drugs or to compare cells from healthy vs. diseased donors, the current level of complexity needs to be increased to reach near-physiological conditions that are required to actually mimic tissue. Such improved conditions mainly include perfusion, a 3D patterned structure, and the temporal control over the conditions (4D). However, we see the near future of our model rather as a basic vascular biology assay with which we can investigate the perfusion-independent, instructive function of the vasculature.

References

1. Potente, M. & Makinen, T. Vascular heterogeneity and specialization in development and disease. *Nat Rev Mol Cell Biol* **18**, 477-494 (2017).
2. Asahara, T. et al. Bone marrow origin of endothelial progenitor cells responsible for postnatal vasculogenesis in physiological and pathological neovascularization. *Circulation research* **85**, 221-228 (1999).
3. Yoder, M.C. Human endothelial progenitor cells. *Cold Spring Harb Perspect Med* **2**, a006692 (2012).
4. Drake, C.J. Embryonic and adult vasculogenesis. *Birth Defects Res C Embryo Today* **69**, 73-82 (2003).
5. Marcelo, K.L., Goldie, L.C. & Hirschi, K.K. Regulation of endothelial cell differentiation and specification. *Circulation research* **112**, 1272-1287 (2013).
6. Djonov, V., Schmid, M., Tschanz, S.A. & Burri, P.H. Intussusceptive angiogenesis: its role in embryonic vascular network formation. *Circulation research* **86**, 286-292 (2000).
7. Djonov, V., Baum, O. & Burri, P.H. Vascular remodeling by intussusceptive angiogenesis. *Cell Tissue Res* **314**, 107-117 (2003).
8. Ribatti, D. & Crivellato, E. “Sprouting angiogenesis”, a reappraisal. *Dev Biol* **372**, 157-165 (2012).
9. Burri, P.H., Hlushchuk, R. & Djonov, V. Intussusceptive angiogenesis: its emergence, its characteristics, and its significance. *Dev Dyn* **231**, 474-488 (2004).
10. Senger, D.R. & Davis, G.E. Angiogenesis. *Cold Spring Harb Perspect Biol* **3**, a005090 (2011).
11. Sundberg, C. et al. Glomeruloid Microvascular Proliferation Follows Adenoviral Vascular Permeability Factor/Vascular Endothelial Growth Factor-164 Gene Delivery. *The American journal of pathology* **158**, 1145-1160 (2001).
12. Carmeliet, P. & Jain, R.K. Molecular mechanisms and clinical applications of angiogenesis. *Nature* **473**, 298-307 (2011).
13. Krock, B.L., Skuli, N. & Simon, M.C. Hypoxia-induced angiogenesis: good and evil. *Genes Cancer* **2**, 1117-1133 (2011).
14. Jakobsson, L. et al. Endothelial cells dynamically compete for the tip cell position during angiogenic sprouting. *Nat Cell Biol* **12**, 943-953 (2010).
15. Phng, L.K. & Gerhardt, H. Angiogenesis: a team effort coordinated by notch. *Dev Cell* **16**, 196-208 (2009).
16. Armulik, A., Genove, G. & Betsholtz, C. Pericytes: developmental, physiological, and pathological perspectives, problems, and promises. *Dev Cell* **21**, 193-215 (2011).
17. Gaengel, K., Genove, G., Armulik, A. & Betsholtz, C. Endothelial-mural cell signaling in vascular development and angiogenesis. *Arteriosclerosis, thrombosis, and vascular biology* **29**, 630-638 (2009).
18. Crisan, M. et al. Perivascular multipotent progenitor cells in human organs. *Ann N Y Acad Sci* **1176**, 118-123 (2009).
19. Crisan, M. et al. A perivascular origin for mesenchymal stem cells in multiple human organs. *Cell Stem Cell* **3**, 301-313 (2008).
20. Sacchetti, B. et al. Self-renewing osteoprogenitors in bone marrow sinusoids can organize a hematopoietic microenvironment. *Cell* **131**, 324-336 (2007).

21. Feng, J., Mantesso, A., De Bari, C., Nishiyama, A. & Sharpe, P.T. Dual origin of mesenchymal stem cells contributing to organ growth and repair. *Proceedings of the National Academy of Sciences of the United States of America* **108**, 6503-6508 (2011).

22. Putnam, A.J. The Instructive Role of the Vasculature in Stem Cell Niches. *Biomater Sci* **2**, 1562-1573 (2014).

23. Billaud, M. et al. Classification and Functional Characterization of Vasa Vasorum-Associated Perivascular Progenitor Cells in Human Aorta. *Stem Cell Reports* **9**, 292-303 (2017).

24. Guimaraes-Camboa, N. et al. Pericytes of Multiple Organs Do Not Behave as Mesenchymal Stem Cells In Vivo. *Cell Stem Cell* **20**, 345-359.e345 (2017).

25. Korn, C. & Augustin, H.G. Mechanisms of Vessel Pruning and Regression. *Dev Cell* **34**, 5-17 (2015).

26. Kochhan, E. et al. Blood flow changes coincide with cellular rearrangements during blood vessel pruning in zebrafish embryos. *PloS one* **8**, e75060 (2013).

27. Ricard, N. & Simons, M. When it is better to regress: dynamics of vascular pruning. *PLoS Biol* **13**, e1002148 (2015).

28. le Noble, F. et al. Flow regulates arterial-venous differentiation in the chick embryo yolk sac. *Development (Cambridge, England)* **131**, 361-375 (2004).

29. Udan, R.S., Vadakkan, T.J. & Dickinson, M.E. Dynamic responses of endothelial cells to changes in blood flow during vascular remodeling of the mouse yolk sac. *Development (Cambridge, England)* **140**, 4041-4050 (2013).

30. Chen, Q. et al. Haemodynamics-driven developmental pruning of brain vasculature in zebrafish. *PLoS Biol* **10**, e1001374 (2012).

31. Lenard, A. et al. Endothelial cell self-fusion during vascular pruning. *PLoS Biol* **13**, e1002126 (2015).

32. Simonavicius, N. et al. Pericytes promote selective vessel regression to regulate vascular patterning. *Blood* **120**, 1516-1527 (2012).

33. Korn, C. et al. Endothelial cell-derived non-canonical Wnt ligands control vascular pruning in angiogenesis. *Development (Cambridge, England)* **141**, 1757-1766 (2014).

34. van Hinsbergh, V.W., Collen, A. & Koolwijk, P. Role of fibrin matrix in angiogenesis. *Ann N Y Acad Sci* **936**, 426-437 (2001).

35. Sahni, A., Altland, O.D. & Francis, C.W. FGF-2 but not FGF-1 binds fibrin and supports prolonged endothelial cell growth. *Journal of thrombosis and haemostasis : JTH* **1**, 1304-1310 (2003).

36. Sahni, A. & Francis, C.W. Vascular endothelial growth factor binds to fibrinogen and fibrin and stimulates endothelial cell proliferation. *Blood* **96**, 3772-3778 (2000).

37. Sahni, A., Odrljin, T. & Francis, C.W. Binding of basic fibroblast growth factor to fibrinogen and fibrin. *The Journal of biological chemistry* **273**, 7554-7559 (1998).

38. Peng, H. et al. Identification of a binding site on human FGF-2 for fibrinogen. *Blood* **103**, 2114-2120 (2004).

39. Wijelath, E.S. Novel Vascular Endothelial Growth Factor Binding Domains of Fibronectin Enhance Vascular Endothelial Growth Factor Biological Activity. *Circulation research* **91**, 25-31 (2002).

40. Kalluri, R. Basement membranes: structure, assembly and role in tumour angiogenesis. *Nat Rev Cancer* **3**, 422-433 (2003).

41. Yurchenco, P.D. Basement membranes: cell scaffoldings and signaling platforms. *Cold Spring Harb Perspect Biol* **3** (2011).

42. Davis, G.E. & Senger, D.R. Endothelial extracellular matrix: biosynthesis, remodeling, and functions during vascular morphogenesis and neovessel stabilization. *Circulation research* **97**, 1093-1107 (2005).

43. Davis, G.E., Stratman, A.N., Sacharidou, A. & Koh, W. Molecular basis for endothelial lumen formation and tubulogenesis during vasculogenesis and angiogenic sprouting. *International review of cell and molecular biology* **288**, 101-165 (2011).

44. Mott, J.D. & Werb, Z. Regulation of matrix biology by matrix metalloproteinases. *Curr Opin Cell Biol* **16**, 558-564 (2004).

45. Alajati, A. et al. Spheroid-based engineering of a human vasculature in mice. *Nat Methods* **5**, 439-445 (2008).

46. Asakawa, N. et al. Pre-vascularization of in vitro three-dimensional tissues created by cell sheet engineering. *Biomaterials* **31**, 3903-3909 (2010).

47. Nishiguchi, A., Matsusaki, M., Asano, Y., Shimoda, H. & Akashi, M. Effects of angiogenic factors and 3D-microenvironments on vascularization within sandwich cultures. *Biomaterials* **35**, 4739-4748 (2014).

48. Peppas, N.A., Hilt, J.Z., Khademhosseini, A. & Langer, R. Hydrogels in Biology and Medicine: From Molecular Principles to Bionanotechnology. *Advanced Materials* **18**, 1345-1360 (2006).

49. Kirschner, C.M. & Anseth, K.S. Hydrogels in Healthcare: From Static to Dynamic Material Microenvironments. *Acta Mater* **61**, 931-944 (2013).

50. Caliari, S.R. & Burdick, J.A. A practical guide to hydrogels for cell culture. *Nat Methods* **13**, 405-414 (2016).

51. Nicosia, R.F. & Madri, J.A. The microvascular extracellular matrix. Developmental changes during angiogenesis in the aortic ring-plasma clot model. *The American journal of pathology* **128**, 78-90 (1987).

52. Nicosia, R.F., Tchao, R. & Leighton, J. Histotypic angiogenesis in vitro: light microscopic, ultrastructural, and radioautographic studies. *In vitro* **18**, 538-549 (1982).

53. Nicosia, R.F., Tchao, R. & Leighton, J. Interactions between newly formed endothelial channels and carcinoma cells in plasma clot culture. *Clinical & experimental metastasis* **4**, 91-104 (1986).

54. Montesano, R., Mouron, P. & Orci, L. Vascular outgrowths from tissue explants embedded in fibrin or collagen gels: a simple in vitro model of angiogenesis. *Cell biology international reports* **9**, 869-875 (1985).

55. Montesano, R., Pepper, M.S., Vassalli, J.D. & Orci, L. Phorbol ester induces cultured endothelial cells to invade a fibrin matrix in the presence of fibrinolytic inhibitors. *Journal of cellular physiology* **132**, 509-516 (1987).

56. Chen, X. et al. Prevascularization of a fibrin-based tissue construct accelerates the formation of functional anastomosis with host vasculature. *Tissue engineering. Part A* **15**, 1363-1371 (2009).

57. Chen, X. et al. Rapid anastomosis of endothelial progenitor cell-derived vessels with host vasculature is promoted by a high density of cotransplanted fibroblasts. *Tissue engineering. Part A* **16**, 585-594 (2010).

58. Klar, A.S. et al. Tissue-engineered dermo-epidermal skin grafts prevascularized with adipose-derived cells. *Biomaterials* **35**, 5065-5078 (2014).

59. Marino, D., Luginbuhl, J., Scola, S., Meuli, M. & Reichmann, E. Bioengineering dermo-epidermal skin grafts with blood and lymphatic capillaries. *Science translational medicine* **6**, 221ra214 (2014).

60. Montano, I. et al. Formation of human capillaries in vitro: the engineering of prevascularized matrices. *Tissue engineering. Part A* **16**, 269-282 (2010).

61. Bayless, K.J. & Davis, G.E. The Cdc42 and Rac1 GTPases are required for capillary lumen formation in three-dimensional extracellular matrices. *Journal of cell science* **115**, 1123-1136 (2002).

62. Kamei, M. et al. Endothelial tubes assemble from intracellular vacuoles in vivo. *Nature* **442**, 453-456 (2006).

63. Stratman, A.N., Davis, M.J. & Davis, G.E. VEGF and FGF prime vascular tube morphogenesis and sprouting directed by hematopoietic stem cell cytokines. *Blood* **117**, 3709-3719 (2011).

64. Stratman, A.N., Malotte, K.M., Mahan, R.D., Davis, M.J. & Davis, G.E. Pericyte recruitment during vasculogenic tube assembly stimulates endothelial basement membrane matrix formation. *Blood* **114**, 5091-5101 (2009).

65. Stratman, A.N., Schwindt, A.E., Malotte, K.M. & Davis, G.E. Endothelial-derived PDGF-BB and HB-EGF coordinately regulate pericyte recruitment during vasculogenic tube assembly and stabilization. *Blood* **116**, 4720-4730 (2010).

66. Black, A.F., Berthod, F., L'Heureux, N., Germain, L. & Auger, F.A. In vitro reconstruction of a human capillary-like network in a tissue-engineered skin equivalent. *FASEB journal : official publication of the Federation of American Societies for Experimental Biology* **12**, 1331-1340 (1998).

67. Shepherd, B.R. et al. Rapid perfusion and network remodeling in a microvascular construct after implantation. *Arteriosclerosis, thrombosis, and vascular biology* **24**, 898-904 (2004).

68. Koike, N. et al. Tissue engineering: creation of long-lasting blood vessels. *Nature* **428**, 138-139 (2004).

69. Au, P., Tam, J., Fukumura, D. & Jain, R.K. Bone marrow-derived mesenchymal stem cells facilitate engineering of long-lasting functional vasculature. *Blood* **111**, 4551-4558 (2008).

70. White, S.M. et al. Implanted cell-dense prevascularized tissues develop functional vasculature that supports reoxygenation after thrombosis. *Tissue engineering. Part A* **20**, 2316-2328 (2014).

71. Brown, R.A., Wiseman, M., Chuo, C.B., Cheema, U. & Nazhat, S.N. Ultrarapid Engineering of Biomimetic Materials and Tissues: Fabrication of Nano- and Microstructures by Plastic Compression. *Advanced functional materials* **15**, 1762-1770 (2005).

72. Cheema, U. & Brown, R.A. Rapid Fabrication of Living Tissue Models by Collagen Plastic Compression: Understanding Three-Dimensional Cell Matrix Repair In Vitro. *Adv Wound Care (New Rochelle)* **2**, 176-184 (2013).

73. Alekseeva, T., Unger, R.E., Brochhausen, C., Brown, R.A. & Kirkpatrick, J.C. Engineering a microvascular capillary bed in a tissue-like collagen construct. *Tissue engineering. Part A* **20**, 2656-2665 (2014).

74. Singh, R.K., Seliktar, D. & Putnam, A.J. Capillary morphogenesis in PEG-collagen hydrogels. *Biomaterials* **34**, 9331-9340 (2013).

75. Van Den Bulcke, A.I. et al. Structural and rheological properties of methacrylamide modified gelatin hydrogels. *Biomacromolecules* **1**, 31-38 (2000).

76. Benton, J.A., DeForest, C.A., Vivekanandan, V. & Anseth, K.S. Photocrosslinking of gelatin macromers to synthesize porous hydrogels that promote valvular interstitial cell function. *Tissue engineering. Part A* **15**, 3221-3230 (2009).

77. Nichol, J.W. et al. Cell-laden microengineered gelatin methacrylate hydrogels. *Biomaterials* **31**, 5536-5544 (2010).

78. Chen, Y.C. et al. Functional Human Vascular Network Generated in Photocrosslinkable Gelatin Methacrylate Hydrogels. *Advanced functional materials* **22**, 2027-2039 (2012).

79. Lin, R.Z., Chen, Y.C., Moreno-Luna, R., Khademhosseini, A. & Melero-Martin, J.M. Transdermal

regulation of vascular network bioengineering using a photopolymerizable methacrylated gelatin hydrogel. *Biomaterials* **34**, 6785-6796 (2013).

80. Khetan, S. & Burdick, J.A. Patterning network structure to spatially control cellular remodeling and stem cell fate within 3-dimensional hydrogels. *Biomaterials* **31**, 8228-8234 (2010).

81. Hanjaya-Putra, D. et al. Controlled activation of morphogenesis to generate a functional human microvasculature in a synthetic matrix. *Blood* **118**, 804-815 (2011).

82. Hanjaya-Putra, D. et al. Spatial control of cell-mediated degradation to regulate vasculogenesis and angiogenesis in hyaluronan hydrogels. *Biomaterials* **33**, 6123-6131 (2012).

83. Kusuma, S. et al. Self-organized vascular networks from human pluripotent stem cells in a synthetic matrix. *Proceedings of the National Academy of Sciences of the United States of America* **110**, 12601-12606 (2013).

84. Shen, Y.I. et al. Engineered human vascularized constructs accelerate diabetic wound healing. *Biomaterials* **102**, 107-119 (2016).

85. Chwalek, K., Tsurkan, M.V., Freudenberg, U. & Werner, C. Glycosaminoglycan-based hydrogels to modulate heterocellular communication in in vitro angiogenesis models. *Scientific reports* **4**, 4414 (2014).

86. Tsurkan, M.V. et al. Defined polymer-peptide conjugates to form cell-instructive starPEG-heparin matrices in situ. *Advanced materials (Deerfield Beach, Fla.)* **25**, 2606-2610 (2013).

87. Lutolf, M.P. Integration column: artificial ECM: expanding the cell biology toolbox in 3D. *Integrative biology : quantitative biosciences from nano to macro* **1**, 235-241 (2009).

88. Kyburz, K.A. & Anseth, K.S. Synthetic mimics of the extracellular matrix: how simple is complex enough? *Ann Biomed Eng* **43**, 489-500 (2015).

89. Cruz-Acuna, R. & Garcia, A.J. Synthetic hydrogels mimicking basement membrane matrices to promote cell-matrix interactions. *Matrix Biol* **57-58**, 324-333 (2017).

90. Guvendiren, M. & Burdick, J.A. Engineering synthetic hydrogel microenvironments to instruct stem cells. *Curr Opin Biotechnol* **24**, 841-846 (2013).

91. Moon, J.J. et al. Biomimetic hydrogels with pro-angiogenic properties. *Biomaterials* **31**, 3840-3847 (2010).

92. Cuchiara, M.P., Gould, D.J., McHale, M.K., Dickinson, M.E. & West, J.L. Integration of Self-Assembled Microvascular Networks with Microfabricated PEG-Based Hydrogels. *Advanced functional materials* **22**, 4511-4518 (2012).

93. Vigen, M., Ceccarelli, J. & Putnam, A.J. Protease-sensitive PEG hydrogels regulate vascularization in vitro and in vivo. *Macromolecular bioscience* **14**, 1368-1379 (2014).

94. Blache, U. et al. Dual Role of Mesenchymal Stem Cells Allows for Microvascularized Bone Tissue-Like Environments in PEG Hydrogels. *Adv Healthc Mater* **5**, 489-498 (2016).

95. Zachary, I. & Morgan, R.D. Therapeutic angiogenesis for cardiovascular disease: biological context, challenges, prospects. *Heart (British Cardiac Society)* **97**, 181-189 (2011).

96. Wong, C., Inman, E., Spaethe, R. & Helgerson, S. Fibrin-based biomaterials to deliver human growth factors. *Thrombosis and haemostasis* **89**, 573-582 (2003).

97. Briquez, P.S., Clegg, L.E., Martino, M.M., Gabhann, F.M. & Hubbell, J.A. Design principles for therapeutic angiogenic materials. *Nature Reviews Materials* **1**, 15006 (2016).

98. Schense, J.C., Bloch, J., Aebischer, P. & Hubbell, J.A. Enzymatic incorporation of bioactive peptides into fibrin matrices enhances neurite extension. *Nature biotechnology* **18**, 415-419 (2000).

99. Schense, J.C. & Hubbell, J.A. Cross-linking exogenous bifunctional peptides into fibrin gels with

factor XIIIa. *Bioconjugate chemistry* **10**, 75-81 (1999).

100. Ehrbar, M. et al. Cell-demanded liberation of VEGF121 from fibrin implants induces local and controlled blood vessel growth. *Circulation research* **94**, 1124-1132 (2004).

101. Ehrbar, M. et al. The role of actively released fibrin-conjugated VEGF for VEGF receptor 2 gene activation and the enhancement of angiogenesis. *Biomaterials* **29**, 1720-1729 (2008).

102. Largo, R.A. et al. Long-term biostability and bioactivity of “fibrin linked” VEGF121in vitro and in vivo. *Biomaterials Science* **2**, 581 (2014).

103. Ghajar, C.M. et al. The effect of matrix density on the regulation of 3-D capillary morphogenesis. *Biophysical journal* **94**, 1930-1941 (2008).

104. Kniazeva, E. & Putnam, A.J. Endothelial cell traction and ECM density influence both capillary morphogenesis and maintenance in 3-D. *American journal of physiology. Cell physiology* **297**, C179-187 (2009).

105. Sacchi, V. et al. Long-lasting fibrin matrices ensure stable and functional angiogenesis by highly tunable, sustained delivery of recombinant VEGF164. *Proceedings of the National Academy of Sciences of the United States of America* **111**, 6952-6957 (2014).

106. Patterson, J. & Hubbell, J.A. Enhanced proteolytic degradation of molecularly engineered PEG hydrogels in response to MMP-1 and MMP-2. *Biomaterials* **31**, 7836-7845 (2010).

107. Patterson, J. & Hubbell, J.A. SPARC-derived protease substrates to enhance the plasmin sensitivity of molecularly engineered PEG hydrogels. *Biomaterials* **32**, 1301-1310 (2011).

108. Zisch, A.H. et al. Cell-demanded release of VEGF from synthetic, biointeractive cell ingrowth matrices for vascularized tissue growth. *FASEB journal : official publication of the Federation of American Societies for Experimental Biology* **17**, 2260-2262 (2003).

109. Phelps, E.A., Landazuri, N., Thule, P.M., Taylor, W.R. & Garcia, A.J. Bioartificial matrices for therapeutic vascularization. *Proceedings of the National Academy of Sciences of the United States of America* **107**, 3323-3328 (2010).

110. Martino, M.M. & Hubbell, J.A. The 12th-14th type III repeats of fibronectin function as a highly promiscuous growth factor-binding domain. *FASEB journal : official publication of the Federation of American Societies for Experimental Biology* **24**, 4711-4721 (2010).

111. Martino, M.M., Briquez, P.S., Ranga, A., Lutolf, M.P. & Hubbell, J.A. Heparin-binding domain of fibrin(ogen) binds growth factors and promotes tissue repair when incorporated within a synthetic matrix. *Proceedings of the National Academy of Sciences of the United States of America* **110**, 4563-4568 (2013).

112. Zieris, A. et al. FGF-2 and VEGF functionalization of starPEG-heparin hydrogels to modulate biomolecular and physical cues of angiogenesis. *Biomaterials* **31**, 7985-7994 (2010).

113. Martino, M.M. et al. Growth factors engineered for super-affinity to the extracellular matrix enhance tissue healing. *Science (New York, N.Y.)* **343**, 885-888 (2014).

114. Wylie, R.G. et al. Spatially controlled simultaneous patterning of multiple growth factors in three-dimensional hydrogels. *Nature materials* **10**, 799-806 (2011).

115. Metzger, S. et al. Modular poly(ethylene glycol) matrices for the controlled 3D-localized osteogenic differentiation of mesenchymal stem cells. *Advanced healthcare materials* **4**, 550-558 (2015).

116. Levenberg, S. et al. Differentiation of human embryonic stem cells on three-dimensional polymer scaffolds. *Proceedings of the National Academy of Sciences of the United States of America* **100**, 12741-12746 (2003).

117. Levenberg, S. et al. Engineering vascularized skeletal muscle tissue. *Nature biotechnology* **23**, 879-884 (2005).

118. Liu, C.H., Wang, Z., Sun, Y. & Chen, J. Animal models of ocular angiogenesis: from development to pathologies. *FASEB journal : official publication of the Federation of American Societies for Experimental Biology* (2017).

119. Walchli, T. et al. Wiring the Vascular Network with Neural Cues: A CNS Perspective. *Neuron* **87**, 271-296 (2015).

120. Scott, A.W. & Bressler, S.B. Long-term follow-up of vascular endothelial growth factor inhibitor therapy for neovascular age-related macular degeneration. *Current opinion in ophthalmology* **24**, 190-196 (2013).

121. Jain, R.K. Antiangiogenesis strategies revisited: from starving tumors to alleviating hypoxia. *Cancer cell* **26**, 605-622 (2014).

122. Simons, M. et al. State-of-the-Art Methods for Evaluation of Angiogenesis and Tissue Vascularization: A Scientific Statement From the American Heart Association. *Circulation research* **116**, e99-132 (2015).

123. Lienemann, P.S. et al. Locally controlling mesenchymal stem cell morphogenesis by 3D PDGF-BB gradients towards the establishment of an in vitro perivascular niche. *Integrative biology : quantitative biosciences from nano to macro* **7**, 101-111 (2015).

124. Zhang, J. et al. A Genome-wide Analysis of Human Pluripotent Stem Cell-Derived Endothelial Cells in 2D or 3D Culture. *Stem Cell Reports* **8**, 907-918 (2017).

125. Muller, K., Naumann, S., Weber, W. & Zurbriggen, M.D. Optogenetics for gene expression in mammalian cells. *Biological chemistry* **396**, 145-152 (2015).

126. Brown, T.E. & Anseth, K.S. Spatiotemporal hydrogel biomaterials for regenerative medicine. *Chemical Society reviews* (2017).

127. Bergers, G. & Hanahan, D. Modes of resistance to anti-angiogenic therapy. *Nat Rev Cancer* **8**, 592-603 (2008).

128. Jain, R.K. Normalizing tumor microenvironment to treat cancer: bench to bedside to biomarkers. *Journal of clinical oncology : official journal of the American Society of Clinical Oncology* **31**, 2205-2218 (2013).

129. Song, H.H., Park, K.M. & Gerecht, S. Hydrogels to model 3D in vitro microenvironment of tumor vascularization. *Advanced drug delivery reviews* **79-80**, 19-29 (2014).

130. Chwalek, K., Bray, L.J. & Werner, C. Tissue-engineered 3D tumor angiogenesis models: potential technologies for anti-cancer drug discovery. *Advanced drug delivery reviews* **79-80**, 30-39 (2014).

131. Taubenberger, A.V. et al. 3D extracellular matrix interactions modulate tumour cell growth, invasion and angiogenesis in engineered tumour microenvironments. *Acta biomaterialia* **36**, 73-85 (2016).

132. Bray, L.J. et al. Multi-parametric hydrogels support 3D in vitro bioengineered microenvironment models of tumour angiogenesis. *Biomaterials* **53**, 609-620 (2015).

133. Roudsari, L.C., Jeffs, S.E., Witt, A.S., Gill, B.J. & West, J.L. A 3D Poly(ethylene glycol)-based Tumor Angiogenesis Model to Study the Influence of Vascular Cells on Lung Tumor Cell Behavior. *Scientific reports* **6**, 32726 (2016).

134. Bertassoni, L.E. et al. Hydrogel bioprinted microchannel networks for vascularization of tissue engineering constructs. *Lab Chip* **14**, 2202-2211 (2014).

135. Kageyama, T. et al. Rapid engineering of endothelial cell-lined vascular-like structures in in situ crosslinkable hydrogels. *Biofabrication* **6**, 025006 (2014).

136. Arrigoni, C. et al. Rational Design of Prevascularized Large 3D Tissue Constructs Using Computational Simulations and Biofabrication of Geometrically Controlled Microvessels.

Advanced healthcare materials **5**, 1617-1626 (2016).

137. Zheng, Y. et al. In vitro microvessels for the study of angiogenesis and thrombosis. *Proceedings of the National Academy of Sciences of the United States of America* **109**, 9342-9347 (2012).

138. Nguyen, D.H. et al. Biomimetic model to reconstitute angiogenic sprouting morphogenesis in vitro. *Proceedings of the National Academy of Sciences of the United States of America* **110**, 6712-6717 (2013).

139. Kolesky, D.B., Homan, K.A., Skylar-Scott, M.A. & Lewis, J.A. Three-dimensional bioprinting of thick vascularized tissues. *Proceedings of the National Academy of Sciences of the United States of America* **113**, 3179-3184 (2016).

140. Kolesky, D.B. et al. 3D bioprinting of vascularized, heterogeneous cell-laden tissue constructs. *Advanced materials (Deerfield Beach, Fla.)* **26**, 3124-3130 (2014).

141. Lee, V.K. et al. Creating perfused functional vascular channels using 3D bio-printing technology. *Biomaterials* **35**, 8092-8102 (2014).

142. Brandenberg, N. & Lutolf, M.P. In Situ Patterning of Microfluidic Networks in 3D Cell-Laden Hydrogels. *Advanced materials (Deerfield Beach, Fla.)* **28**, 7450-7456 (2016).

143. Wang, X. et al. Engineering anastomosis between living capillary networks and endothelial cell-lined microfluidic channels. *Lab Chip* **16**, 282-290 (2016).

144. Wang, X. et al. An on-chip microfluidic pressure regulator that facilitates reproducible loading of cells and hydrogels into microphysiological system platforms. *Lab Chip* **16**, 868-876 (2016).

145. Hsu, Y.H., Moya, M.L., Hughes, C.C., George, S.C. & Lee, A.P. A microfluidic platform for generating large-scale nearly identical human microphysiological vascularized tissue arrays. *Lab Chip* **13**, 2990-2998 (2013).

146. Yeon, J.H., Ryu, H.R., Chung, M., Hu, Q.P. & Jeon, N.L. In vitro formation and characterization of a perfusable three-dimensional tubular capillary network in microfluidic devices. *Lab Chip* **12**, 2815-2822 (2012).

147. van Duinen, V., Trietsch, S.J., Joore, J., Vulto, P. & Hankemeier, T. Microfluidic 3D cell culture: from tools to tissue models. *Curr Opin Biotechnol* **35**, 118-126 (2015).

148. Phan, D.T.T. et al. A vascularized and perfused organ-on-a-chip platform for large-scale drug screening applications. *Lab Chip* **17**, 511-520 (2017).

149. Sobrino, A. et al. 3D microtumors in vitro supported by perfused vascular networks. *Scientific reports* **6**, 31589 (2016).

150. Nguyen, E.H. et al. Versatile synthetic alternatives to Matrigel for vascular toxicity screening and stem cell expansion. **1**, 0096 (2017).

151. Shi, S. & Gronthos, S. Perivascular niche of postnatal mesenchymal stem cells in human bone marrow and dental pulp. *Journal of bone and mineral research : the official journal of the American Society for Bone and Mineral Research* **18**, 696-704 (2003).

152. Corselli, M. et al. The tunica adventitia of human arteries and veins as a source of mesenchymal stem cells. *Stem cells and development* **21**, 1299-1308 (2012).

153. Kfoury, Y. & Scadden, D.T. Mesenchymal cell contributions to the stem cell niche. *Cell Stem Cell* **16**, 239-253 (2015).

154. Ghajar, C.M., Blevins, K.S., Hughes, C.C., George, S.C. & Putnam, A.J. Mesenchymal stem cells enhance angiogenesis in mechanically viable prevascularized tissues via early matrix metalloproteinase upregulation. *Tissue engineering* **12**, 2875-2888 (2006).

155. Ghajar, C.M. et al. Mesenchymal cells stimulate capillary morphogenesis via distinct proteolytic mechanisms. *Experimental cell research* **316**, 813-825 (2010).

156. Melero-Martin, J.M. et al. Engineering robust and functional vascular networks in vivo with human adult and cord blood-derived progenitor cells. *Circulation research* **103**, 194-202 (2008).

157. Traktuev, D.O. et al. Robust functional vascular network formation in vivo by cooperation of adipose progenitor and endothelial cells. *Circulation research* **104**, 1410-1420 (2009).

158. Alimperti, S. et al. Three-dimensional biomimetic vascular model reveals a RhoA, Rac1, and N-cadherin balance in mural cell-endothelial cell-regulated barrier function. *Proceedings of the National Academy of Sciences of the United States of America* **114**, 8758-8763 (2017).

159. Engler, A.J., Sen, S., Sweeney, H.L. & Discher, D.E. Matrix elasticity directs stem cell lineage specification. *Cell* **126**, 677-689 (2006).

160. Petrie, T.A. et al. Multivalent integrin-specific ligands enhance tissue healing and biomaterial integration. *Science translational medicine* **2**, 45ra60 (2010).

161. Kilian, K.A., Bugarija, B., Lahn, B.T. & Mrksich, M. Geometric cues for directing the differentiation of mesenchymal stem cells. *Proceedings of the National Academy of Sciences of the United States of America* **107**, 4872-4877 (2010).

162. Kilian, K.A. & Mrksich, M. Directing stem cell fate by controlling the affinity and density of ligand-receptor interactions at the biomaterials interface. *Angewandte Chemie (International ed. in English)* **51**, 4891-4895 (2012).

163. Gobaa, S. et al. Artificial niche microarrays for probing single stem cell fate in high throughput. *Nat Methods* **8**, 949-955 (2011).

164. Cosgrove, B.D. et al. N-cadherin adhesive interactions modulate matrix mechanosensing and fate commitment of mesenchymal stem cells. *Nature materials* **15**, 1297-1306 (2016).

165. Murphy, W.L., McDevitt, T.C. & Engler, A.J. Materials as stem cell regulators. *Nature materials* **13**, 547-557 (2014).

166. Seliktar, D. Designing cell-compatible hydrogels for biomedical applications. *Science (New York, N.Y.)* **336**, 1124-1128 (2012).

167. Ranga, A. et al. Neural tube morphogenesis in synthetic 3D microenvironments. *Proceedings of the National Academy of Sciences of the United States of America* **113**, E6831-e6839 (2016).

168. Ranga, A. et al. 3D niche microarrays for systems-level analyses of cell fate. *Nature communications* **5**, 4324 (2014).

169. Enemchukwu, N.O. et al. Synthetic matrices reveal contributions of ECM biophysical and biochemical properties to epithelial morphogenesis. *The Journal of cell biology* **212**, 113-124 (2016).

170. Li, S. et al. Hydrogels with precisely controlled integrin activation dictate vascular patterning and permeability. *Nature materials* **16**, 953-961 (2017).

171. Gjorevski, N. et al. Designer matrices for intestinal stem cell and organoid culture. *Nature* **539**, 560-564 (2016).

172. Benoit, D.S., Schwartz, M.P., Durney, A.R. & Anseth, K.S. Small functional groups for controlled differentiation of hydrogel-encapsulated human mesenchymal stem cells. *Nature materials* **7**, 816-823 (2008).

173. Caliari, S.R., Vega, S.L., Kwon, M., Soulas, E.M. & Burdick, J.A. Dimensionality and spreading influence MSC YAP/TAZ signaling in hydrogel environments. *Biomaterials* **103**, 314-323 (2016).

174. Ehrbar, M. et al. Enzymatic formation of modular cell-instructive fibrin analogs for tissue engineering. *Biomaterials* **28**, 3856-3866 (2007).

175. Ehrbar, M. et al. Biomolecular hydrogels formed and degraded via site-specific enzymatic reactions. *Biomacromolecules* **8**, 3000-3007 (2007).

176. Liu, H., Kennard, S. & Lilly, B. NOTCH3 expression is induced in mural cells through an autoregulatory loop that requires endothelial-expressed JAGGED1. *Circulation research* **104**, 466-475 (2009).

177. Lienemann, P.S. et al. A versatile approach to engineering biomolecule-presenting cellular microenvironments. *Advanced healthcare materials* **2**, 292-296 (2013).

178. Smith, A.O., Bowers, S.L., Stratman, A.N. & Davis, G.E. Hematopoietic stem cell cytokines and fibroblast growth factor-2 stimulate human endothelial cell-pericyte tube co-assembly in 3D fibrin matrices under serum-free defined conditions. *PloS one* **8**, e85147 (2013).

179. Morello, R. et al. Regulation of glomerular basement membrane collagen expression by LMX1B contributes to renal disease in nail patella syndrome. *Nature genetics* **27**, 205-208 (2001).

180. Kruegel, J. & Miosge, N. Basement membrane components are key players in specialized extracellular matrices. *Cellular and molecular life sciences : CMLS* **67**, 2879-2895 (2010).

181. Ricard-Blum, S. The collagen family. *Cold Spring Harb Perspect Biol* **3**, a004978 (2011).

182. Suh, J.H. & Miner, J.H. The glomerular basement membrane as a barrier to albumin. *Nature reviews. Nephrology* **9**, 470-477 (2013).

183. Stratman, A.N. et al. Interactions between mural cells and endothelial cells stabilize the developing zebrafish dorsal aorta. *Development (Cambridge, England)* **144**, 115-127 (2017).

184. Morrow, D. et al. Notch and vascular smooth muscle cell phenotype. *Circulation research* **103**, 1370-1382 (2008).

185. Wang, Y., Pan, L., Moens, C.B. & Appel, B. Notch3 establishes brain vascular integrity by regulating pericyte number. *Development (Cambridge, England)* **141**, 307-317 (2014).

186. Kofler, N.M., Cuervo, H., Uh, M.K., Murtomaki, A. & Kitajewski, J. Combined deficiency of Notch1 and Notch3 causes pericyte dysfunction, models CADASIL, and results in arteriovenous malformations. *Scientific reports* **5**, 16449 (2015).

187. Volz, K.S. et al. Pericytes are progenitors for coronary artery smooth muscle. *eLife* **4** (2015).

188. High, F.A. et al. Endothelial expression of the Notch ligand Jagged1 is required for vascular smooth muscle development. *Proceedings of the National Academy of Sciences of the United States of America* **105**, 1955-1959 (2008).

189. Jin, S. et al. Notch signaling regulates platelet-derived growth factor receptor-beta expression in vascular smooth muscle cells. *Circulation research* **102**, 1483-1491 (2008).

190. Scheppke, L. et al. Notch promotes vascular maturation by inducing integrin-mediated smooth muscle cell adhesion to the endothelial basement membrane. *Blood* **119**, 2149-2158 (2012).

191. Poulos, M.G. et al. Endothelial Jagged-1 is necessary for homeostatic and regenerative hematopoiesis. *Cell reports* **4**, 1022-1034 (2013).

192. Lilly, B. & Kennard, S. Differential gene expression in a coculture model of angiogenesis reveals modulation of select pathways and a role for Notch signaling. *Physiological genomics* **36**, 69-78 (2009).

193. Kurpinski, K. et al. Transforming growth factor-beta and notch signaling mediate stem cell differentiation into smooth muscle cells. *Stem cells (Dayton, Ohio)* **28**, 734-742 (2010).

194. Papadimitropoulos, A. et al. Expansion of human mesenchymal stromal cells from fresh bone marrow in a 3D scaffold-based system under direct perfusion. *PloS one* **9**, e102359 (2014).

195. Guven, S. et al. Engineering of large osteogenic grafts with rapid engraftment capacity using mesenchymal and endothelial progenitors from human adipose tissue. *Biomaterials* **32**, 5801-5809 (2011).

196. Osinga, R. et al. Generation of a Bone Organ by Human Adipose-Derived Stromal Cells Through

Endochondral Ossification. *Stem cells translational medicine* **5**, 1090-1097 (2016).

197. Zeisberger, S.M. et al. Optimization of the culturing conditions of human umbilical cord blood-derived endothelial colony-forming cells under xeno-free conditions applying a transcriptomic approach. *Genes to cells : devoted to molecular & cellular mechanisms* **15**, 671-687 (2010).

198. Niemisto, A., Dunmire, V., Yli-Harja, O., Zhang, W. & Shmulevich, I. Robust quantification of in vitro angiogenesis through image analysis. *IEEE transactions on medical imaging* **24**, 549-553 (2005).

199. Love, M.I., Huber, W. & Anders, S. Moderated estimation of fold change and dispersion for RNA-seq data with DESeq2. *Genome biology* **15**, 550 (2014).

200. Huber, W. et al. Orchestrating high-throughput genomic analysis with Bioconductor. *Nat Methods* **12**, 115-121 (2015).

201. Horton, E.R. et al. Definition of a consensus integrin adhesome and its dynamics during adhesion complex assembly and disassembly. *Nat Cell Biol* **17**, 1577-1587 (2015).

202. Mayorca-Guiliani, A.E. et al. ISDoT: in situ decellularization of tissues for high-resolution imaging and proteomic analysis of native extracellular matrix. *Nature medicine* **23**, 890-898 (2017).

203. Zeeberg, B.R. et al. High-Throughput GoMiner, an 'industrial-strength' integrative gene ontology tool for interpretation of multiple-microarray experiments, with application to studies of Common Variable Immune Deficiency (CVID). *BMC bioinformatics* **6**, 168 (2005).

204. de Hoon, M.J. et al. Predicting gene regulation by sigma factors in Bacillus subtilis from genome-wide data. *Bioinformatics (Oxford, England)* **20 Suppl 1**, i101-108 (2004).

205. Saldanha, A.J. Java Treeview--extensible visualization of microarray data. *Bioinformatics (Oxford, England)* **20**, 3246-3248 (2004).

206. Gomez-Barrena, E. et al. Bone fracture healing: cell therapy in delayed unions and nonunions. *Bone* **70**, 93-101 (2015).

207. Dimitriou, R., Jones, E., McGonagle, D. & Giannoudis, P.V. Bone regeneration: current concepts and future directions. *BMC medicine* **9**, 66 (2011).

208. Kanczler, J.M. & Oreffo, R.O.C. OSTEOGENESIS AND ANGIOGENESIS: THE POTENTIAL FOR ENGINEERING BONE. *European Cells and Materials* **15**, 100-114 (2008).

209. Tsigkou, O. et al. Engineered vascularized bone grafts. *Proceedings of the National Academy of Sciences of the United States of America* **107**, 3311-3316 (2010).

210. Correia, C. et al. In vitro model of vascularized bone: synergizing vascular development and osteogenesis. *PloS one* **6**, e28352 (2011).

211. Nguyen, L.H. et al. Vascularized bone tissue engineering: approaches for potential improvement. *Tissue engineering. Part B, Reviews* **18**, 363-382 (2012).

212. Amini, A.R., Laurencin, C.T. & Nukavarapu, S.P. Bone Tissue Engineering: Recent Advances and Challenges. *Crit Rev Biomed Eng.* **40**, 363–408 (2012).

213. Stegen, S., van Gastel, N. & Carmeliet, G. Bringing new life to damaged bone: the importance of angiogenesis in bone repair and regeneration. *Bone* **70**, 19-27 (2015).

214. Mercado-Pagan, A.E., Stahl, A.M., Shanjani, Y. & Yang, Y. Vascularization in bone tissue engineering constructs. *Annals of biomedical engineering* **43**, 718-729 (2015).

215. Caplan, A.I. & Correa, D. The MSC: an injury drugstore. *Cell stem cell* **9**, 11-15 (2011).

216. Bose, S., Roy, M. & Bandyopadhyay, A. Recent advances in bone tissue engineering scaffolds. *Trends in biotechnology* **30**, 546-554 (2012).

217. Lutolf, M.P. & Hubbell, J.A. Synthetic biomaterials as instructive extracellular microenvironments

for morphogenesis in tissue engineering. *Nat Biotechnol* **23**, 47-55 (2005).

218. Slaughter, B.V., Khurshid, S.S., Fisher, O.Z., Khademhosseini, A. & Peppas, N.A. Hydrogels in regenerative medicine. *Advanced materials (Deerfield Beach, Fla.)* **21**, 3307-3329 (2009).

219. Sala, A. et al. Engineering 3D cell instructive microenvironments by rational assembly of artificial extracellular matrices and cell patterning. *Integrative biology : quantitative biosciences from nano to macro* **3**, 1102-1111 (2011).

220. Ali, S., Saik, J.E., Gould, D.J., Dickinson, M.E. & West, J.L. Immobilization of Cell-Adhesive Laminin Peptides in Degradable PEGDA Hydrogels Influences Endothelial Cell Tubulogenesis. *BioResearch open access* **2**, 241-249 (2013).

221. Schweller, R.M. & West, J.L. Encoding Hydrogel Mechanics via Network Cross-Linking Structure. *ACS Biomaterials Science & Engineering* **1**, 335-344 (2015).

222. Ehrbar, M. et al. Biomolecular Hydrogels Formed and Degraded via Site-Specific Enzymatic Reactions. *Biomacromolecules* **8**, 3000-3007 (2007).

223. Ehrbar, M. et al. Elucidating the role of matrix stiffness in 3D cell migration and remodeling. *Biophysical journal* **100**, 284-293 (2011).

224. Caplan, A.I. & Correa, D. PDGF in bone formation and regeneration: new insights into a novel mechanism involving MSCs. *J Orthop Res* **29**, 1795-1803 (2011).

225. Hollinger, J.O., Hart, C.E., Hirsch, S.N., Lynch, S. & Friedlaender, G.E. Recombinant human platelet-derived growth factor: biology and clinical applications. *J Bone Joint Surg Am* **90 Suppl 1**, 48-54 (2008).

226. Lienemann, P.S., Lutolf, M.P. & Ehrbar, M. Biomimetic hydrogels for controlled biomolecule delivery to augment bone regeneration. *Adv Drug Deliv Rev* **64**, 1078-1089 (2012).

227. Ahn, H.J., Lee, W.J., Kwack, K. & Kwon, Y.D. FGF2 stimulates the proliferation of human mesenchymal stem cells through the transient activation of JNK signaling. *FEBS Lett* **583**, 2922-2926 (2009).

228. Martin, I., Muraglia, A., Campanile, G., Cancedda, R. & Quarto, R. Fibroblast Growth Factor-2 Supports ex Vivo Expansion and Maintenance of Osteogenic Precursors from Human Bone Marrow*. *Endocrinology* **138**, 4456-4462 (1997).

229. Bianchi, G. et al. Ex vivo enrichment of mesenchymal cell progenitors by fibroblast growth factor 2. *Experimental Cell Research* **287**, 98-105 (2003).

230. Tsutsumi, S. et al. Retention of multilineage differentiation potential of mesenchymal cells during proliferation in response to FGF. *Biochem Biophys Res Commun* **288**, 413-419 (2001).

231. Coutu, D.L., Francois, M. & Galipeau, J. Inhibition of cellular senescence by developmentally regulated FGF receptors in mesenchymal stem cells. *Blood* **117**, 6801-6812 (2011).

232. Quarto, N., Wan, D.C. & Longaker, M.T. Molecular mechanisms of FGF-2 inhibitory activity in the osteogenic context of mouse adipose-derived stem cells (mASCs). *Bone* **42**, 1040-1052 (2008).

233. Lai, W.T., Krishnappa, V. & Phinney, D.G. Fibroblast growth factor 2 (Fgf2) inhibits differentiation of mesenchymal stem cells by inducing Twist2 and Spry4, blocking extracellular regulated kinase activation, and altering Fgf receptor expression levels. *Stem cells* **29**, 1102-1111 (2011).

234. Lei, L. et al. Optimization of release pattern of FGF-2 and BMP-2 for osteogenic differentiation of low-population density hMSCs. *Journal of biomedical materials research. Part A* **103**, 252-261 (2015).

235. Benoit, D.S., Durney, A.R. & Anseth, K.S. The effect of heparin-functionalized PEG hydrogels on three-dimensional human mesenchymal stem cell osteogenic differentiation. *Biomaterials* **28**, 66-77 (2007).

236. Nguyen, M.K., Jeon, O., Krebs, M.D., Schapira, D. & Alsberg, E. Sustained localized presentation of RNA interfering molecules from in situ forming hydrogels to guide stem cell osteogenic differentiation. *Biomaterials* **35**, 6278-6286 (2014).

237. Hagmann, S. et al. FGF-2 addition during expansion of human bone marrow-derived stromal cells alters MSC surface marker distribution and chondrogenic differentiation potential. *Cell Prolif* **46**, 396-407 (2013).

238. Handorf, A.M. & Li, W.J. Fibroblast growth factor-2 primes human mesenchymal stem cells for enhanced chondrogenesis. *PloS one* **6**, e22887 (2011).

239. Ito, T., Sawada, R., Fujiwara, Y. & Tsuchiya, T. FGF-2 increases osteogenic and chondrogenic differentiation potentials of human mesenchymal stem cells by inactivation of TGF-beta signaling. *Cytotechnology* **56**, 1-7 (2008).

240. Solchaga, L.A. et al. FGF-2 enhances the mitotic and chondrogenic potentials of human adult bone marrow-derived mesenchymal stem cells. *J Cell Physiol* **203**, 398-409 (2005).

241. Kaigler, D. et al. Endothelial cell modulation of bone marrow stromal cell osteogenic potential. *FASEB J* **19**, 665-667 (2005).

242. Wang, J. et al. In vitro osteogenesis of human adipose-derived stem cells by coculture with human umbilical vein endothelial cells. *Biochem Biophys Res Commun* **412**, 143-149 (2011).

243. Kang, Y., Kim, S., Fahrenholtz, M., Khademhosseini, A. & Yang, Y. Osteogenic and angiogenic potentials of monocultured and co-cultured human-bone-marrow-derived mesenchymal stem cells and human-umbilical-vein endothelial cells on three-dimensional porous beta-tricalcium phosphate scaffold. *Acta biomaterialia* **9**, 4906-4915 (2013).

244. Leszczynska, J., Zyzynska-Granica, B., Koziak, K., Ruminski, S. & Lewandowska-Szumiel, M. Contribution of endothelial cells to human bone-derived cells expansion in coculture. *Tissue engineering. Part A* **19**, 393-402 (2013).

245. Deckers, M.M.L. et al. Bone Morphogenetic Proteins Stimulate Angiogenesis through Osteoblast-Derived Vascular Endothelial Growth Factor A. *Endocrinology* **143**, 1545-1553 (2002).

246. Bai, Y. et al. Effects of combinations of BMP-2 with FGF-2 and/or VEGF on HUVECs angiogenesis in vitro and CAM angiogenesis in vivo. *Cell and tissue research* **356**, 109-121 (2014).

247. Langenfeld, E.M. & Langenfeld, J. Bone Morphogenetic Protein-2 Stimulates Angiogenesis in Developing Tumors. *Molecular Cancer Research* **2**, 141–149 (2004).

248. Rothhammer, T., Bataille, F., Spruss, T., Eissner, G. & Bosserhoff, A.K. Functional implication of BMP4 expression on angiogenesis in malignant melanoma. *Oncogene* **26**, 4158-4170 (2007).

249. Folkman, J. & C., H. Angiogenesis in vitro. *Nature* **288**, 551-556 (1980).

250. Smith, A.O., Bowers, S.L.K., Stratman, A.N. & Davis, G.E. Hematopoietic Stem Cell Cytokines and Fibroblast Growth factor-2 Stimulate Human Endothelial Cell- Pericyte Tube Co-Assembly in 3D Fibrin Matrices under Serum-Free Defined Conditions. *PloS one* **8**, e85147 (2013).

251. Milleret, V., Simona, B.R., Lienemann, P.S., Voros, J. & Ehrbar, M. Electrochemical control of the enzymatic polymerization of PEG hydrogels: formation of spatially controlled biological microenvironments. *Adv Healthc Mater* **3**, 508-514 (2014).

252. Weber, F.E. et al. Disulfide bridge conformers of mature BMP are inhibitors for heterotopic ossification. *Biochem Biophys Res Commun* **286**, 554-558 (2001).

253. Niemistö, A., Dunmire, V., Yli-Harja, O., Zhang, W. & Shumlevich, I. Robust Quantification of In Vitro Angiogenesis Through Image Analysis. *IEEE TRANSACTIONS ON MEDICAL IMAGING* **24**, 549-553 (2005).

254. Metzger, S. et al. Cell-Mediated Proteolytic Release of Growth Factors from Poly(Ethylene Glycol) Matrices. *Macromolecular bioscience* **16**, 1703-1713 (2016).

Curriculum Vitae

Ulrich Blache
Scheideggstrasse 124
CH-8038 Zürich
Ulrich.Blache@werb.de
Mobil: +41 762143406

Education

2014 – 2017	**Ph.D. Student** at ETH Zurich, Switzerland, Department of Health Sciences and Technology
2012 – 2013	**Research Assistant** at the Martin-Luther University in Halle/Saale, Germany, Institute for Physiological Chemistry
2012	**M.Sc. in Cell Biology** University of Leipzig, Germany Master-Thesis at University of Basel, Switzerland
2010	**B.Sc. in Biology** University of Leipzig, Germany
2004 – 2005	**Civilian Service** at the St. Elisabeth Hospital, Leipzig, Germany
2004	**Abitur**, Rudolf-Hildebrandt-Gymnasium, Markkleeberg, Germany

Fellowships

2014 – 2017	**Marie Curie Fellowship** Recipient of the European Union (ITN) Early Stage Researcher (ESR)
2008 – 2012	**Rosa Luxemburg Fellowship** Recipient of the German Federal Ministry of Education and Science

Publications

Blache U and Ehrbar M (2017): Inspired by nature: hydrogels as versatile tools for vascular engineering. In: *Advances in Wound Care* ahead of print

Blache U, Guerrero J, Güven S, Klar AS and Scherberich A (2018): In vitro formation of microvascular networks and models. Book chapter (peer-reviewed) in: *Tissue Engineering and Regeneration: Vascularization for Tissue Engineering and Regenerative Medicine*, Springer (2018)

Vess A*, **Blache U***, Leitner L, Kurz ARM, Ehrenpfordt A, Sixt M and Posern G (2017): A dual phenotype of MDA-MB-468 cancer cells reveals mutual regulation of tensin3 and adhesion plasticity. In: *Journal of Cell Science* 130/13 (2017); *equal contribution

Metzger S*, **Blache U***, Lienemann PS, Karlsson M, Weber FE, Weber W and Ehrbar M (2016): Cell-Mediated Proteolytic Release of Growth Factors from Poly(Ethylene Glycol) Matrices. In: *Macromolecular Bioscience* 16/11 (2016); *equal contribution

Blache U, Metzger S, Vallmajo-Martin Q, Martin I, Djonov V and Ehrbar M (2016): Dual Role of Mesenchymal Stem Cells Allows for Microvascularized Bone Tissue-Like Environments in PEG Hydrogels. In: *Advanced Healthcare Materials* 5/4 (2016)

Blache U, Silván U, Plodinec M, Sütterlin R, Jakob R, Klebba I, Bentires-Alj M, Aebi U and Schönenberger C-A (2013): A Tumorigenic Actin Mutant Alters Fibroblasts Morphology and Multicellular Assembly Properties. In: *Cytoskeleton* 70/10 (2013)

Blache U, Jakob T, Su W and Wilhelm C (2011): The Impact of Cell-specific Absorption Properties on the Correlation of Electron Transport Rates Measured by Chlorophyll Fluorescence and Photosynthetic Oxygen Production in Planktonic Algae. In: *Plant Physiology and Biochemistry* 49/8 (2011)

Under revision or in preparation

Lienemann PS, Papageorgiou P, **Blache U**, Metzger S, Kiveliö AS, Milleret V, Vallmajo-Martin Q, Sala A, Hohnel S, Roch A, Reuten R, Koch M, Naveiras O, Weber FE, Weber W, Lutolf MP and Ehrbar M: Augmenting bone regeneration through enhanced recruitment and manipulation of endogenous skeletal stem cells in artificial niches

Blache U, Vallmajo-Martin Q, Horton ER, Guerrero J, Djonov V, Scherberich A, Erler JT, Martin I, Snedeker JG, Milleret V and Ehrbar M: Notch-inducing PEG-hydrogels mimic the extracellular matrix switch of MSCs in the perivascular microenvironment